UNIVERSIDAD DEL ROSARIO
Escuela de Medicina y Ciencias de la Salud
Programa de Doctorado en Ciencias Biomédicas y Biológicas

Doctoral Thesis

Successional Dynamics, Edaphic and Microclimatic Heterogeneity Shape Reproductive Phenology, Functional Traits, and Early-Life Community Assembly in Upper Andean Mountain Forests

Presented by
Carolina Álvarez Garzón
BSc Biology
Advisor: Dr. Juan Manuel Posada

Bogotá, D. C., Colombia

Jul 2025

Successional Dynamics, Edaphic and Microclimatic Heterogeneity Shape Reproductive Phenology, Functional Traits, and Early-Life Community Assembly in Upper Andean Mountain Forests

Author: Carolina Álvarez Garzón
Program: Doctorado en Ciencias Biomédicas y Biológicas, Universidad del Rosario
Year: 2025

Funding and Support

Colciencias, Universidad del Rosario (Convocatoria Interna de Investigación 2023), Fundación Manigua Desde la Tierra

---

Bibliographic Details
Document type: Doctoral thesis (Ph.D.)
Place of publication: Bogotá, D. C., Colombia
Total pages: [163]
Author's ORCID: 0000-0002-4505-1034

---

1 Acknowledgments

This dissertation stands on the collective efforts of many colleagues, institutions, friends, and family members. I am very grateful to Dr. Juan M. Posada for guiding me through this work, for our helpful conversations, and for carefully reviewing and improving the manuscript. I am deeply grateful to Lizeht Velazco, Angelica Moreno, David Leal, and Valeria Vargas, students of the Biology Group at Universidad del Rosario, for their generous fieldwork; in particular, Brayan Polanía skillfully coordinated sample collection under often challenging conditions, Gabriela del Mar Castaño and Antony Ortiz offered persistent assistance in the field and laboratory.

The research forms part of Proyecto Rastrojos, a collaborative initiative led by Universidad del Rosario and the Instituto de Investigación de Recursos Biológicos Alexander von Humboldt, in partnership with Fundación Cedrela and Pontificia Universidad Javeriana. Core funding came from Universidad del Rosario through the small-grant project "*Dinámicas de regeneración y descomposición de hojarasca en un gradiente sucesional de bosque Altoandino*." At the same time, plot establishment and monitoring benefited from additional support by "*Estudio de dinámicas socio-ecológicas ante escenarios de cambio climático en bosques secundarios peri-urbanos Altoandinos*" lead by Juan M. Posada and funded by COLCIENCIAS (No. FP44842-046-2017). Fundación Manigua Desde la Tierra financed greenhouse operations. I extend special thanks to Professor Fernando A. O. Silveira for his mentorship during my internship at the Federal University of Minas Gerais (UFMG); the fellowship provided by FAPEMIG—Fundação de Amparo à Pesquisa do Estado de Minas Gerais—made this training period possible and highly productive.

I am grateful to the landowners and Fundación Natura, whose generosity and logistical help made locality access possible: Carlos Castillo and the staff of Reserva Biológica El Encenillo; Martha Giraldo and Estefanía Cabo (Torca); Gonzalo Martínez (Tabio); Pedro Rodríguez (Guatavita); and Juan Ramón Giraldo (Fusca).

Warm thanks go to Ana Belén Hurtado and Carlos Vargas for their expert seedling identifications. The botanist Mateo Hernández provided expert species identifications, and I also thank Nicol Rueda, Ana Belén Hurtado, and Isabel Restrepo for their thoughtful readings and invaluable advice on scientific writing. On a personal note, I am in debt to my parents, siblings, and Guille, whose unwavering

encouragement sustained me through each stage of this journey. To my closest friends—whose countless coffees and listening ears turned challenges into solutions—thank you for your unconditional support. Without your patience, humor, and well-timed “descargas,” this thesis would not have come to an end.

2 Table of Contents

3 List of Tables

4 List of Figures

5 General Introduction

FAO´s Global Forest Resources Assessment indicates that only about one-third of the global forest area qualifies as primary (≈1.11 billion ha), while the tropical forests contain the largest share of forests and have experienced persistent primary-forest loss; these trends imply that natural regenerating (secondary) forests make up the majority of tropical forest cover (FAO, 2020; Poorter et al., 2016; Poorter, Craven, et al., 2021; Poorter, Rozendaal, Bongers, Almeida, et al., 2021). These secondary forests store considerable carbon and preserve much of Earth's biodiversity (Chazdon et al., 2016), yet their long-term contribution to climate mitigation and conservation pivots on how quickly—and in which direction—succession proceeds (Baccini et al., 2019; Mitchard, 2018; Tebby et al., 2017).

Functional traits—morphological, physiological, and phenological attributes that mediate resource use—link plant performance to local conditions and shift predictably along successional gradients (Lohbeck, Poorter, Martínez-Ramos, et al., 2014; Poorter, Rozendaal, Bongers, Almeida, et al., 2021; Violle et al., 2007). In tropical forests, succession is commonly described as a transition from 'fast' to 'slow' traits strategy: early in succession acquisitive pioneers capture resources rapidly but die young, whereas later in succession conservative species invest in dense, long-lived tissues that can tolerate stress (Díaz et al., 2016; Reich, 2014; Wright et al., 2004). Empirical patterns, however, are more nuanced: a pan-tropical synthesis revealed that the community-weighted mean of wood density rises with succession in wet forests but declines in dry forests, with both trajectories converging only after several decades (Poorter et al., 2019). Forest succession in highly disturbed upper Andean Tropical Mountain Forests (UATMF; 2,600–3,200 m a.s.l.) follows the inverse trend, favoring conservative strategies in early-successional stands and more acquisitive strategies in late-successional stands, likely due to stressful abiotic conditions early in succession (Castillo-Figueroa et al., 2023). However, this study has mainly focused on leaf and wood traits, while reproductive traits remain understudied in tropical montane systems. For instance, the FunAndes database reports seed traits for <15 % of Andean taxa, limiting trait-based forecasts of succession (Báez, Cayuela, et al., 2022). In addition, recent chronosequences also report both decoupling of seed and vegetative trait axes (Barczyk et al., 2024) and tight integration between them (Guzmán et al., 2023). These gaps motivate a focus on seed temporal supply (phenology), seed-trait variation and seed banks, and seedling recruitment across succession.

We link these four components to established succession theory. Within Pickett's hierarchical framework, phenology governs species availability by opening or closing recruitment windows; seed traits (size, dormancy, dispersal syndromes) regulate movement into safe sites; and seedling functional traits determine performance under local filters (e.g., light, moisture, and edaphic stress; Pickett et al., 1987). This mapping aligns with Grubb's regeneration niche (Grubb, 1977) and with gap-phase (Brokaw, 1985) and initial-vs-relay floristics (Chazdon et al., 2007; Egler, 1954; van Breugel et al., 2007) models: early stands are dominated by small-seeded pioneers with persistent seed banks and high fecundity that rapidly colonize high-light gaps, whereas older stands increasingly recruit large-seeded, shade-tolerant taxa, often dispersed by animals and lacking persistent seed banks (Chazdon et al., 2007; Egler, 1954; Grubb, 1977; van Breugel et al., 2007). Mechanistically, the tolerance–fecundity (seed size–shade tolerance) trade-off predicts that large seeds enhance establishment in stressful microsites (shade, drought), while small seeds maximize colonization in benign sites—a pattern that structures turnover along successional light and resource gradients (Dalling & Hubbell, 2002). Coexistence processes further interact with succession: temporal "storage" via persistent seed banks (Wright, 2002) and seasonality promote recruitment when conditions align, and Janzen–Connell effects impose distance- and density-dependent mortality that is strongest for abundant seeds/seedlings, maintaining diversity through time (Comita et al., 2014).

Phenology further regulates the seasonal timing of reproduction by synchronizing energy and nutrient flows to pollinators and frugivores (E-Vojtkó et al., 2022). In tropical lowland forests, flowering and fruiting peaks correlate with irradiance rather than rainfall (Chapman et al., 2018; Wright & Calderón, 2006). Additionally, small but significative changes in day length can synchronize flowering near the Equator (Borchert et al., 2015). Whether comparable signals operate under the colder, cloudier Andean climate remains unclear.

Seed availability initiates regeneration (Álvarez-Buylla & Martínez-Ramos, 1990; Kuzee & Wijdeven, 2000), yet seed traits can play an important role in determining which recruits persist. Trait-based ecology predicts coordinated shifts in regeneration and vegetative traits along succession. In early successional habitats, seedlings typically originate from small, low-resource seeds and express acquisitive leaves (high SLA, low LDMC) that maximize rapid carbon gain and colonization. In shaded late-successional understories, conservative strategies prevail: larger, resource-rich deeds buffer establishment risk, and leaves show lower SLA and higher LDMC (Leishman et al., 2000), favoring tissue longevity and shade tolerance (Díaz et al., 2016; Moles & Westoby, 2004; Reich, 2014; Wright et al., 2004).

Soil seed banks buffer regeneration after disturbance but often diverge from canopy composition because (i) dispersal limitation and microhabitat heterogeneity shape local propagule pools (Medeiros-Sarmento et al., 2020; Williams-Linera et al., 2016) and (ii) species differ in seed longevity and dormancy cycling, which regulate how long seeds persist and when they germinate (Baskin & Baskin, 2014). In the Colombian Upper Andean Tropical Mountain Forest (UATMF), spatial distance explains more turnover in seedlings and adults than stand age (Hurtado-M et al., 2021), yet comparable tests for seed banks are lacking. Understanding how environmental drivers filter species from the soil to the seedling stage remains essential for effective restoration planning.

These knowledge gaps obscure how seed supply, trait variation, and recruitment are linked across succession. We use Poorter et al. (2023) synthesis and Pickett´s hierarchical model to map phenology and seed/seed bank traits to species availability, and seedling traits to performance (Pickett et al., 1987; Poorter et al., 2023). I place all data in a single model in which climate and soils act as abiotic filters, phylogenetic structure captures shared ancestry, and spatial distance represents dispersal limitation. I fit this framework to monthly phenological censuses, eight seed traits, five vegetative traits, and complete inventories of viable seeds, seedlings, and adults for 64 woody species across twenty UATMF plots arrayed along an early-to-late successional gradient. This model integrates three assembly axes: (i) temporal—seed availability driven by phenology; (ii) functional—alignment between seed and whole-plant traits along succession; and (iii) demographic—filters from the soil seed bank to established seedlings. Together, these axes allow us to test the specific pathways linking propagule supply to establishment.

In the first chapter of my dissertation, I tested three expectations about phenology along a succession gradient. First, I expected early-successional stands to show higher reproductive activity and greater per-event intensity because open canopies increase irradiance and carbon gain, which promote flowering and fruiting in fast-strategy pioneers with short lifespans and high fecundity (Wright & van Schaik, 1994). Second, I expected flowering to peak in months of highest solar radiation. In contrast, fruit-ripening would peak in cloudier periods, reflecting (i) light as a proximate cue for flowering and (ii) moisture and biotic interactions that favor fruit development and dispersal (Wright & van Schaik, 1994). Third, I expected weak phylogenetic conservatism in phenology across the flora but a stronger signal in late-successional stands because environmental filtering under deep shade favors clades with conserved, conservative schedules, yielding phylogenetic clustering (Davies et al., 2013). Recognizing these

ecological and evolutionary links helps predict phenological responses to environmental change and how temporal niche differences promote coexistence in Andean biodiversity hotspots.

In the second chapter, I asked whether regeneration traits provide additional information on assembly beyond leaf and wood traits along an upper-Andean successional gradient. Rather than assume a single spectrum, I test the hypothesis of partial coordination among seeds, leaves, and wood along a whole plant fast-slow axis, as proposed for global trait spectra and cross-organ economics (fast=adquisitive; slow=conservative), Thus acquisitive species should pair lighter, weakly protected seeds with high SLA and low LDMC, whereas conservative species should pair heavy, betterl-defended seeds with low SLA and high LDMC.

From these ideas, I derived three predictions. (i) Early-successional plots, shaped by high light and acidic Andean soils with high aluminum saturation, should converge on conservative vegetative traits (low SLA, high LDMC, and low Amax) and similarly conservative seed traits, reducing functional diversity (Ordoñez et al., 2020). (ii) Late, stands should remain uniform in vegetative traits yet diverge in seed traits that partition establishment niches, aided by diverse frugivore assemblages. (iii) Dispersal limitation should favor anemochory in disturbed early plots, whereas frugivore-rich late forests should host a wider array of zoochorous strategies. To test these ideas, I measured five vegetative traits (SLA, LDMC, WD, Hmax, and Amax) and five regeneration traits (seed mass, seed nitrogen, seed carbon, dispersal mode, and monthly flowering-fruiting activity peaks) for 64 woody species sampled in 20 plots spanning a well-defined successional gradient.

In the final chapter, I examine how soil seed banks, seedlings, and adult plant communities vary with forest succession stand (early vs. late) and local environment across four upper-Andean localities (Tabio, Guasca, Torca-Bogotá, and Guatavita). I quantify α-diversity (species richness and density) and β-diversity (turnover in composition) as functions of soil measures (pH, volumetric water content, bulk density, available nutrients) and soil temperature. From this model, I derived four predictions. First, seedling species richness increases from early- to late-successional stands because closed canopies and deeper organic layers create more shaded, moist microsites for establishment; by contrast, seed bank richness decreases or remains similar, as late-successional species contribute few persistent seeds. Second, floristic similarity between the seed bank and seedlings decreases with succession because recruitment filters and overstory composition diverge. Third, seed bank and seedling densities decrease in late forests,

where light and resources are scarcer at fine spatial scales. Fourth, patch-scale abiotic heterogeneity (especially soil moisture, bulk density, and temperature) explains more variation in community composition than the successional stage alone, producing stronger turnover among localities than along the successional gradient. To evaluate these ideas, I relate seed-bank and seedling composition to soil pH, volumetric water content, bulk density, nutrient availability, and soil temperature and organic layer in early and late stands at each locality.

By integrating reproductive phenology with seed functional traits and soil seed-bank dynamics, my dissertation provides valuable insights for Andean restoration and conservation programs. Flowering and dispersal timelines indicate the months when viable seed rain peaks, informing the scheduling for nursery collections (Ordoñez et al., 2025). The coupled seed-leaf-wood trait spectrum clarifies how early successional forests versus late successional stands favor different ecological strategies, enabling managers to match seed sources and planting densities to local constraints on light, water, and nutrients (Castillo-Figueroa et al., 2023; Homeier et al., 2021). Finally, models of seed-bank diversity and its environmental drivers reveal which plots harbor dormant diversity and which require enrichment planting, enabling more cost-effective allocation of restoration budgets and facilitating long-term monitoring (Gelviz-Gelvez et al., 2016; Medeiros-Sarmento et al., 2020; Piquer-Doblas et al., 2024). Collectively, these insights refine successional theory while providing science-based guidelines to support restoration and conservation actions, facilitating recruitment and safeguarding biodiversity in Upper Andean tropical Mountain forests, one of the most threatened ecosystems on Earth.

6 Reproductive Schedules vary with succession in Andean Mountain Forests

6.1 Abstract

Although secondary forests now account for nearly half of the world's tropical forest area and play a vital role in biodiversity conservation and carbon cycling, the phenological processes that govern their ecological recovery—particularly at high elevations in upper Andean Mountain Forest—remain poorly understood. In this study, I investigated whether reproductive phenology activity and intensity shift predictably across successional stages. I monitored flowering and fruiting monthly for 491 individuals across 66 woody species in early- and late-successional forests of the upper Andean Tropical Mountain Forests (2,600–3,100 m a.s.l., Eastern Cordillera, Colombia). In the analysis, I used circular statistics, generalized additive models, and phylogenetic signal analysis. I found that flowering peaked in April in late-successional stands and in late August in early-successional forests; community-level fruiting (unripe and ripe) peaked from July to October, reflecting a lag from earlier flowering cohorts; flowering activity increased with precipitation and cloud cover and declined with increasing mean and low temperatures. Additionally, the dynamics of unripe and ripe fruit activities were closely tracked by cloudiness and rainfall, with low solar radiation best explaining the dynamics of ripe fruit. Forests produced flowers and fruits year-round. In addition, all phenophases were strongly positively correlated with each other. We found a weak phylogenetic signal in early succession and a stronger one in late successional forests, suggesting increased synchrony among related species in the latter. These findings demonstrate that reproductive phenology in upper Andean forests is driven by temperature, cloud cover, and rainfall dynamics, as well as by shifts associated with succession and phylogenetic structure. Moreover, our results on the dynamics of phenophases offer valuable insights for the conservation of pollinators and seed dispersers, as well as for the availability of seeds for restoration programs, thereby increasing the resilience of these forests under climate change.

***Keywords**:* Reproductive phenology; Successional gradient; Upper Andean Mountain Forest; Solar-radiation and cloud dynamics; Phylogenetic conservatism; Tropical secondary forest recovery.

6.2 Introduction

Disturbance and intensive land-use change have transformed vast areas of old-growth forest into regrowth stands. Secondary formations now comprise a large share of tropical forest areas and dominate many

human-modified landscapes (Chazdon et al., 2007, 2016; Poorter, Craven, et al., 2021). These recovering forests support biodiversity, but their contributions depend on successional trajectories (Poorter, Craven, et al., 2021). Recovery can stall or reverse under severe drought or continued degradation. Biodiversity responses vary with climate, soils, and disturbance regimes (Boukili & Chazdon, 2017; Chazdon, 2008; Chazdon et al., 2007; Norden et al., 2015; Poorter, Craven, et al., 2021; Poorter, Rozendaal, Bongers, de Jarcilene, et al., 2021).

Understanding how species respond to environmental gradients along successional trajectories is, therefore, essential for explaining forest recovery (Craven et al., 2015; Larson & Funk, 2016; Lohbeck, Poorter, et al., 2013; Lohbeck, Poorter, Martínez-Ramos, et al., 2014). Functional traits—morphological, physiological, and phenological characteristics that define resource uptake and use— link plant performance to local conditions (Violle et al., 2007). Along successional gradients, environmental filters change, and these filters select species with different strategies along the fast–slow (acquisitive-conservative) spectrum (Reich, 2014). For instance, fast-growing pioneers flower soon after establishment, reproduce frequently, and disperse many small seeds. In contrast, late-successional species postpone reproduction, flower less often, and invest more resources per seed (Dalling & Hubbell, 2002; Williamson et al., 2008). Patterns differ across climates: conservative drought-tolerance traits often dominate early in dry forests, whereas acquisitive traits are common early in wet tropical forests (Poorter, Rozendaal, Bongers, de Jarcilene, et al., 2021). Deciduous and compound-leaved trees decline with forest age in both types, presumably because canopy development moderates a hot, dry microclimate (Poorter, Rozendaal, Bongers, de Jarcilene, et al., 2021). Water availability shapes both the onset and direction of trait change and can drive convergence in community-level trait values once continuous cover is established (Lohbeck, Poorter, Martínez-Ramos, et al., 2014). In upper Andean forests, community-weighted mean wood density can be high early in succession because shrubs dominate, trees are scarce, and abiotic stress is intense (Castillo-Figueroa et al., 2023). Reproductive phenology is a functional trait: its timing and intensity govern allocation, exposure to stress, and interactions with pollinators and dispersers. Phenophases map onto key bottlenecks in regeneration (pollen delivery and fruit set, dispersal and pre-dispersal loss, germination cues, and access to safe sites) and shape seed rain, seed bank carryover, and seedling recruitment (E-Vojtkó et al., 2022b). At monthly scales, irradiance and photoperiod cue flowering (Chapman et al., 2018; Wright & Calderón, 2006). At shorter time scales, moisture and temperature modulate fruit development after a lag from flowering (Borchert et al., 2015). At broader scales, climatic seasonality and drought severity best explain variation in reproductive activity across the

Neotropics (Mendoza et al., 2017), while short-term anomalies in moisture, vapor-pressure deficit, temperature, and insolation, alongside biotic interactions, further modulate local phenological schedules (Hawes & Peres, 2016; B. Larson & Barrett, 2000; Tschapka & Helversen, 2007). In addition, phylogeny constrains reproductive timing because related species share sensory and developmental pathways for floral induction and fruit development (e.g., photoperiod and temperature thresholds). As a result, early phenophases such as bud burst and anthesis tend to be more phylogenetically conserved than later phases such as fruit maturation, which are more labile and track local climate and dispersal interactions. In shaded, cool, late-successional understories, environmental filtering can reinforce this conservatism by favoring lineages with similar schedules, whereas more heterogeneous light regimes in early stands weaken such clustering (Basnett et al., 2019; Brito et al., 2017; Du et al., 2015). This background motivates examining the phylogenetic structure of phenology across successional stages. UATMF is a biodiversity hotspot (Myers et al., 2000; Rahbek et al., 2019), yet we lack tests of how phenology changes with succession at high elevation. Here, I integrate field observations, climate records, phylogeny, and successional stages (early and late) to test environmental forcing, evolutionary history, and successional stand shape on reproductive schedules in these forests.

I proposed three hypotheses. (H1) Flowering activity and intensity should be higher in early successional stands and increase with solar radiation and air temperature because high light enhances photosynthesis and cues floral induction (Uriarte et al., 2018; Wright & Calderón, 2018a). Fruiting activity and intensity should increase with soil moisture and lower temperature, after a lag from flowering, because developing fruits require water and cooler conditions, which reduce heat and water stress that can cause fruit abortion (Rodrigo & Herrero, 2002). (H2) The lag between fruiting and flowering peaks will be longer in late stands because cooler, shaded understories reduce light and thermal time, slowing fruit growth and ripening (Lorer et al., 2024). Lastly, (H3) Overall phylogenetic conservatism in reproductive timing is weak across the flora but stronger in late stands, where environmental filtering under shade favors clades with conserved schedules (Davies et al., 2013).

6.3 Materials and Methods

Study area

We conducted our study along a successional gradient in UATMF within the Eastern Andean Cordillera, specifically in peri-urban areas around Bogotá, Colombia (Figure 6.1A). This region has undergone

significant transformations due to agriculture, cattle ranching, mining, and urbanization. For this study, we selected 20 permanent plots from the "Rastrojos" project (Hurtado-M et al., 2021). We focused on four localities in Guasca (Gsc), Tabio (Tb), Guatavita (Gvt), and Torca (Tc, Bogotá), with altitudes ranging from 2,600 to 3,100 m above sea level, characterized by moderate to steep slopes. Cattle pastures and agriculture are the dominant activities around the Guatavita (distance between plots 120 – 150 m) and Tabio plots (distance between plots 105 – 640 m), while Guasca (distance between plots 65 – 810 m) experienced limestone mining until the 1990s and is now part of a private reserve. The plots in Torca (50-750 m apart) are within Bogotá's political boundaries and are surrounded by secondary vegetation and urban development.

We conducted censuses in 20 of the 20 x 20 m plots, with 11 plots in early successional forests and 9 in late successional forests (Table 10.1). We classified forest successional stages based on stand age (as estimated by landowners), community composition, forest structure, and aboveground biomass (Clerici et al., 2016; Hurtado-M et al., 2021). Forest age ranges from 10 to 25 years old (early succession) to 60-80 years or older for late successional forests (Table 10.1). Our classification aligns with the physiognomy and structure of the forests, indicating that early successional stands exhibit high stem density and low canopy height, whereas late successional stages display a multi-layered structure with low stem density and a taller, more heterogeneous canopy (Hurtado-M et al., 2021; Figure 6.1A-C).

Climatic variables

Climatic data for the four localities were obtained from nearby weather stations of the Instituto de Hidrología, Meteorología y Estudios Ambientales (IDEAM) covering the last 30 years (IDEAM, 2022). This long-term dataset offers a comprehensive overview of precipitation patterns in the region, enabling an assessment of climatic trends and variability.

We also collected data on local weather: precipitation (mm), temperature (°C), solar radiation (Whm^{-2}), and wind velocity (ms^{-1}) at three localities using an all-in-one weather station (Atmos 41, Meter, Pullman, WA, USA); we recorded data every 15 minutes for one year.

We used our solar radiation measurements, along with a radiation model based on Campbell & Norman (1998), to estimate cloud cover in the study area. We calculated the daily clear-sky potential radiation (Rp; Campbell & Norman, 1998), assuming an atmospheric transmittance of 0.75. We then

compared these potential values with the daily global solar energy measured at our stations (Solar radiation Wh) and calculated cloudiness as follows:

$$Cloudiness = 1 - \frac{Rm}{Rp}$$

This ratio expresses the fraction of incoming radiation attenuated by clouds, as any shortfall from the modeled potential is attributed primarily to cloud cover (Kearney et al., 2014). We calculated all correlation variables for phenology against climate using the monthly means of each climatic parameter, and we also extracted their first (Q1) and third (Q3) quartiles to capture the influence of more extreme conditions on reproductive activity.

Phenological patterns

We quantified phenological patterns across 491 individuals representing all 66 tree and shrub species recorded in the 20 plots (see Table 10.2), which together accounted for 100% of the total species in the study area. Monitoring was conducted monthly from February 2021 to February 2022, using at least five randomly selected individuals per species.

We recorded the activity, intensity, and peak-month activity and intensity for each phenophase in at least five individuals. Initially, we visually examined the crown of each individual to identify the presence of different phenophases: (i) open flowers (flowering), (ii) unripe fruits, and (iii) ripe fruits. We calculated community activity as the percentage of all individuals in each phenophase (Morellato et al., 2010). Then, to evaluate the intensity of phenological events, we visually sampled three branches using the semi-quantitative scale developed by Fournier (1974), which comprises five categories ranging from 0 to 4, with 25% intervals (Morellato et al., 2000). The Fournier Intensity Index, as established by Fournier (1974), was calculated monthly for each of the three phenophases across all species. The formula used for this calculation was (Fournier, 1974):

$$FI = \left(\sum Intensity \;\; i/(N * 4) * 100\right)$$

To determine the overall intensity for each species, we summed the intensity (*i*) values obtained monthly for all individuals and divided this total by the maximum possible value (N x 4) (Oliveira et al., 2021). Next, we employed circular analyses to examine the frequency of species exhibiting peak activity

by converting months into angles. The months were defined by 30° intervals, with January at 0°, February at 30°, and so on (Oliveira et al., 2021). We evaluated the activity and intensity of each phenophase using circular statistics (Hudson & Keatley, 2010) and identified the peak monthly activity and intensity for each phenophase as the month with the highest recorded index (Oliveira et al., 2021). We specifically examined the activity and intensity of flowers, unripe fruits, and ripe fruits to understand their distribution throughout the year and across different stages of forest succession.

To assess the uniformity of these circular distributions, we applied both the Rayleigh and Hermans-Rasson tests (Agostinelli, 2022; Lund et al., 2024) using the R packages *circular* and *CircStats*. The Hermans-Rasson test provided further insights into the presence of multiple modes within the data, offering a comprehensive view of the periodicity of floral and fruiting events (Agostinelli, 2022). The Rayleigh test was used to identify significant modes in the data, revealing whether the activity or intensity of flower or fruit ripeness was concentrated around specific periods (Lund et al., 2024). We applied Rao's homogeneity test to evaluate the uniformity of the data distributions, confirming whether the activity and intensity of flowers and the stages of fruit development followed a uniform circular pattern. Rao's homogeneity test allowed us to compare dispersion and directional consistency across datasets, such as flower activity and intensity during forest succession stages (Lund et al., 2024).

Trait-environmental relationships

We first explored bivariate associations between climate (precipitation, temperature, wind velocity, cloudiness, and solar radiation) and reproduction (flower and fruit activity and intensity) with Spearman rank correlations, a non-parametric metric that captures monotonic links and remains robust to non-normality (Huang et al., 2021; Stefanidis et al., 2023; Yaseen et al., 2023). After removing collinear climatic predictors with $|\rho| > 0.90$, we calculated a full correlation matrix between each phenological variable and the retained climatic predictor (monthly means, first monthly quartiles, and third monthly quartiles of climatic variables).

To quantify those links while allowing for non-linear responses, we used generalized additive models (GAMs) (Polansky & Robbins, 2013; Yao & Ding, 2024). For each phenological response, we compared a candidate set comprising (i) univariate smooths for every climatic predictor that showed a significant Spearman correlation and (ii) a multivariate model that included smooth terms for all significant predictors. Models used thin-plate regression splines, Gaussian error, and restricted maximum

likelihood. We ranked candidates by AIC and deviance explained, selected the model with the lowest AIC, and verified that the smooths had low concavity. Partial-dependence plots illustrate how gradients of temperature, precipitation, radiation, wind, and cloudiness modulated reproductive activity and intensity. We assessed goodness of fit using marginal R^2 and observed-versus-predicted scatterplots, and we checked residuals for autocorrelation and heteroscedasticity. All analyses were implemented in R 4.4.3 (R Core Team, 2024). We modeled phenophase activity and intensity as functions of the same-month climate data (monthly means and Q1/Q3). We did not include lagged climate predictors; potential delays between flowering and fruiting were evaluated descriptively from the timing of their community peaks.

Phylogenetic analyses

We first standardized all species names against the Leipzig Catalogue of Vascular Plants (LCVP; Freiberg et al., 2020), ensuring consistency between our trait dataset and phylogenetic backbone. A community-level phylogeny was then reconstructed using *V.PhyloMaker2* (Jin & Qian, 2022), which extracts relevant clades from the seed-plant Mega phylogeny of Smith and Brown, (2018) and scales branch lengths according to divergence-time estimates from Zanne et al., (2014). The resulting tree topology and divergence times follow the protocol of Jin and Qian, (2022), yielding a well-resolved hypothesis of relationships for the upper Andean mountain forest community (Figure 10.2).

To assess phylogenetic signals in reproductive phenology, we pruned this composite tree to match the species present in each successional stage (Early vs. Late) and each phenophase (flowering, unripe fruit, and ripe fruit). We applied the circular-trait extension of Blomberg's K to the Cartesian components of peak-activity angles, and we computed Rao's ϕ statistic for the raw angular data using the method of Pavoine et al., (2010). In each case, 1,000 permutations of trait values across the tree were used to generate null distributions under random trait–phylogeny association. Observed ϕ values falling outside the 95 % permutation envelope were taken as evidence of a significant phylogenetic signal, whereas values within this range supported the null hypothesis of phylogenetically random trait distribution.

6.4 Results

Climatic variables

Analysis of precipitation data over the past 30 years (data source IDEAM) shows two distinct wet seasons in the sampling areas. The first typically occurs between March and May, with peak precipitation

exceeding 150 mm per month, while the second occurs from October to November, reaching 200 mm per month. In contrast, precipitation dropped below 50 mm during the dry months of June to September and December to February (Figure 6.1).

In the census year (2021- 2022), seasonal variation in microclimatic variables across our Andean highland localities was different from the long-term average. Mean daily precipitation peaked later than average in the first half of the year (May; 5.14 ± 1.31 mm d^{-1}), had a higher than usual peak in October (5.05 ± 0.89 mm d^{-1}), but an unusually wet period in the middle of the year (August; 4.19 ± 0.60 mm d^{-1}). From December through April, mean precipitation remained below 2.90 mm d^{-1}. Mean air temperature ranged from 10.33 ± 0.14 °C in June to 12.11 ± 0.17 °C in December. Mean cloud cover varied between 44.10 ± 1.43 % in January and 55.20 ± 2.02 % in May. Mean wind speed remained near 1.00 ± 0.04 m s^{-1} throughout the year, but with a small increase in August (Figure 6.2).

Phenological activity and intensity among successional stages

We observed that flowering activity (the percentage of individuals that flowered) peaked around April in the late-successional forest but occurred in late August in the early-successional stands. After running Rao´s test for equality of polar vectors (Table 10.3), we found that the difference between the two peaks was statistically significant. In contrast, unripe- and ripe-fruit activities did not differ in mean phase among the early and late successional forests. However, the equality-of-dispersion test showed no difference in phenophase synchrony for flowering or unripe and ripe-fruit activity. Similarly, we found that intensity distributions of flowering, unripe, and ripe fruit remained consistent across successional stages (Table 10.3; Figure 10.1). All other phenophases displayed homogeneous dispersions (Table 10.3; Figure 10.1).

When examining variations between successional stages, we found that flowering activity was high in April in late-successional forests and again in August. In contrast, early successional forests exhibited lower overall activity and less pronounced flowering peaks than late successional forests (Figure 6.3A). The unripe fruit phase exhibited high activity from July to September, particularly in late-successional forests, where fruiting peaked in August. Early successional forests displayed lower activity in unripe fruit (Figure 6.3B). Ripe fruiting activities peaked in August to October (Figure 6.3C) and were again higher in late than in early successional forests.

When comparing phenophase activity and intensity, we found that flowering and fruiting intensities were approximately 70% lower than their corresponding activity levels within the same successional stage (Figure 6.3 and Figure 6.4). Flowering intensity peaked in early and late-successional forests during the dry season (February), with early forests exhibiting the highest flowering intensity (Figure 6.4A). In late-successional stands, the intensity of unripe and ripe fruits was highest in August and September, coinciding with the second rainy season (Figure 6.4B and C).

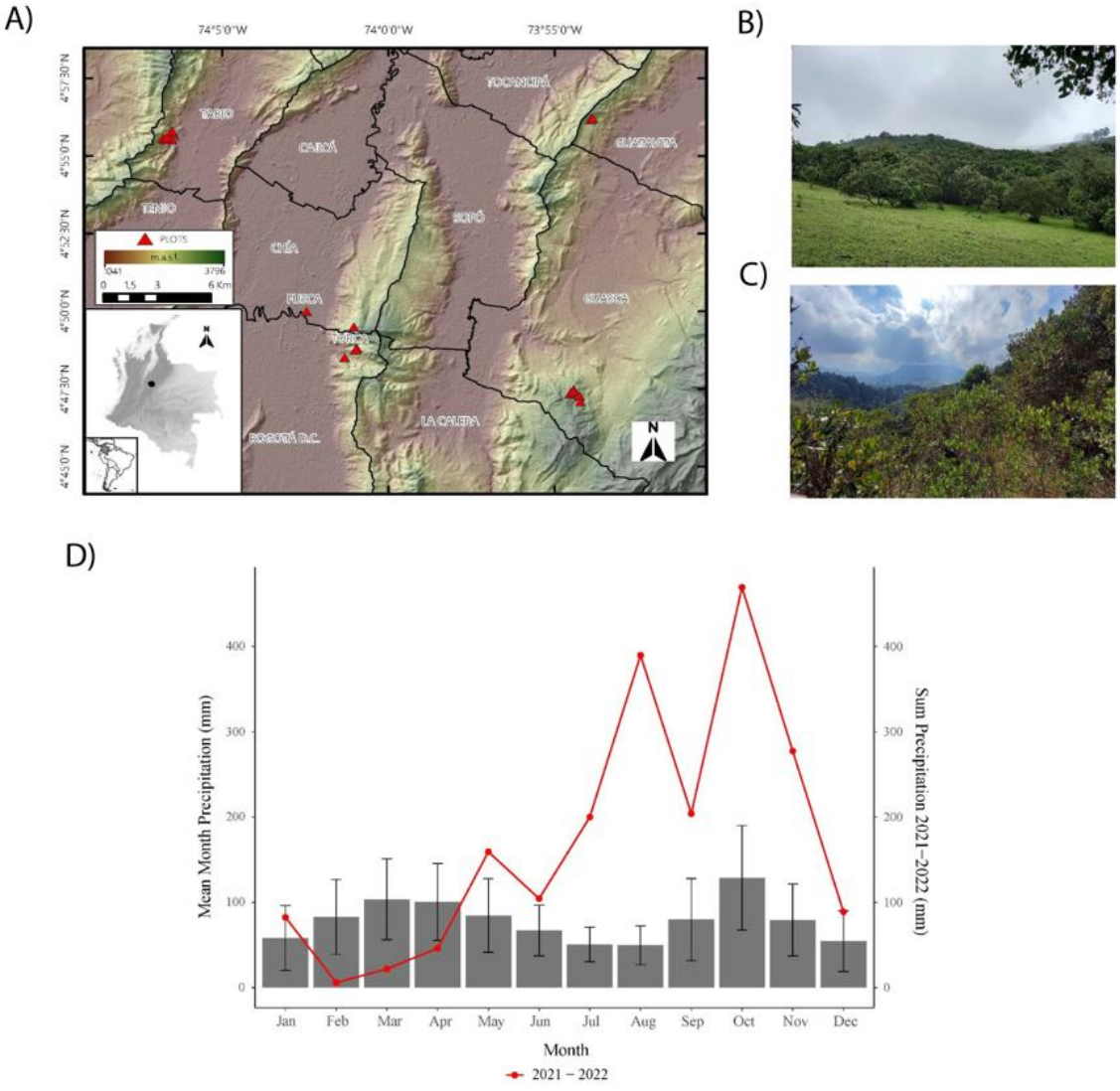

Figure 6.1. Description of the study area in Upper Andean Mountain Tropical Forests.

A) Location map of the 20 permanent plots in the Eastern Andean Cordillera near Bogotá, Colombia. B) Picture of a late successional forest in Tabio, Cundinamarca, Colombia. C) Picture of an early successional forest in Tabio, Cundinamarca, Colombia. These images illustrate the structural differences between the two stages of succession. D) The Average monthly precipitation at the study localities over the last 30 years is represented by gray bars, with standard deviation data from IDEAM. The red line in the graph represents the total monthly precipitation (in millimeters) for the four localities studied from 2021 to 2022.

We also found that phenological phases exhibited strong positive associations in both activity and intensity. In terms of activity, flowering correlated strongly with both ripe and unripe fruit, with the relationship between the two being the strongest. Intensity metrics followed a similar pattern: flowering intensity correlated with ripe fruit and unripe fruit (Figure 6.5).

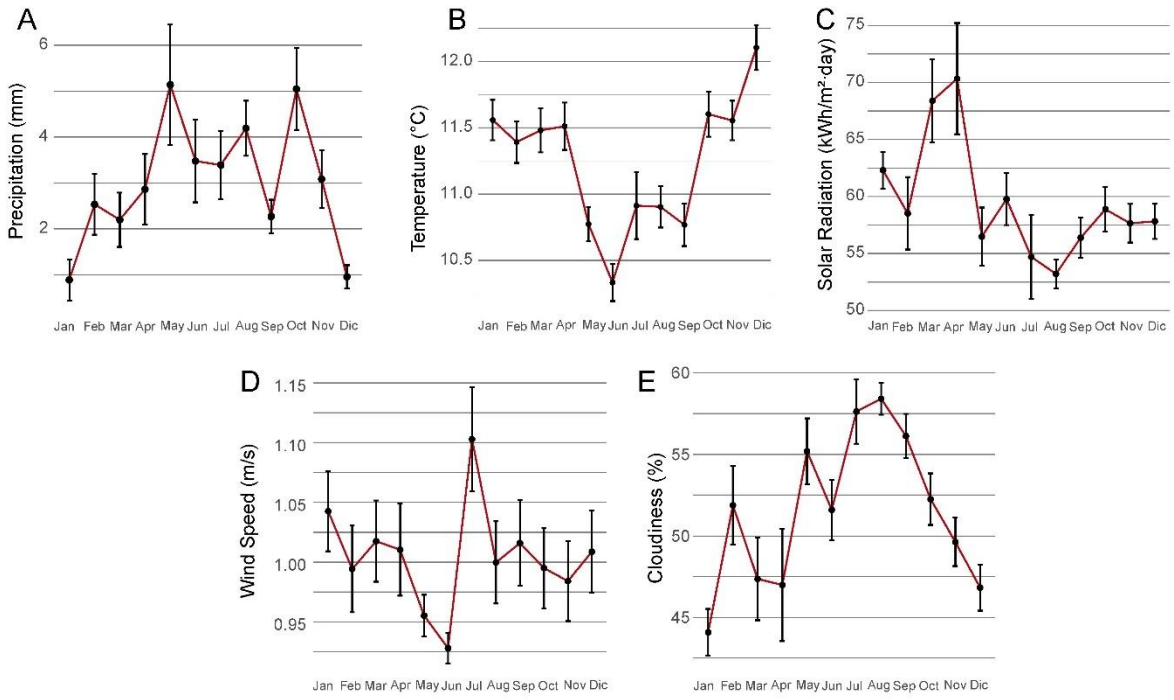

Figure 6.2. Monthly climate profile of the upper-Andean study area. Panels illustrate the annual course of five microclimatic variables derived from continuous 15-minute records at three field stations.

(A) precipitation (mm), (B) mean air temperature (°C), (C) global solar irradiance (kWh m^{-2} day^{-1}), (D) wind speed (m s^{-1}), and (E) fractional cloudiness (%). Each point represents the average daily value for a given month, averaged across stations with complete data, and the error bars show the Standard Error of those monthly means. All metrics, therefore, reflect average daily conditions.

Drivers of phenological activity and intensity

Spearman correlations revealed that flower activity does not correlate with environmental variables (Figure 6.5A). Unripe-fruit activity increased with mean monthly cloudiness (%) and precipitation (%) but fell as mean monthly temperature and first-quartile temperature increased (°C). Ripe-fruit activity showed the strongest negative relation to first-quartile temperature (°C), increasing with mean temperature (°C), and with mean cloud cover (%; Figure 6.5A). We fitted separate generalized additive models to each phenophase activity (Table 10.4) and found that first-quartile monthly temperature best predicted flower activity (AIC = 90.02; deviance explained = 20.3%) and unripe-fruit activity (AIC = 86.25; deviance explained = 62.8%), whereas first-quartile solar radiation best explained ripe-fruit activity (AIC = 89.59; deviance explained = 87.5%).

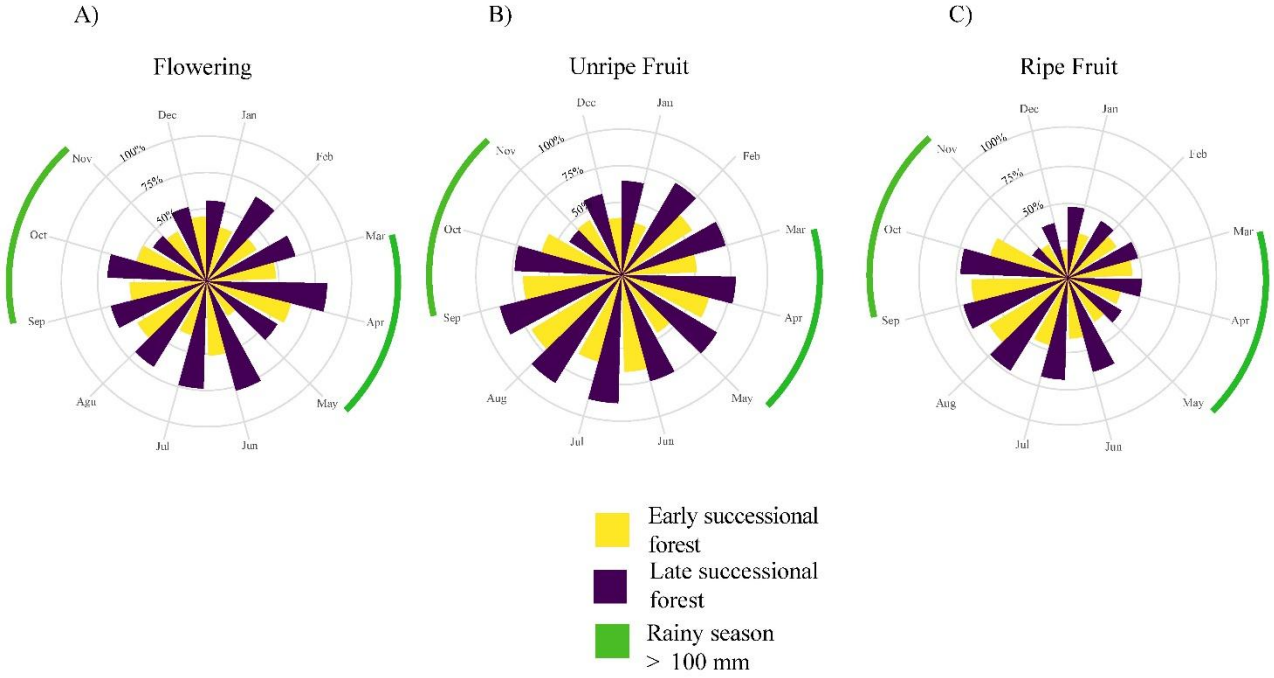

Figure 6.3. Phenological Activity in early and late successional Upper Andean Mountain Tropical Forests.

Percentage of individuals in A) flowering, B) unripe, and C) ripe fruiting stages in early and late forests from 2021 to 2022. Purple bars are % of individuals in each phenophase in early successional forests, and yellow bars are % of individuals in late successional forests. The two green semi-circles represent the two rainy seasons evaluated from 30 years of precipitation data for the study zone.

On the other hand, we found that flower intensity correlated negatively with the first quartile of monthly solar radiation (kWh m-2) (Figure 6.5B). GAMs confirmed these trends (Table 10.4): first-quartile solar radiation best-predicted flower intensity (AIC = 54.91; deviance explained = 76.5%) and ripe-fruit intensity (AIC = 49.84; deviance explained = 47.4%), whereas unripe-fruit intensity responded most strongly to first-quartile temperature (AIC = 68.39; deviance explained = 41.5%).

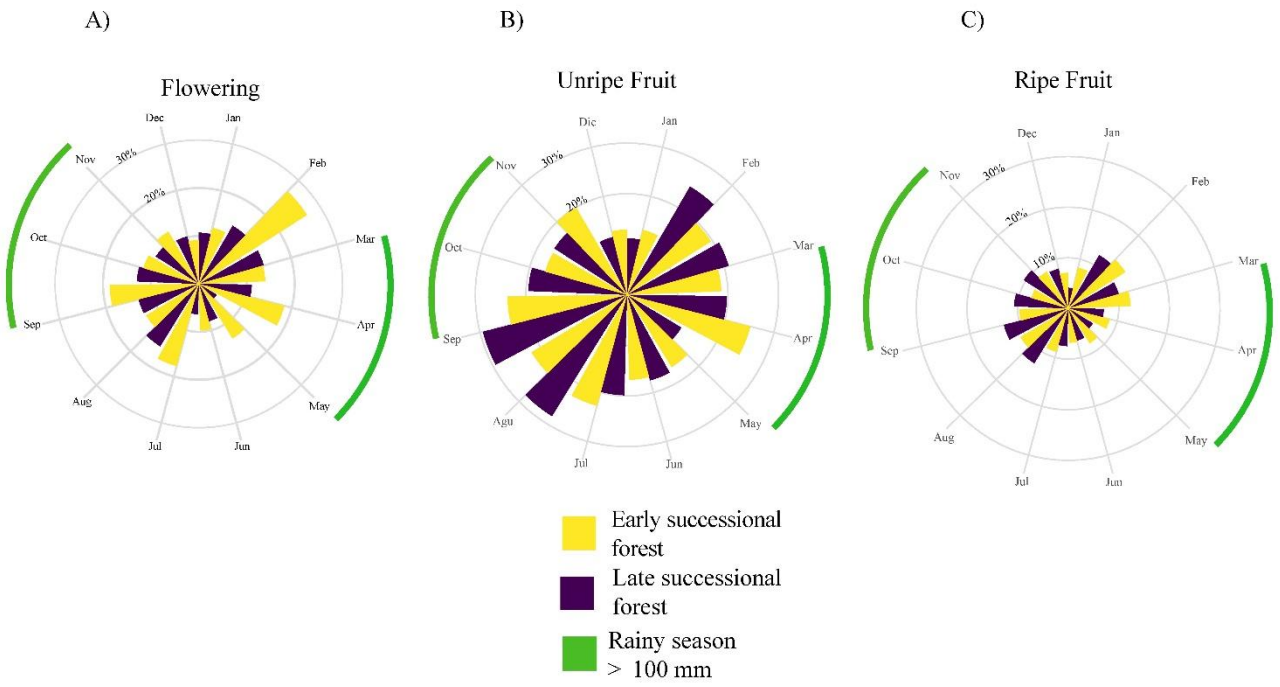

Figure 6.4. Phenological Intensity Type Forest in Upper Andean Mountain Tropical Forests.

Percentage of intensity in A) flowering, B) unripe, and C) ripe fruiting stages in early and late successional forests from 2021 to 2022. Purple bars represent the percentage of intensity in each phenophase in early successional forests, and yellow bars represent the percentage of intensity in late successional forests. The two green semi-circles represent the two rainy seasons evaluated from 30 years of precipitation data for the study zone.

By contrast, high reproductive intensity occurred when cool, cloudy conditions persisted throughout the month; we related climate and phenological activity within the same month. Thus, when we mention a 'lag', we refer not to a lagged climate effect, but to the temporal offset between community-level peaks of flowering and fruiting. Because our time series has a monthly resolution, we cannot detect shorter (e.g., weekly) or species-specific delays."

Phylogenetic signal in reproductive phenology

Rao's φ values increased from early to late successional stages for all three phenophases (**Error! Reference source not found.**). Flowering activity exhibited the strongest shift, from φ = 0.135 in early succession to φ = 0.438 in late succession (Δ = –0.303). Unripe fruiting increases from φ = 0.210 to φ = 0.348 (Δ = –0.138), and ripe fruiting from φ = 0.138 to φ = 0.447 (Δ = –0.309),

Blomberg's K analysis of the components of peak phenophase angle data corroborated the φ results. In early-successional communities, the phylogenetic signal remained weak across all phenophases (**Error! Reference source not found.**). In contrast, late-successional communities showed stronger phylogenetic signal in both circular dimensions of the peak-angle data—the cosine component (Kx) and the sine component (Ky) (**Error! Reference source not found.**). Taken together, Rao's φ and Blomberg's K therefore demonstrate that reproductive phenology is significantly more phylogenetically structured in late- than in early-successional upper-Andean Mountain Forest communities.

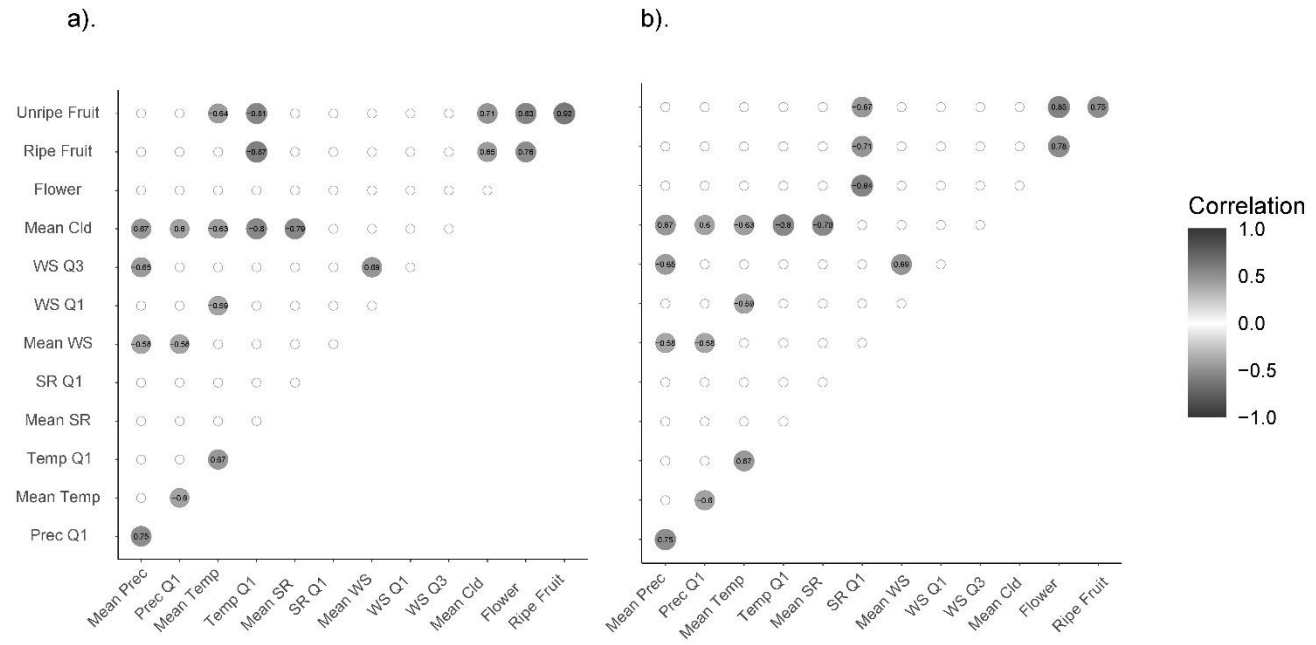

Figure 6.5. Correlation structure linking climate and reproductive phenology in upper-Andean forests.

Heat maps depicting Pearson correlation coefficients between monthly climate descriptors and three phenological phases for (a) reproductive activity—the proportion of individuals in flower, with unripe fruit, or with ripe fruit—and (b) reproductive intensity—the mean percentage of crown surface occupied by each phase. Climate variables include mean precipitation (Mean Prec) and its first quartile (Prec Q1); mean air temperature (Mean Temp) and its first quartile (Temp Q1); mean global solar irradiance (Mean SR) and its first quartile (SR Q1); mean wind speed (Mean WS) together with its first (WS Q1) and third quartiles (WS Q3); and mean cloudiness (Mean Cld). Only correlations significant at $P \leq 0.05$ are shown; non-significant cells are omitted. Shading denotes the magnitude and sign of the coefficient (scale bar at right), and the overlaid numbers give the exact coefficient value ($-1 \leq r \leq 1$). All climate metrics are derived from daily averages that are subsequently aggregated to monthly means.

6.5 Discussion

Our study reveals that both early and late successional forests maintain flower and fruiting activity and intensity throughout the year. This year-round availability of flowers and fruits represents a critical resource for pollinators and frugivores, ensuring a continuous supply of pollen and nectar rewards that

can enhance pollen viability and foraging efficiency (Wright & Calderón, 2018a; Zimmerman et al., 2007). By maintaining reproductive activity even outside peak seasons, these forests provide temporal stability in trophic interactions, helping sustain pollinator populations and frugivore assemblages (Chacoff et al., 2020). In turn, this continuous resource flow supports higher levels of species diversity and ecosystem resilience, as mutualistic networks remain intact throughout the year rather than collapsing during seasonal lows (Collins et al., 2002; Peterson et al., 2003). Such phenological continuity may therefore underpin the remarkable biodiversity characteristic of upper Andean mountain forests (Pérez-Escobar et al., 2022).

Our first hypothesis was not supported as phenophase activity and intensity were generally higher in late forests than in early successional forests. The potential reasons could be that more conservative species tend to appear early in succession, as demonstrated by Castillo-Figueroa et al., (2023) for the same forests. Forest productivity and soil fertility were lower at our study site during early succession, likely reducing reproductive productivity. Our pattern resembles gradients reported in Brazilian Atlantic forests, where flowering intensity peaks later in succession, coinciding with advanced canopy closure (Cardoso et al., 2018). However, our results show that the difference in fruiting intensity between late and early successional forests was relatively weak, contrasting with the findings in Andean cloud forests (Castillo-Figueroa et al., 2023; Hurtado-M et al., 2021). Our findings do not contradict earlier studies. Instead, they indicate that short-term, resource-tracking processes operate across the gradient; moisture and cloudiness pulses after flowering possibly reduce thermal and water stress and synchronize fruiting in both early and late stands. Consistent with this, fruiting activity and intensity rose with cloudiness and precipitation and fell when solar radiation was low, and a mid-year wet pulse in 2021–2022 coincided with fruiting peaks in both forest stages (Figs. 6.3–6.5; Table 10.4). Similar patterns have been reported in other Neotropical forests, where shared climatic drivers and plant–animal mutualisms involving generalist pollinators and seed dispersers can synchronize reproductive output and thereby limit divergence in fruiting among habitats (Boyle & Bronstein, 2012; Lasky et al., 2016).

Our second hypothesis predicted that higher solar radiation would increase flowering, whereas fruit development would benefit from cloudier and wetter months. Our prediction was partially supported. Contrary to expectation, flowering activity was not correlated with monthly average solar global radiation; instead, it declined during colder months (i.e., lower mean and first-quartile temperatures), suggesting thermal constraints on floral initiation even when light was abundant. Indeed, cooler months – with greater cloudiness, not peak irradiance - best predicted flowering activity in the GAMs. Precipitation showed a

positive correlation with activity but did not enter the best model once temperature and radiation were considered, so we view precipitation as a proxy for cloudy, humid periods rather than a direct driver of flowering.

In contrast, fruiting activity supported our prediction: both unripe- and ripe-fruit activity increased with cloudiness and rainfall, and low solar radiation (first-quartile solar radiation) best explained ripe-fruit activity. At Upper Antean Mountain forest, cloudy, humid months favor fruit development (filling), not pre-dispersal fruit drop (Cao et al., 2018; Iwasaki et al., 2019; Li et al., 2021). Interestingly, shade-house trials demonstrate that fruits grow best under intermediate light levels, while excessive sunlight can cause tissue burn (Ortiz et al., 2021). Conversely, lower temperatures may prolong the unripe stage (La Spada et al., 2024).

Our results suggest that Phenological activity depends on discrete periods with low monthly temperatures and high cloudiness, which set the calendar of each phase. The principal flowering peak occurred in April, when maximum solar input (70 kWh m^{-2}) coincided with the mean temperature (11.5 °C) and low precipitation (≈ approximately 3 mm $month^{-1}$), suggesting that day length activated flowering even under severe precipitation shortages. A second, smaller peak emerged in June, after temperatures dropped below 10.5°C and the season's first showers exceeded 3 mm in mean daily precipitation. Unripe-fruit activity then dominated July–September—the period when the usual mid-year drought failed, and cloud cover surpassed 55 %—while ripe-fruit activity lagged by about a month, cresting in August–October and tracking an exceptionally intense late wet season (up to 5 mm d^{-1} in October). Conversely, during the warmest, driest months (January and December), activity in all phenophases dipped below 50%, showing that even a strong photoperiod cue requires minimal precipitation to sustain development.

By contrast, our findings indicate that high reproductive intensity was achieved only when cool, cloudy weather persisted throughout the month. The highest floral intensity occurred in February, characterized by low precipitation (2–3 mm), moderate irradiance (55–60 kWh m^{-2}), suggesting that plants converted drought-stored carbon into a brief but vigorous bloom. Because we modeled only contemporaneous climate–phenology links at monthly resolution, testing explicit flower→fruit delays would require lagged predictors or higher-frequency sampling. In contrast, floral intensity declined in June—despite high activity—because cloudiness above 50% and reduced radiation (~60 kWh m^{-2}) limited daily carbon gain. Unripe-fruit intensity peaked in September under high cloudiness, continued humidity,

and winds ≥ 1 m s^{-1}, conditions that optimize pericarp growth, but collapsed in January (< 1 mm rain, 65 kWh m^{-2}, < 45 % clouds) when high radiation and water stress curtailed allocation. Ripe-fruit intensity was similar to the floral pattern, remaining high in February but declining sharply in November and December as warm temperatures (above 11.5–12 °C) and strong irradiance elevated transpiration demand.

Several long-term studies corroborate—and sometimes nuance—the two-step pattern we detect—first, the activity signal. At Barro Colorado Island, flowering dates remain locked to the same cool, overcast weeks each year—even during intense El Niño droughts—implying a photoperiod or dawn-light cue very similar to the "low-temperature and high-cloud" windows that trigger our April and June peaks (S. J. Wright & Calderón, 2006). In Ugandan cloud forests, Chapman et al., (2018) also found that fruit initiation rises in months with below-average temperatures and elevated cloudiness, matching our July–September burst of unripe fruits. Large-scale modelling of dipterocarps in Southeast Asia reaches the same conclusion: low-temperature cues, not rainfall means, synchronize community-wide flowering. Second, the intensity filter. Our finding that high reproductive investment requires the persistence of cool, cloudy weather echoes liana studies from Australia's Wet Tropics, where diffuse light sustained over several weeks, rather than its brief appearance, drives the largest fruit crops. Likewise, Adamescu et al (2018) suggest that fruit production in Central African canopy trees increases only when low-irradiance conditions persist for a full month, consistent with the idea that carbohydrate reserves must accumulate to support reproduction. Patterns may differ in wetter lowland systems where heat and water are not limited, but our high-elevation forests are cool and humid, so we expect cloudier months to favor fruit development. Taken together, this study supports our proposal that cool-cloudy pulses set the phenological calendar, whereas sustained microclimatic conditions determine the scale of investment; however, it also warns that the second filter can shift toward wetter or more energy-rich forests.

Our results also showed strong positive correlations between the activity and intensity of flowering, unripe fruit, and ripe fruit phases. These patterns, together with the offset peaks of each phase, are consistent with a within-year sequence (flower → unripe fruit → ripe fruit) that could provide relatively continuous floral and fruit resources at the community level. However, we did not explicitly evaluate whether resource supply is continuous for particular pollinator or frugivore guilds (e.g., by defining minimum resource thresholds or tracking species turnover within guilds across months). Because flowering peaks reliably precede fruit peaks by one to two months, our observed 1–2-month offset implies that an April bloom was followed by elevated ripe-fruit activity in August–October; this timing can inform

seed-collection planning (Benavidez et al., 2023; González & Loiselle, 2016; Ordoñez et al., 2025). Whether this temporal coupling ensures an uninterrupted food stream depends on factors we did not measure, such as species overlap, fruiting duration, and consumer mobility. Furthermore, the exceptional climate of our census year—characterized by an extended early dry spell, the absence of the usual mid-year drought, and record late-season rainfall—may have amplified these phase-to-phase links (Corredor-Londoño et al., 2020). Therefore, while phase correlations offer a useful forecasting tool, they should not be interpreted as evidence of year-round resource constancy.

Finally, our third hypothesis predicted a phylogenetic influence on reproductive activity (flower, unripe, and ripe fruit). Although the overall signal was weak, it was stronger in late-successional forests compared to early-successional stands. Phylogenetic analyses revealed weak conservatism in early-successional communities but significant clustering in late-successional stands, suggesting stronger evolutionary constraints on phenological timing within late-successional forests. Early succession is primarily driven by abiotic factors, which can select for broad stress tolerance, ecological strategies, and phenotypic flexibility, resulting in phylogenetically over-dispersed assemblages (Hai et al., 2020; Liu et al., 2021; Purschke et al., 2013). As forest structural complexity and resource increase, biotic interactions and niche differentiation become dominant, resulting in clusters of distantly related lineages that partition predictable microclimates (Norden et al., 2012; Purschke et al., 2013; Satdichanh et al., 2018). This shift highlights how the successional stage modulates the balance between ecological plasticity and phylogenetic constraint, a balance that will shape the resilience of Andean Mountain phenologies under accelerating climatic variability.

Our results constitute a critical first reference point for a region where such information was previously lacking. We emphasize the need for multi-year monitoring to distinguish potential phenological patterns driven by non-climatic cues (e.g., day length) from weather-driven fluctuations. More censuses are also needed to confirm our finding that flowers and fruits remain available throughout the year. This continuous resource supply, even as phenological peaks shift in response to rainfall and radiation, buffers pollinator and frugivore guilds (Butler et al., 2023), sustains complex interaction networks (Christmann et al., 2023), and may contribute to the resilience of upper-Andean mountain ecosystems in the face of increasing climatic variability (Báez et al., 2022).

6.6 Conclusions

Our year-long, community-level survey of 66 woody species in upper Andean Mountain forests shows that reproductive phenology shifts with succession. Late-successional stands concentrate flowering activity during dry months and exhibit phylogenetically clustered peaks across all three phenophases. In contrast, early-successional forests exhibit flowering and fruiting throughout the year; however, reproductive intensity is highly seasonal, with pronounced peaks and periods of low activity. Our results are consistent with a two-step climate filter. Step 1 (trigger): short cool, cloudy periods align with the onset of phenophases (e.g., flowering peaks in April in late stands and in late August in early stands; unripe/ripe fruit peaks July–October). Step 2 (persistence): high phenophase intensity occurred only when cool, cloudy conditions persisted across the month (e.g., February flowering intensity; September unripe-fruit intensity). Hot, sunny months (January and December) had low production. See Figure 10.1 for a monthly synthesis across stages.

Our data show a ~1–2-month offset between flowering and fruiting peaks and positive correlations among phenophases. These patterns suggest that flowers and fruits co-occur for much of the year at the community level. By "resource continuity," we mean the maintenance of floral or fruit resources above ecologically meaningful thresholds for particular pollinator or frugivore guilds, without significant temporal gaps. We did not quantify such thresholds or link resource dynamics to specific mutualists, nor did we assess seed-collection feasibility in an operational sense. Therefore, we refrain from inferring strictly year-round resource continuity or defining seed-collection schedules from these data. Because our phenology series covers only the 2021–2022 hydrological year, which differed from long-term climate means, we interpret the observed timing as year-specific rather than as a long-term phenological pattern.

Finally, our phylogenetic analyses reveal increasing evolutionary constraints on reproductive activity and intensity along the successional gradient, suggesting that abiotic filters predominate in early successional forest communities. In contrast, stronger biotic competition promotes niche differentiation and lineage structuring in late successional forest communities.

Therefore, management and restoration strategies in upper-mountain forests should capitalize on the year-round availability of flowers and fruits while targeting the pronounced activity peaks—particularly in August and September—for coordinated seed collection**.** Second, detailed knowledge of phenological schedules is vital for protecting pollinators and seed dispersers, whose life cycles hinge on these seasonal

pulses. Under a drier future climate, our data suggest that flowering activity and intensity may be predictable, but fruiting could be delayed or diminished, reducing the period when food is available. Anticipating this shift will enable practitioners to retime plantings, broaden the range of nectar- and fruit-producing species, and develop conservation programs that are better buffered against the effects of climate change.

7 Integrating Vegetative and Regenerative Trait Axes Across Successional Gradients in Upper Andean Mountain Forests

7.1 Abstract

Functional-trait ecology postulates that plant species persist only when their regeneration and vegetative traits align with local environmental filters. However, the combined role of seed and whole-plant traits remains poorly studied. In upper Andean Mountain forests, rapid land-use change threatens biodiversity, but limited data on seed traits hamper predictions of community assembly and restoration trajectories. In this study, we tested for coordination among seed, leaf, and wood traits along an acquisitive–conservative axis and assessed whether regeneration traits add explanatory power beyond vegetative traits. We quantified nine seed and phenological traits—including seed mass, C and N content, coat permeability, respiration, dispersal mode, and four phenological traits that capture timing and synchrony—the peak flowering/fruiting angle (circular mean month of activity) and the vector length for flowering/fruiting (synchrony).—and five vegetative traits (specific leaf area, leaf dry matter content, maximum assimilation rate, wood density, maximum (potential) tree height) for 64 woody species. Sampling took place in 20 permanent 20 × 20 m plots spanning early (≤ 50 yr) and late-successional (> 60 yr) stands at 2,600–3,200 m a.s.l. in the Eastern Cordillera of Colombia. We combined Gower distances, factor analysis of mixed data (FAMD), RLQ ordination, and Gaussian General Linear Models (GLMs) to couple traits with environmental, structural, and edaphic variables. We identified two principal seed-trait axes: size–chemistry and phenology–permeability. Zoochorous species spanned the entire trait space, whereas anemo- and autochorous species clustered around low-mass, early-flowering syndromes. RLQ analysis revealed covariance among environment, community composition, and the 13 functional traits. n early-successional stands, greater canopy openness and higher exchangeable aluminum were associated with species with high leaf dry matter content (LDMC) and relatively heavy, nutrient-rich seeds. In contrast, late-successional forests with higher aboveground biomass, warmer soils, and thicker organic horizons were associated with taller trees and a higher prevalence of zoochorous species spanning a broad range of seed masses and fruiting phenologies. Functional divergence, dispersion, and Rao's entropy increased with aboveground biomass (i.e., forest

succession), whereas functional evenness declined with warmer surface soils; functional richness was constant. Heavier seeds occurred in warmer soils; bulk-dense soils had low seed nitrogen (N) content, but deep organic layers increased it. Our results reveal a single acquisitive–conservative spectrum that links seed and vegetative traits across succession, while dispersal mode and seed phenology form a separate axis, most pronounced in mature stands. Recognizing how aluminum toxicity and canopy openness shape these axes clarifies the trajectory of functional diversity and provides a concrete, trait-based outline for restoring threatened upper Andean montane forests.

Keywords: aluminum stress; canopy openness; community assembly; dispersal syndromes; functional diversity; RLQ analysis; seed mass; soil organic layer

7.2 Introduction

Functional trait ecology provides a framework to understand how organismal attributes interact with abiotic and biotic filters to structure plant communities (Funk et al., 2017; Lavorel & Garnier, 2002). In resource-poor locations—such as dry forests, exposed slopes, or nutrient-stripped mine spoils—environmental filtering favors species with stress-tolerant traits (Fazlioglu et al., 2021). Communities therefore converge on conservative traits, including low specific leaf area (SLA), high leaf dry-matter content (LDMC), and high wood density (WD) (Bernard-Verdier et al., 2012; Csecserits et al., 2021; Poorter et al., 2023). Functional richness, divergence, and dispersion are low because most species share similar solutions (Poorter et al., 2019; Sanaphre-Villanueva et al., 2016).

Disturbance, in contrast, generates transiently open sites that are resource-rich — as in many tropical early successional forests — so stands favor acquisitive traits early in succession. Fast, acquisitive species with high SLA and low WD dominate these open gaps. Slow, conservative species prevail once canopies close and competition intensifies (Lohbeck, Poorter, et al., 2013; Lohbeck, Poorter, Martínez-Ramos, et al., 2014; Pinho et al., 2018), establishing a continuum of acquisitive and conservative traits along the forest successional gradient. Across tropical forests, community-weighted means of SLA, LDMC, WD, and maximum height (Hmax) consistently shift toward conservative values as light and nutrients decline (Lohbeck et al., 2015). As conditions change, these patterns of traits can expand again—or contract once more—depending on the local environment (Purschke et al., 2013; Umaña et al., 2020; Zhang et al., 2015). Under severe drought, however, this pattern may flip entirely, with diversity increasing rather than shrinking (Poorter et al., 2023).

Traits such as SLA, WD, and SM thus encapsulate ecological strategies with contrasting investments in resource capture, defense, and persistence, clarifying why some species succeed in specific environments whereas others fail (Gross et al., 2017; Huxley et al., 2023; Westoby, 1998; Yan et al., 2023; Zirbel et al., 2017). However, reproductive traits that define the "regeneration niche" remain understudied (Rosbakh et al., 2018). Seed mass, nutrient content, dispersal mode, and flowering/fruiting phenology dictate a plant's first interaction with the post-disturbance environment and may align—or decouple—from leaf and stem economics (Gomes et al., 2019; Hawes et al., 2020). Empirical work shows that early successional forests favor small, wind-dispersed seeds, whereas shaded understories favor larger, animal-dispersed propagules (Ellison et al., 1993; Foster, 1986; Garwood, 1983; Puerta-Piñero et al., 2013). Recent studies from African mountain forests (Luna-Nieves et al., 2022) and the Himalayas (Vázquez-Ramírez & Venn, 2023) report similar shifts, suggesting that montane systems worldwide may follow comparable rules, but quantitative data for upper Andean Mountain forests remain rare (Báez et al., 2022; Faccion et al., 2021; Homeier et al., 2021).

Functional trait ecology also predicts that species persist only when their seeds and seedlings match the local assembly filters that govern dispersal, persistence, and germination (Grubb, 1977; Poschlod et al., 2013). In shaded understories, seedlings must tolerate low light levels, which favor conservative leaf strategies (e.g., Kitajima, 1994). Seeds that invest heavily in reserves and protective tissue are favored. Large seeds supply enough carbon and nitrogen to support slow, shade-tolerant growth. Conversely, recently disturbed areas with high light availability and abundant nutrients favor colonists with small, lightly physical protected seeds capable of rapid germination and fast initial growth (Kaur et al., 2021), thus maximizing colonization speed. It is still unclear whether the assembly rules identified in lowland tropical forests apply unchanged to tropical montane systems. Evidence from an elevational gradient in Ecuador suggests they may not: as altitude increased, the community’s seed-trait composition shifted while leaf traits remained essentially constant, implying that seeds and leaves respond to different environmental filters in these high-elevation forests (Barczyk et al., 2024). By contrast, experiments in lower mountain forests revealed a trade-off between rapid germination and subsequent seedling growth (Guzmán et al., 2023). Together, these studies underscore the need for integrative work that unites regeneration and vegetative traits.

Saatkamp et al., (2018) propose a seed-ecological spectrum in which seed traits cluster along four conceptual functional axes. First, the resource-investment axis captures the classical seed-size versus seed-number trade-off, adjusted by nutrient content: plants invest either in a few large, resource-rich propagules

or in many small, resource-poor ones. Second, a persistence-to-rapid-germination axis reflects variation in seed-coat thickness or permeability and metabolic rate, ranging from long-lived, well-defended seeds to metabolically active seeds that germinate quickly when conditions become favorable. Third, the germination-timing axis involves dormancy class and sensitivity to environmental filters such as light, temperature, or chemical signals. Finally, a dispersal-and-establishment axis combines seed mass, shape, surface structures, seasonality of release, and dispersal vector to determine where and when seeds arrive and seedlings take root. Because these axes remain hypothetical, Saatkamp et al. (2018) encourage empirical studies that link seed traits to vegetative spectra, such as the leaf-economic spectrum.

Upper Andean montane forests provide an ideal setting to test this framework. Steep altitudinal gradients create sharp shifts in temperature and moisture, while early-successional stands often occur adjacent to old-growth forests (Castillo-Avila et al., 2025; Homeier et al., 2010; Malizia et al., 2020; Maza et al., 2022). Agriculture, recurrent fire, and selective logging operate as strong disturbance filters in tropical forests, restructuring species pools and altering successional trajectories (Armenteras et al., 2011; Castillo-Figueroa et al., 2023; Chazdon, 2003; Hurtado-M et al., 2022). If the seed-ecological spectrum aligns with vegetative strategies, we should see coordinated shifts in seed, leaf, and wood traits across successional gradients. However, most Andean studies focus solely on vegetative traits (Castellanos-Castro & Newton, 2015; Castillo-Figueroa et al., 2023), and fewer than 15% of regional species have any seed-trait data in global databases (Báez, Cayuela, et al., 2022). Generating this missing data will help clarify trait-mediated recovery and guide the conservation of these biodiverse but threatened ecosystems.

We aimed to test whether reproductive and vegetative traits conform to a single acquisitive–conservative spectrum and to track how that spectrum reorganizes through succession in upper-Andean montane forest. To do so, we compiled three complementary trait matrices: (i) a seed-only matrix containing nine seed traits—seed mass (SM), nitrogen (SN) and carbon (SC) concentrations, coat permeability (SP), respiration rate (SR), and the sine and cosine of peak flowering and fruiting dates—for 18 species; (ii) an expanded whole-plant matrix with 12 traits (the seven most diagnostic seed traits plus SLA, LDMC, WD, Amax and Hmax) for 41 species; and (iii) a successional matrix that integrates 13 traits, after gap-filling by imputation, for all 64 species recorded in 20 plots spanning. From these data, we formulated four a priori hypotheses: H1—We test whether seed, leaf, and wood traits are coordinated along a common acquisitive–conservative axis across succession. Acquisitive strategies should pair small low seed mass, high respiration per mass, and higher permeability with high SLA, high Amax, low WD, and generally lower Hmax; species with conservative strategies should show the opposite. This treats seed traits as the regeneration axis of the

whole-plant spectrum and asks whether their positions align with one another. H2— functional community composition will shift from predominantly acquisitive strategies in high resource availability in early successional forests (low biomass forests), to more conservative strategies in late successional stands; and H3—If seed traits organize along acquisitive conservative axis, dispersal syndromes should also shift predictably with succession: anemochory/autochory (typically smaller, lightly provisioned, more permeable seeds) should dominate early succession, whereas zoochory (often larger, nutrient-rich, better-protected seeds) should increase with late succession, enlarging the occupied seed-trait space. .

7.3 Materials and methods

Study area and plot network

We worked in four upper-Andean localities on the eastern flank of the Eastern Colombian Cordillera near Bogotá—Torca (Bogotá D.C.), Tabio, Guasca, and Guatavita (Figure 7.1). Elevations range from 2,600 to 3,200 m, and the climate is bimodal, with wet seasons in April–June and September–November. Mean annual precipitation ranges from 600 to 1,200 mm. These upper Andean tropical mountain forests retain only 20–40 % of their original cover due to a long history of grazing, cropping, mining, and urban expansion (Calbi et al., 2021; Etter & van Wyngaarden, 2000; Hurtado-M et al., 2021; Rubiano et al., 2017).

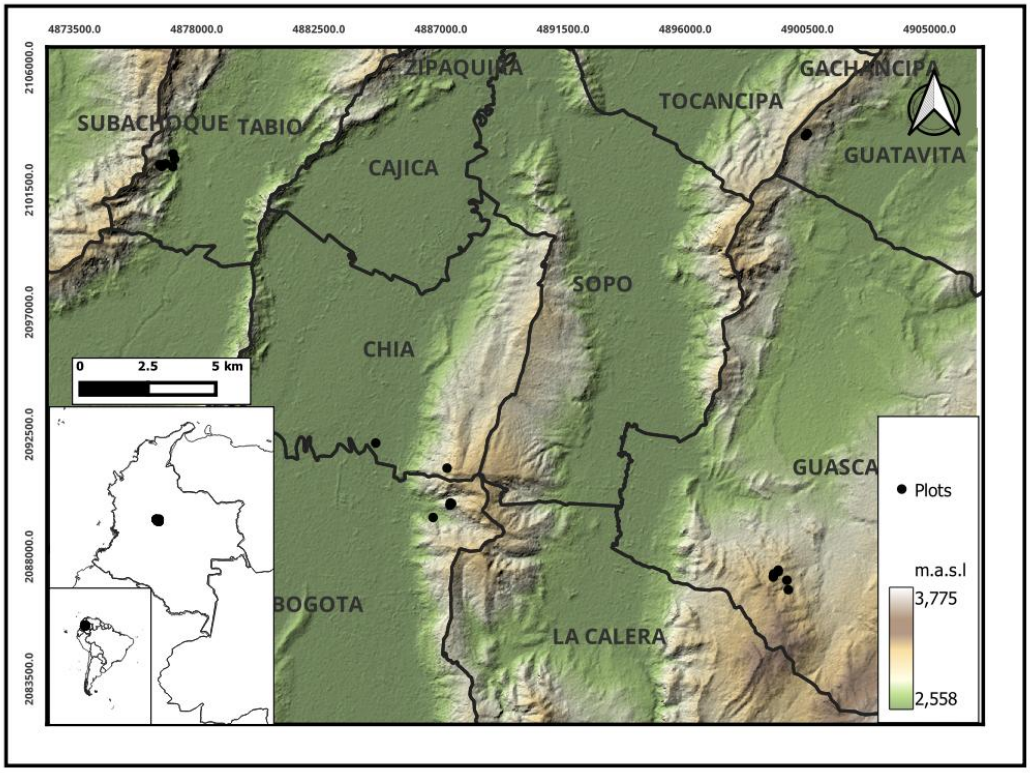

Figure 7.1. Description of the study area. Location map of the 20 permanent plots of the Rastrojos project in the Eastern Andean Cordillera near Bogotá, Colombia.

Our study took place in a network of permanent plots, known as the "Rastrojos" network, where we selected 20 plots (each 20 × 20 m) in early successional (EF) and late successional forest (LF) (Table 7.1). Plots in Torca are in a landscape dominated by secondary forests with some peri-urban areas and a few mature forest remnants; Tabio plots are also in an area covered by early successional forests with few small late successional forest patches; Guasca plots are in the privately protected Encenillo Reserve on former limestone quarries, and the reserve is covered in large areas of early and late forests; and Guatavita plots are found in small early forests surrounded in an agro-pastoral matrix.

Table 7.1. Geographic position, successional stage, and stand structure attributes of the 20 permanent forest plots surveyed in four upper Andean localities (Guatavita, Guasca, Tabio, and Torca).

For each plot we provide: Plot ID, successional category (Early successional forest = mid-regeneration stands ≤ 50 yr; Late successional forest = stands with no significant anthropogenic disturbance for > 60 yr), geographic coordinates (longitude and latitude in degrees, minutes, seconds; WGS-84), elevation (m a.s.l.), canopy openness (%)

derived from hemispherical photographs, leaf-area index (LAI), aboveground biomass expressed as megagrams of carbon per hectare (AGB MgC ha^{-1}), and mean organic-layer thickness (m). These structural variables characterize the vertical complexity and carbon stocks of the forest sites used in subsequent ecological and statistical analyses.

Locality	Plot ID	Succession	Longitude	Latitude	Elevation (m)	Canopy openness (%)	LAI	AGB (MgC ha^{-1})	Organic Layer (m)
Guatavita	1	Early	4° 56' 9,716"	73° 53' 54,237"	3036	17.89	2.52	13.01	0.10
	2	Early	4° 56' 12,618"	73° 53' 51,825"	3028	13.14	2.67	11.26	0.08
Guasca	3	Late	4° 47' 20,318"	73° 54' 31,812"	3140	6.86	3.84	79.23	0.11
	4	Early	4° 47' 28,667"	73° 54' 25,886"	3086	6.21	4.38	33.78	0.02
	5	Late	4° 47' 24,124"	73° 54' 31,332"	3107	9.62	3.17	78.86	0.12
	6	Early	4° 47' 26,609"	73° 54' 25,904"	3095	9.38	3.29	24.51	0.03
	15	Early	4° 47' 16.5"	73° 54' 15.4"	3150	7.80	3.84	49.33	0.02
	16	Late	4° 47' 05,2"	73° 54' 13,8"	3225	8.24	3.51	76.61	0.12
Tabio	7	Early	4° 55' 40,858"	74° 6' 29,194"	2696	5.85	3.39	31.50	0.06
	8	Early	4° 55' 47,149"	74° 6' 31,021"	2708	10.91	2.88	20.20	0.09
	9	Late	4° 55' 33,961"	74° 6' 47,225"	2821	4.02	3.97	58.72	0.18
	10	Late	4° 55' 31,683"	74° 6' 31,579"	2685	7.68	3.36	48.81	0.13

Locality	Plot ID	Succession	Longitude	Latitude	Elevation (m)	Canopy openness (%)	LAI	AGB (MgC ha^{-1})	Organic Layer (m)
	19	Late	4° 55' 31.79"	74° 06'44.42"	2800	5.85	3.67	43.42	0.15
	20	Early	4° 55' 35.03"	74° 06'40.15"	2821	8.38	3.14	38.40	0.08
Torca	11	Late	4° 48' 48,674"	74° 0' 58,527"	2946	7.36	3.08	87.02	0.45
	12	Late	4° 48' 47,937"	74° 0' 56,997"	2966	11.42	2.71	65.37	0.22
	13	Early	4° 48' 31,216"	74° 1' 19,178"	2709	8.82	3.19	33.63	0.11
	14	Late	4° 48' 45,912"	74° 0' 58,852"	2954	7.89	3.16	81.02	0.11
	17	Late	4° 49' 30,41"	74° 01' 02,49"	3046	8.87	2.98	45.64	0.33
	18	Early	4° 50' 00,4"	74° 01'08,8"	2783	8.87	3.19	66.44	0.11

Forest structure and successional context

In every plot, we determined the successional status using four pre-existing data related to forest structure and edaphic conditions: above-ground biomass (AGB), canopy openness (CO), leaf-area index (LAI), and soil organic-layer thickness (OLT) (Castillo-Figueroa et al., 2023; Raj et al., 2021; Rozendaal et al., 2021; Souza et al., 2019). We estimated above-ground biomass (AGB; Mg C ha^{-1}) using stem diameters (DBH) and standard allometric equations for Andean forests (Pérez & Díaz, 2010; Sierra et al., 2007), and expressed them as carbon stocks, assuming a 50% carbon content. Canopy openness (CO, %) and LAI (LAI, m^2 leaf m^{-2} ground) were derived from nine hemispherical photographs per plot and analyzed with Gap Light Analyzer 2.0, which computes gap fraction and effective LAI from image-based light transmittance. The

organic-layer thickness (OLT, m) was measured as the depth of the O horizon (litter + humus) to the mineral soil in a pit at the outside edge of plots (Table 7.1).

Seed and vegetative trait sampling

We collected seed and phenological data in these 20 plots through monthly observations over at least one annual cycle. We determined peak flowering and fruiting for each species as the date when the highest proportion of individuals were in flower or fruit (Chapter six of this document; Morellato et al., 2013). Because these peak dates span the calendar year, we converted each date into an angle θ on a 0–360° scale and then projected it onto the unit circle by computing x = cos (θ) and y = sin (θ) (García et al., 2016). This sine, cosine transformation resolves the artificial gap between 359° and 1° by mapping temporally adjacent dates to neighboring points in Cartesian space. In the resulting two-dimensional coordinates, standard Euclidean-based methods, such as principal components analysis, factorial analysis of mixed data, and distance-based clustering, can treat flowering-time data in the same manner as any other quantitative trait (Pei & Yeh, 2001; Sherlock & Kakad, 2001). By retaining both sine and cosine, we preserve the unique identity of each peak date and ensure that calculated distances reflect true phenological proximity (Pei & Yeh, 2001).

Guided by these phenological records, we selected five individuals per species and collected at least 100 mature seeds per species in crown areas exposed to full sunlight (Cornelissen et al., 2003; Perez-Harguindeguy et al., 2013). After air-drying the seeds in the laboratory, we stored them in paper bags under complete darkness for subsequent analyses (Shipley et al., 2006). To determine seed mass, we oven-dried the seeds at 80 °C until they reached a constant weight (Perez-Harguindeguy et al., 2013). For seeds weighing <0.001 g, we used the average mass of 100 seeds. We classified dispersal syndromes based on field observations and regional literature (Maecha Vega et al., 2012). Seed coat permeability was evaluated by immersing batches of 10 seeds (up to 10 replicates per species) in water for 72 hours. After soaking, seeds were drained on a 100-µm mesh, gently shaken five times to shed free water, and then rolled once between two layers of lint-free tissue for 30 s (no compressive pressure) to achieve a surface-dry condition. Percent permeability was calculated as:

$$\%\ Permeability = \frac{Weight_2 - Weight_1}{Weight_1} x\ 100$$

where $Weight_1$ is the initial dry mass, and $Weight_2$ is the mass after imbibition. The permeability trait value for each species was taken as the mean percentage permeability across all replicates (Wu & Shen, 2021). We measured the respiration of imbibed seeds after 72 hours (SR, μmol CO_2 $Kg^{-1}s^{-1}$) using a LI-6800 Portable Photosynthesis System (LI-COR, Lincoln, NE, USA), as described by Patanè et al., (2006). We then determined seed nitrogen (N) and carbon (C) content by oven-drying the seeds at 80 °C until a constant weight was achieved. Seeds were finely ground and analyzed in a Thermo Flash 1112 Elemental Analyzer (Thermo Fisher Scientific, Waltham, MA, USA) (Bu et al., 2018; Soriano et al., 2011).

Leaf and stem traits were obtained from the central database of the Rastrojos project, where traits were measured between 2016 and 2019 on fully expanded sun leaves from at least three individuals per species, following standard procedures (Perez-Harguindeguy et al., 2013). The traits measured were Specific leaf area (SLA, g m^{-2}), leaf dry matter content (LDMC, g g^{-1}), and maximum photosynthetic capacity (Amax, μmol CO^2 g^{-1} s^{-1}) using a Li-Cor 6400XT Photosynthesis System (LI-COR). Maximum plant height (Hmax, m) was the highest reported height value from either field surveys in the plots, herbarium vouchers, or literature. Lastly, we collect sapwood cores at a height of 1.30 m on trees and shrubs using a 5 mm increment borer. If a shrub had no clear stem at that height, we sampled down to 1.10 m but never lower (Castillo-Figueroa et al., 2023). We took cores from an average of five individuals per species. We measured each core's fresh volume by water displacement and then oven-dried it at 105 °C for 72 hours to determine the dry mass (Chave et al., 2006). We calculated wood density (WD, g cm^{-3}) by dividing the dry mass by the fresh volume.

Trait space data set

For our trait-space analyses, we assembled three complementary data sets. (i) Seed matrix: eighteen woody species were scored for nine regeneration traits—seed mass (SM), nitrogen (SN %), carbon (SC %) concentration, coat permeability (SP %), mass-specific respiration rate (SR), dispersal mode (anemochory, autochory, zoochory), and the sine and cosine of peak flowering and fruiting dates. Table 7.2, by design, lists all taxa with any seed-trait information (n = 63), showing NA where a trait was not measured; only the 18 species with full coverage entered the seed-matrix ordinations (Table 7.2). (ii) Whole-plant matrix: forty-one species were described by the seven most diagnostic seed traits plus five vegetative attributes—specific leaf area (SLA), leaf dry-matter content (LDMC), wood density (WD), maximum photosynthetic rate (Amax), and maximum height (Hmax, m). (iii) Successional matrix: the same 13 traits were extended to all 64 species recorded in 20 plots (Table 10.5); five continuous traits (WD, Amax, SM, SN, SC) were gap-

filled with the *missForest* random-forest algorithm, flowering and fruiting angles were decomposed into sine and cosine components (zero where events were absent), and unobserved dispersal modes were coded as "unknown". Post-imputation checks yielded a gap-free 64 × 13 matrix in which median absolute changes in community-weighted means were 0 % (maximum = 4.3 %; Table 10.6) and functional-diversity indices shifted by ≤ 2.6 % (Table 10.7), confirming negligible bias; only functional richness dropped sharply, as expected from convex-hull sensitivity. All quantitative traits were centered and scaled to unit variance before ordination, while dispersal mode remained a categorical factor. Within the seed matrix, we assessed pairwise Spearman rank correlations among traits and phenological variables and evaluated their significance with permutation-based p-values ($\alpha = 0.05$; Legendre & Legendre, 2012a).

Table 7.2. Functional seed traits for woody species of the Upper Andean Mountain Forest community.

For each species (name, code, family), we report the mean (μ) and standard deviation (SD) for seed mass (SM, g), seed nitrogen content (SN, %), seed carbon content (SC, %), C: N ratio (C: N), and dispersal mode (DM). Flowering and fruiting peak angles (°) indicate the average timing of reproductive events on a circular (0–360°) scale, and DM specifies the primary mechanism of seed dispersal. Values recorded as NA indicate that trait data for the corresponding species were unavailable.

Specie	Code	Family	Seed Mass (g)		Seed Nitrogen (%)		Seed Carbon (%)		Seed C: N Ratio		DM	Flower peak angle (°)	Fruit peak angle (°)	Seed Coat Permeability (%)		Seed Respiration (µmol CO2/Kg/s)	
			µ	SD	µ	SD	µ	SD	µ	SD				µ	SD	µ	SD
Abatia parviflora	Abapar	Salicaceae	NA	NA	NA	NA	NA	NA	NA	NA	Anemochory	180.00	75.00	NA	NA	NA	NA
Ageratina asclepiadea	Ageasc	Asteraceae	0.01	0.00	NA	NA	NA	NA	NA	NA	Anemochory	240.00	240.00	NA	NA	NA	NA
Ageratina fastigiata	Agefas	Asteraceae	0.01	NA	2.26	0.26	23.62	0.82	10.56	1.34	Anemochory	140.00	90.00	NA	NA	NA	NA
Ageratina glyptophlebia	Agegly	Asteraceae	0.05	0.00	2.40	0.51	23.31	1.71	10.08	2.44	Anemochory	130.00	75.00	NA	NA	NA	NA
Aiouea dubia	Aiodub	Lauraceae	1.25	0.23	2.12	0.08	56.43	1.70	26.65	1.45	Zoochory	300.00	NA	NA	NA	NA	NA
Alnus acuminata	Alnacu	Betulaceae	0.00	0.00	2.64	1.45	54.52	6.76	27.63	15.27	Anemochory	270.00	330.00	129.64	50.25	- 348.28	0.98
Baccharis macrantha	Bacmac	Asteraceae	0.02	0.01	3.01	0.57	49.77	6.75	16.73	1.29	Anemochory	90.00	90.00	NA	NA	NA	NA
Barnadesia spinosa	Barspi	Asteraceae	NA	NA	NA	NA	NA	NA	NA	NA	Anemochory	15.00	NA	NA	NA	NA	NA
Bejaria resinosa	Bejres	Ericaceae	0.01	0.01	4.46	4.05	50.65	9.33	16.78	8.44	Anemochory	360.00	285.00	NA	NA	NA	NA
Bucquetia glutinosa	Bucglu	Melastomataceae	NA	NA	NA	NA	NA	NA	NA	NA	Autochory	105.00	360.00	NA	NA	NA	NA

Specie	Code	Family	Seed Mass (g)		Seed Nitrogen (%)		Seed Carbon (%)		Seed C: N Ratio		DM	Flower peak angle (°)	Fruit peak angle (°)	Seed Coat Permeability (%)		Seed Respiration (µmol CO2/Kg/s)	
			µ	SD	µ	SD	µ	SD	µ	SD				µ	SD	µ	SD
Cavendishia bracteata	Cavbra	Ericaceae	0.01	0.00	3.20	2.12	51.48	3.72	21.19	11.29	Zoochory	60.00	300.00	45.52	47.43	NA	NA
Cavendishia nitida	Cavnit	Ericaceae	0.01	0.00	20.80	9.21	53.42	6.82	3.60	3.24	Zoochory	210.00	240.00	13.27	12.76	NA	NA
Cedrela montana	Cedmon	Meliaceae	0.02	0.01	6.93	0.53	50.69	2.30	7.35	0.61	Anemochory	60.00	292.50	288.06	41.72	-13.07	1.83
Citharexylum sulcatum	Citsul	Verbenaceae	0.08	0.01	1.50	0.96	53.32	2.52	52.21	32.04	Zoochory	210.00	300.00	NA	NA	NA	NA
Clethra fimbriata	Clefim	Clethraceae	0.01	0.01	4.49	0.10	56.25	3.19	12.51	0.44	Anemochory	120.00	300.00	NA	NA	NA	NA
Clethra mexicana	Clelan	Clethraceae	0.00	0.00	NA	NA	NA	NA	NA	NA	Anemochory	255.00	105.00	211.12	177.22	NA	NA
Clusia multiflora	Clumul	Clusiaceae	0.00	0.00	4.24	0.57	50.76	7.90	11.96	0.73	Zoochory	150.00	105.00	6.76	2.49	NA	NA
Critoniopsis bogotana	Cribog	Asteraceae	0.03	0.02	1.85	0.11	47.95	2.87	26.11	3.00	Anemochory	75.00	270.00	NA	NA	NA	NA
Croton bogotanus	Crobog	Euphorbiaceae	0.03	0.02	2.40	1.04	53.14	6.82	25.96	10.36	Zoochory	210.00	45.00	147.77	38.71	-1.71	0.19
Cybianthus iteoides	Cybite	Primulaceae	NA	NA	NA	NA	NA	NA	NA	NA	Zoochory	90.00	NA	NA	NA	NA	NA

Specie	Code	Family	Seed Mass (g)		Seed Nitrogen (%)		Seed Carbon (%)		Seed C: N Ratio		DM	Flower peak angle (°)	Fruit peak angle (°)	Seed Coat Permeability (%)		Seed Respiration (µmol CO2/Kg/s)	
			µ	SD	µ	SD	µ	SD	µ	SD				µ	SD	µ	SD
Daphnopsis caracasana	Dapcar	Thymelaeaceae	0.35	0.67	2.62	0.55	47.23	1.63	18.60	3.32	Zoochory	45.00	165.00	24.35	13.54	-2.68	0.42
Linochilus rosmarinifolius	Linros	Asteraceae	0.03	0.01	4.25	1.13	46.87	11.37	11.08	0.57	Anemochory	15.00	75.00	NA	NA	NA	NA
Drimys granadensis	Drigra	Winteraceae	NA	NA	NA	NA	NA	NA	NA	NA	Zoochory	255.00	270.00	62.66	9.88	NA	NA
Duranta mutisii	Durmut	Verbenaceae	0.14	0.02	NA	NA	NA	NA	NA	NA	Zoochory	NA	NA	NA	NA	NA	NA
Escallonia resinosa	Escdis	Escalloniaceae	NA	NA	NA	NA	NA	NA	NA	NA	Autochory	292.50	45.00	NA	NA	NA	NA
Gaiadendron punctatum	Gaipun	Loranthaceae	0.03	0.01	2.04	0.21	59.72	1.46	29.56	3.29	Zoochory	90.00	270.00	61.76	6.06	NA	NA
Hedyosmum sp1	Hedsp1	Chloranthaceae	NA	NA	NA	NA	NA	NA	NA	NA	Zoochory	NA	NA	NA	NA	NA	NA
Hesperomeles goudotiana	Hesgou	Rosaceae	0.01	0.00	0.34	0.24	22.99	0.73	97.28	49.37	Zoochory	30.00	195.00	44.19	27.98	-1.35	0.07
Ilex kunthiana	Ilekun	Aquifoliaceae	0.00	0.00	1.77	0.51	35.63	11.96	21.42	8.55	Zoochory	210.00	180.00	106.95	35.09	-229.40	82.78
Lippia hirsuta	Liphir	Verbenaceae	NA	NA	NA	NA	NA	NA	NA	NA	Anemochory	195.00	NA	NA	NA	NA	NA

Specie	Code	Family	Seed Mass (g)		Seed Nitrogen (%)		Seed Carbon (%)		Seed C: N Ratio		DM	Flower peak angle (°)	Fruit peak angle (°)	Seed Coat Permeability (%)		Seed Respiration (µmol CO2/Kg/s)	
			µ	SD	µ	SD	µ	SD	µ	SD				µ	SD	µ	SD
Macrocarpaea glabra	Macgla	Gentianaceae	0.00	0.00	17.88	13.09	55.52	3.72	5.37	3.82	Autochory	195.00	130.00	NA	NA	NA	NA
Macleania rupestris	Macrup	Ericaceae	0.02	0.01	6.61	1.00	56.85	3.90	8.71	0.84	Zoochory	222.86	90.00	58.15	80.09	-16.66	13.94
Maytenus laxiflora	Maylax	Celastraceae	0.01	0.00	NA	NA	NA	NA	NA	NA	Autochory	150.00	NA	94.29	8.68	-4.58	0.10
Miconia elaeoides	Micela	Melastomataceae	NA	NA	NA	NA	NA	NA	NA	NA	Anemochory	NA	NA	NA	NA	NA	NA
Miconia ligustrina	Miclig	Melastomataceae	0.00	0.00	2.91	0.64	55.99	6.91	19.66	3.65	Zoochory	150.00	195.00	NA	NA	NA	NA
Miconia squamulosa	Micsqu	Melastomataceae	0.00	0.01	1.69	0.42	50.24	4.84	31.54	9.80	Zoochory	150.00	90.00	50.73	13.87	-19.73	17.35
Morella parvifolia	Morpar	Myricaceae	0.02	0.01	1.84	1.33	54.46	2.38	46.57	29.69	Anemochory	150.00	210.00	NA	NA	NA	NA
Morella pubescens	Morpub	Myricaceae	0.02	0.01	1.63	0.51	58.55	6.59	39.86	16.32	Zoochory	180.00	255.00	NA	NA	NA	NA
Myrsine coriacea	Myrcor	Primulaceae	NA	NA	NA	NA	NA	NA	NA	NA	Zoochory	75.00	300.00	NA	NA	NA	NA
Myrsine dependens	Myrdep	Primulaceae	0.01	0.00	1.65	0.26	59.18	1.97	36.58	6.45	Zoochory	60.00	270.00	NA	NA	NA	NA

Specie	Code	Family	Seed Mass (g)		Seed Nitrogen (%)		Seed Carbon (%)		Seed C: N Ratio		DM	Flower peak angle (°)	Fruit peak angle (°)	Seed Coat Permeability (%)		Seed Respiration (µmol CO2/Kg/s)	
			µ	SD	µ	SD	µ	SD	µ	SD				µ	SD	µ	SD
Myrsine latifolia	Myrlat	Primulaceae	0.03	0.01	1.13	0.40	61.54	5.44	60.10	20.11	Zoochory	210.00	90.00	41.93	8.06	NA	NA
Myrcianthes leucoxyla	Myrleu	Myrtaceae	0.02	0.01	1.17	0.40	48.54	1.05	46.00	16.06	Zoochory	120.00	135.00	58.90	43.76	-121.59	0.57
Ocotea calophylla	Ococal	Lauraceae	NA	NA	NA	NA	NA	NA	NA	NA	Zoochory	NA	NA	NA	NA	NA	NA
Oreopanax bogotensis	Orebog	Araliaceae	NA	NA	NA	NA	NA	NA	NA	NA	Zoochory	NA	NA	NA	NA	NA	NA
Oreopanax incisus	Oreinc	Araliaceae	0.01	0.00	5.63	-	60.90	6.02	10.82	1.07	Zoochory	270.00	195.00	126.27	6.45	-72.14	0.26
Palicourea angustifolia	Palang	Rubiaceae	0.01	0.00	2.34	0.62	56.49	2.94	28.44	18.40	Zoochory	45.00	292.50	43.59	7.96	-3.53	0.84
Palicourea demissa	Paldem	Rubiaceae	0.03	0.02	1.70	0.49	53.96	1.48	34.29	11.06	Zoochory	360.00	90.00	NA	NA	NA	NA
Palicourea paniculata	Pallin	Rubiaceae	0.01	0.00	3.20	0.26	56.42	1.77	17.70	1.30	Zoochory	30.00	60.00	51.98	3.48	NA	NA
Piper bogotense	Pipbog	Piperaceae	0.00	0.00	3.29	0.17	49.24	3.05	14.97	0.68	Zoochory	90.00	255.00	26.41	7.55	-3.57	2.62
Prunus buxifolia	Prubux	Rosaceae	0.09	0.11	3.48	0.53	51.97	4.01	15.20	2.42	Zoochory	30.00	240.00	18.30	NA	NA	NA

Specie	Code	Family	Seed Mass (g)		Seed Nitrogen (%)		Seed Carbon (%)		Seed C: N Ratio		DM	Flower peak angle (°)	Fruit peak angle (°)	Seed Coat Permeability (%)		Seed Respiration (µmol CO2/Kg/s)	
			µ	SD	µ	SD	µ	SD	µ	SD				µ	SD	µ	SD
Palicourea boqueronensis	Psyboq	Rubiaceae	0.01	0.00	1.87	0.13	25.12	0.56	13.47	0.90	Zoochory	255.00	195.00	27.85	39.39	NA	NA
Frangula goudotiana	Fragou	Rhamnaceae	0.01	0.00	3.44	1.50	53.21	6.37	21.07	16.86	Zoochory	270.00	180.00	143.79	119.75	-35.87	37.28
Frangula sphaerosperma	Frasph	Rhamnaceae	0.02	0.01	2.69	0.34	55.51	3.74	20.85	2.52	Zoochory	150.00	360.00	121.41	66.21	-26.01	0.16
Solanum cornifolium	Solcor	Solanaceae	0.00	0.00	6.41	0.35	56.92	3.37	8.88	0.29	Autochory	60.00	230.00	75.35	26.05	-18.88	18.34
Symplocos theiformis	Symthe	Symplocaceae	0.04	0.04	0.61	0.29	52.04	1.56	99.64	35.09	Zoochory	90.00	60.00	NA	NA	NA	NA
Ulex europaeus	Uleeur	Fabaceae	0.01	0.00	6.64	0.87	53.18	2.39	8.12	0.96	Autochory	60.00	150.00	36.78	30.22	-72.15	0.22
Vallea stipularis	Valsti	Elaeocarpaceae	0.00	0.00	NA	NA	NA	NA	NA	NA	Autochory	90.00	292.50	NA	NA	NA	NA
Varronia cylindrostachya	Varcyl	Boraginaceae	NA	NA	NA	NA	NA	NA	NA	NA	Zoochory	90.00	255.00	NA	NA	NA	NA
Vasconcellea pubescens	Vaspub	Caricaceae	0.03	0.00	8.00	0.43	62.84	4.89	7.85	0.35	Zoochory	330.00	NA	NA	NA	NA	NA
Verbesina arborea	Verarb	Asteraceae	NA	NA	NA	NA	NA	NA	NA	NA	Anemochory	330.00	120.00	NA	NA	NA	NA

Specie	Code	Family	Seed Mass (g)		Seed Nitrogen (%)		Seed Carbon (%)		Seed C: N Ratio		DM	Flower peak angle (°)	Fruit peak angle (°)	Seed Coat Permeability (%)		Seed Respiration (µmol CO2/Kg/s)	
			µ	SD	µ	SD	µ	SD	µ	SD				µ	SD	µ	SD
Viburnum triphyllum	Vibtri	Adoxaceae	0.04	0.01	1.99	0.21	54.03	2.44	27.57	4.27	Zoochory	90.00	225.00	28.92	12.42	-4.77	0.19
Weinmannia tomentosa	Weitom	Cunoniaceae	0.01	0.01	2.34	0.75	24.79	2.12	11.56	3.77	Autochory	240.00	255.00	NA	NA	NA	NA
Xylosma spiculifera	Xylspi	Salicaceae	0.01	0.00	4.33	0.41	63.73	1.52	14.82	1.38	Zoochory	150.00	210.00	50.06	3.93	-6.16	0.05

Environmental monitoring

Plant-available nutrients and near-surface soil conditions were obtained from the Rastrojos' project database. These included exchangeable inorganic nutrients in soil solution, which approximated nutrient supply to roots. Anion and cation PRS® probes (Western AG, Canada) were installed at four points per plot (n=14 plots) for a 30-day adsorption period. Each probe was inserted vertically to a depth of 10 cm during the November 2016 rainy season. At every sampling point, four anion and four cation probes were installed. Pooled eluates from the eight probes produced one composite sample, yielding sixteen samples per plot and four replicates. At Western AG Laboratories, phosphorus (P) and aluminum (Al) were measured colorimetrically using inductively coupled plasma spectrometry (https://www.westernag.ca/). We used available P as an indicator of fertility, whereas Al reflects acidity-related toxicity that can inhibit root elongation and nutrient uptake. Bulk density (g cm^{-3}) was measured in five random cores per plot at two depths (0–15 cm and 15–30 cm); these variable captures compaction and porosity, which regulate aeration, infiltration, and root penetration. TMS-4 multiparameter sensors (TOMST, Czech Republic) were used to measure surface soil temperature and volumetric soil water content (VWC; $m^3\ m^{-3}$). Sensors were positioned vertically to a depth of 14 cm in each plot, corresponding to the rooting zone most relevant to seedlings; recordings were done every 15 min for four months. Thus, VWC and temperature track water and thermal stress that affect flowering, fruit filling, germination cues, and seedling establishment. We filled in the gaps using data from the nearest locality.

Seed-trait space ordination

We computed Gower distances to visualize overall species dissimilarity and conducted a Principal Coordinates Analysis (PCoA). We used Factor Analysis of Mixed Data (FAMD; Lê et al., 2008) to integrate those continuous traits with dispersal mode (anemochory, autochory, zoochory) as a categorical variable, ensuring each data block contributed equally to the ordination. We retained axes whose eigenvalues exceeded the broken-stick threshold. Finally, we tested whether the dispersal mode structured trait space by performing a permutational multivariate analysis of variance (MANOVA, 999 permutations; Anderson & Walsh, 2013) and confirmed that any significant group differences reflected shifts in centroid rather than dispersion using a *betadisper* homogeneity test.

We assessed the contribution of each seed trait to community dissimilarity by correlating its Euclidean distance matrix with the overall Gower dissimilarity matrix using Spearman's rank correlation.

We then selected the five traits with the highest correlations for a distance-based redundancy analysis (dbRDA) implemented via the *capscale* function in vegan (Legendre & Legendre, 2012b). We evaluated the complete dbRDA model with 999 permutations and tested each predictor using permutation-based ANOVA, reporting F-statistics and p-values adjusted by the Benjamini–Hochberg method.

RLQ ordination

We used RLQ to test whether environmental gradients (R) are associated with species traits (Q) through the observed species composition (L). Practically, we first ordinated R (sites × environment) and Q (species × traits) with Hill–Smith PCA to handle mixed variable types, and L (sites × species) with correspondence analysis to obtain site/species weights. RLQ then finds the linear combinations of environmental variables and traits that maximize their covariance when linked by L; the resulting axes summarize the dominant environment–trait co-structure mediated by composition. We evaluated the global association and the significance of the first two RLQ axes with 999 permutations that break the R–Q link while preserving the structure of L (row/column permutations sensu Dray et al., 2014). Loadings on each axis identify the environmental variables and traits driving the association. For interpretation, we show a triplot plus separate R–L, R–Q, and L–Q overlays (Dolédec et al., 1996; R Core Team, 2024; Dray et al., 2014).

Community-weighted means and functional diversity

We used the FD package (R 4.4.3) to compute, for each plot, (a) community-weighted means (CWMs), which weights each trait by species abundance, and (b) five complementary functional diversity (FD) indices that describe different aspects of how traits are distributed within communities: FRic (functional richness; convex-hull volume = breadth of occupied trait space), FEve (functional evenness; regularity of spacing along the minimum spanning tree), FDiv (functional divergence; relative prominence of extreme trait values), FDis (functional dispersion; mean distance to the multivariate centroid), and Rao's Q (expected pairwise trait distance between two individuals). Circular CWMs for flowering and fruiting peaks were computed as abundance-weighted circular means (unit-vector averaging of angles) and reported as the month of peak activity. We use CWMs to describe shifts across succession, and FD indices to quantify changes in trait breadth, spacing, and spread that can indicate filtering, niche differentiation, or packing. Cautionary note on CWM-based models: Community-weighted means are intrinsic community-level variables derived from the same species composition matrix and thus may not be

statistically independent across plots. This lack of independence can lead to biased effect sizes and inflated Type I error rates when CWM–environment relationships are tested with standard parametric models (Peres-neto et al., 2017; Zelený, 2018). In our study, we therefore treat CWM–environment regressions primarily as descriptive summaries of trait shifts along structural and edaphic gradients, and we interpret their P-values cautiously. Our main inferential framework for trait–environment relationships is the RLQ/fourth-corner analysis, which uses permutation schemes specifically designed for the R–L–Q table structure and avoids the inflated Type I error rates reported for simple CWM regressions (Peres-neto et al., 2017). The CWM models are used to visualize and summarize these multivariate trait–environment patterns at the plot scale.

Generalized linear models

We modeled each response (FRic, FEve, FDiv, FDis, RaoQ, and nine CWMs) against nine predictors (aboveground biomass (AGB, MgC ha^{-1}), canopy openness (CO %), Leaf area index (LAI), organic-layer thickness (OLT, m), mean soil surface temperature (Ts, °C), soil volumetric moisture (VWC m^3 m^{-3}), bulk density (BD, cm^3 g^{-1}), Aluminum (Al, µg cm^{-2} d^{-1}) and Phosphorus (P, µg cm^{-2} d^{-1})) using Gaussian GLMs. Full models were evaluated using *MuMIn* (Bartoń, 2010); we averaged coefficients when two or more candidate models fell within $\Delta AIC < 2$. Diagnostics included residual plots, Q–Q plots, and checks of predictors versus fitted values. Significant relationships ($P < 0.05$) and individual predictor–response plots were summarized. This multi-layered methodology links environmental variables, forest structure, species composition, and a complete suite of regeneration and vegetative traits, providing a robust platform to test how functional strategies shift during succession in upper Andean Mountain Forests. Diagnostic checks confirmed homoscedastic, approximately normal residuals and no influential observations. To visualize raw relationships, we plotted each response against each retained predictor in the best GLM and fitted an ordinary least-squares line. These scatterplots are purely descriptive and were not used for hypothesis testing; statistical inference is based on the multivariate GLMs described above.

7.4 Results

Functional seed space

Spearman correlations among nine seed traits for 18 woody species (Table 7.3) revealed consistent sets of relationships. Larger seeds had higher respiration rates (SM g vs. SR µmol CO_2 kg^{-1} s^{-1}, $\rho = 0.55$, $p <$

0.01) and reached their flowering peaks later in the year (SM g vs. Flco, $\rho = 0.39$, $p < 0.05$). Seeds with high carbon content were positively correlated with seed nitrogen content (SC% vs. SN%, $\rho = 0.56$, $p < 0.01$), suggesting a link between energy storage or structure and protein content. Seed permeability decreased as respiration increased (SP% vs. SR µmol CO_2 kg^{-1} s^{-1}, $\rho = –0.40$, $p < 0.01$) and as flowering peaks shifted later in the year (SP% vs. Flco, $\rho = –0.38$, $p < 0.01$). Flowering sine correlated negatively with permeability (Flsin vs. SP%, $\rho = –0.57$, $p < 0.001$) and positively with Flco ($\rho = 0.40$, $p < 0.05$); the fruiting sine opposed both flowering coordinates (Frsin vs. Flco, $\rho = –0.46$, $p < 0.01$; Frsin vs. Flsin, $\rho = –0.35$, $p < 0.05$). No other pairwise correlations were significant.

Table 7.3. Seed-trait correlations of 18 woody species.

Values are Spearman's rank correlation coefficients (ρ) calculated for nine seed functional traits: seed mass (SM gr), seed nitrogen content (SN%), seed carbon content (SC%), seed permeability (SP%), seed respiration (SR µmol CO2 Kg-1 s-1), Flower cosine (Flco), Flower sine (Flsin), Fruit cosine (Frco), and Fruit sine (Frsi). Asterisks denote the level of statistical significance after Bonferroni adjustment: * P < 0.05; ** P < 0.01; *** P < 0.001. Coefficients on the main diagonal equal 1 (trait compared with itself).

Trait	SM g	SN %	SC %	SP %	SR µmol CO_2/ kg/s	Flco	Flsin	Frco	Frsin
SM g	1								
SN %	–0.02	1							
SC %	–0.04	0.56**	1						
SP %	–0.11	0.23	0.19	1					
SR µmol CO_2 /kg/s	0.55**	–0.15	–0.13	–0.40**	1				
Flco	0.14	0.07	–0.22	–0.38**	0.39*	1			
Flsin	0.23	–0.06	–0.25*	–0.57***	0.29	0.40*	1		
Frco	0.13	0.09	0.26	0.25	0.1	–0.22	0.09	1	

Trait	SM g	SN %	SC %	SP %	SR µmol CO_2/ kg/s	Flco	Flsin	Frco	Frsin
Frsin	0.21	–0.21	–0.23	0.08	–0.24	–0.46**	–0.35*	–0.14	1

Using a Gower distance matrix, we derived two principal coordinate axes that explained 67.4% of the trait variation (PCoA1 = 34.5%, PCoA2 = 32.9%; Figure 7.2). Animal-dispersed species were broadly distributed, although more on the negative side of axis one and at the positive end of axis 2. Anemochories and autochorous species were uncommon and grouped on the positive end of axis one and the positive side of axis 2 for autochory, and the negative side of axis 2 for anemochory (Figure 7.2; Figure 10.3). A *Permanova* analysis on the 41 species and 12 traits distance matrix confirmed that the centroids of the three dispersal guilds differ significantly, with dispersal mode accounting for 26 % of total multivariate trait variation; F= 6.75 R^2, p <0.001: Table 10.8). A companion *Permdisp* test showed no difference in within-group dispersion (F = 2.54, p = 0.09; Table 10.8), indicating that these differences arise from shifts in group centroids rather than unequal spread.

Seed-only ordination FMAD (Figure 10.4; Table 10.9) highlighted five variables that dominated trait space. Seed-coat permeability (SP%) led the field, accounting for 23.5% of dimension one and influencing later axes. Dispersal mode (DM) was observed in 22.1% of cases, underscoring its role as a primary organizer of seed traits. Phenology entered through the cosine of the fruit angle (Frco), accounting for 14.9 % of dimension one and 23.3 % of dimension four. Flowering sine (Flsin) and seed respiration (SR µmol CO2 Kg-1 s-1) completed the set, adding 10.5 % and 10.2 %, respectively.

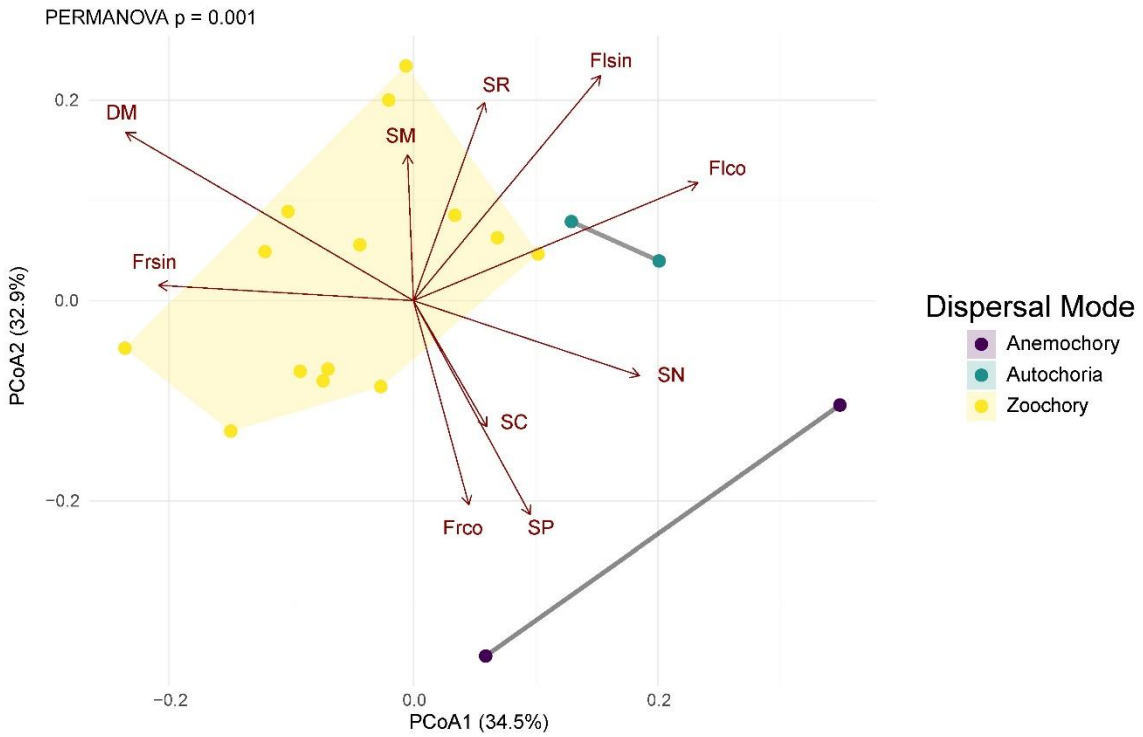

Figure 7.2. Principal coordinates analysis (PCoA) of seed-trait composition for 18 woody species.

The ordination is based on a Gower distance matrix and displays the first two axes, which account for 67.4% of the total variation (PCoA 1 = 34.5%, PCoA 2 = 32.9%). Circles mark species and are colored by their primary dispersal mode: anemochory (violet; wind), autochory (blue; self-dispersal), and zoochory (yellow; animals). Arrows represent trait vectors; arrow length indicates the strength of each trait's correlation with the ordination axes. Trait abbreviations are as follows: SM = seed mass (g), SN = seed nitrogen content (%), SC = seed carbon content (%), SP = seed-coat permeability (%), SR = seed respiration rate (µmol CO2 Kg-1s-1), DM = dispersal mode, Flco/Flsin = cosine and sine of peak flowering date, and Frco/Frsin = cosine and sine of peak fruit-ripening date. A PERMANOVA on the 41 species and 12 traits distance matrix detected significant differences in multivariate seed-trait composition among dispersal modes (p = 0.001).

Multivariate coupling among environment, species composition, and seed, leaf, and wood traits

We found relationships between environmental variables, species composition, and thirteen functional traits (global Model 4: P = 0.001; 999 permutations; Table 10.10). The first axis accounted for 58.0% of

the shared structure, and the second axis contributed 20.4%, resulting in a bivariate ordination that summarized 78.4% of the total covariance. Environmental and trait ordinations displayed similar dispersions (Table 10.10), and their scores correlated tightly along Axis 1 (r = 0.77).

The ordination distinguished three largely independent sets of environmental conditions (Figure 7.3A). First, above-ground forest biomass and soil chemistry varied in parallel but independently: plots with higher canopy opening frequently—but not invariably—coincided with higher concentrations of exchangeable aluminum. These early successional forests harbored species that invest in dense wood (high WD and high LDMC). Second, a moisture–structure cluster was associated with high volumetric soil-water content, elevated bulk density, and a high leaf area index. The tight alignment of these variables indicates that they vary together. Leaf traits with the strongest projections—maximum photosynthetic assimilation rate (Amax) and specific leaf area (SLA)- pointed in the same direction. Third, organic-layer thickness (OLT) lay almost perpendicular to canopy openness, LAI, VWC, and BD, suggesting that OLT varied independently from these variables. Importantly, these environmental contrasts align with the trait gradient: along axis 1, seed mass covaried positively with conservative leaf/wood traits (LDMC, WD) and negatively with acquisitive leaf traits (SLA, Amax). In line with this trait–environment gradient, late-successional plots with higher aboveground biomass and closed canopies tended to host heavier-seeded species with conservative leaf and stem traits, whereas lighter-seeded species with more acquisitive traits dominated open, early-successional plots with lower biomass. At the late-successional, high-biomass end of this gradient, tall zoochorous trees bearing heavy, nutrient-rich seeds were common, whereas early-successional plots with thin organic soil layers, cooler soils, and low aboveground biomass were dominated by short, early-flowering, wind-dispersed shrubs.

.

A group characterized by large aboveground biomass, warmer soils, and deep organic horizons is defined as a late-successional forest. Tall, zoochorous trees bearing heavy, nutrient-rich seeds clustered here, whereas plots with a thin organic soil layer, cooler soils, and low above-ground biomass supported short, early-flowering shrubs that rely on wind dispersal.

Plot scores underscored successional dynamics (Figure 7.3B). Early successional forests were grouped where canopy openness and aluminum levels were highest, whereas late successional stands

clustered in the quadrant defined by high biomass, thick organic layers, moist soils, and a high leaf area index. The OLT/ABG/Ts grouping remained decoupled from the moisture–LAI complex.

Species positions mirrored these environmental trends (Figure 7.3C). Early successional forests with elevated aluminum levels favored species such as *Xylosma spiculifera* and *Myrsine latifolia*. Zoochorous species (*Drimys granadensis*, *Oreopanax incisus*) occupied the late successional forest sector of the ordination, contrasting with anemochory shrubs (*Ageratina glyptophlebia*, *Bucquetia glutinosa*) that populated the early successional end. Intermediate taxa such as *Clethra fimbriata* and *Miconia ligustrina* filled the center, illustrating continuous functional turnover.

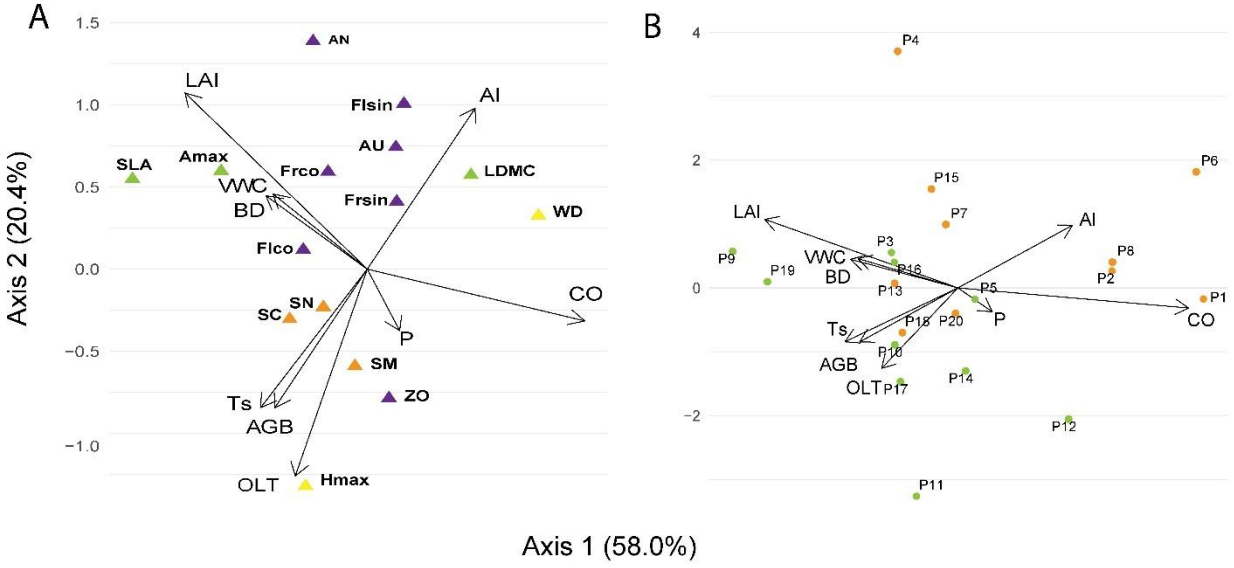

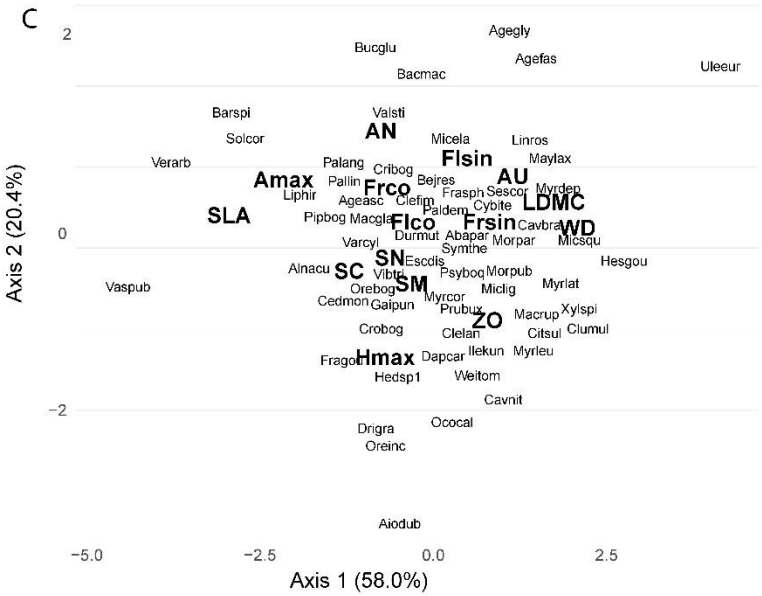

Figure 7.3. RLQ ordinations linking environment (R), species composition (L), and functional traits (Q) in upper-Andean Forest plots. (A) R–Q biplot.

Fig 7.3 A Environmental variables (black labels) and trait centroids (purple triangles, area reproductive traits; orange triangles are seed resource traits; green triangles are leaf traits; and yellow triangles are wood and high plant traits) are plotted in space defined by Axis 1 (58.0%) and Axis 2 (20.4%). (Fig 7.3 B) R–L ordination. The plots are displayed in environmental space, with vectors pointing toward increasing values of each environmental variable. Points mark plots and are colored by successional stage (orange = early, green = late). (Fig 7.3 C) L–Q ordination. Species are represented by three-letter genus–species codes (see Table 10.2) in the same trait space. Environmental variables: P = Phosphorus, µg cm^{-2} d^{-1}; Al = exchangeable Aluminum, µg cm^{-2} d^{-}; BD = bulk density, g cm-3; Ts = soil temperature °C; VWC = volumetric water content%; CO = canopy openness, %; LAI = leaf area index; AGB = aboveground biomass, MgC ha-1; OLT = organic-layer thickness, m. Traits: SC = seed carbon content %; SN = seed nitrogen content, %; SM = seed mass, g; LDMC = leaf dry matter content, g g-1; SLA = specific leaf area cm2 g-1, Amax = maximum photosynthetic capacity, nmol g-1 s-1; WD = wood density g cm-3; AN = anemochory; AU = autochory; ZO = zoochory; Hmax = maximum height, m; Flsin/Flco = sine/cosine of flowering activity, Frsin/Frco = sine/cosine of fruiting activity. Axes one and two together capture 78.4 % of the total co-structure; higher axes contain the remaining variance.

Links between structural and environmental variables, diversity, and CWMs

We found that structural conditions in successional forests were related to four functional diversity metrics (Table 10.12), whereas functional richness showed no structural signal and was best described by an intercept-only model. We found a positive relationship between biomass and functional divergence (AGB: $\beta = 0.0027 \pm 0.0008$, $P = 0.004$; Figure 7.4A), functional dispersion (FDis: $\beta = 4.66 \times 10^{-4} \pm 1.63 \times 10^{-4}$, $P = 0.010$; Figure 7.4B) and Rao's quadratic entropy ($\beta = 8.69 \times 10^{-5} \pm 2.95 \times 10^{-5}$, $P = 0.009$; Figure 7.4C). In contrast, functional Evenness declined as surface soils got warmed (Ts: $\beta = -0.038 \pm 0.016$, $P = 0.031$; Figure 7.4D~~).~~.

We also found that the community-weighted mean maximum height (CWM-Hmax) increased with aboveground biomass ($\beta = 0.076 \pm 0.016$, $P < 0.001$; Figure 7.5A) and warmer soils ($\beta = 0.797 \pm 0.346$, $P = 0.035$; Figure 7.5B). We observed that community weighed mean specific leaf area (CWM-SLA) increases with bulk density ($\beta = 35.9 \pm 14.8$, $P = 0.015$; Figure 7.5D), and soil temperature ($\beta = 5.32 \pm 2.57$, $P = 0.038$; Figure 7.5E) but declined with exchangeable aluminum ($\beta = -0.319 \pm 0.158$, $P = 0.044$; Figure 7.5D–F). Photosynthetic capacity (CWM-Amax) also increased with bulk density ($\beta = 32.1 \pm 16.2$, $P = 0.048$; Figure 7.5C) and higher Ts ($\beta = 8.09 \pm 3.95$, $p = 0.041$). Taken together, the models for leaf economics indicate that sites with more compact soils—typical of early-successional forests—favor communities dominated by species with acquisitive leaves (high specific leaf area, SLA, and maximum leaf area, Amax). In contrast, aluminum-rich soils shift the community means toward thicker, more conservative foliage (low SLA). Aluminum and bulk density varied to some extent independently across plots. For example, some early-successional plots had high exchangeable Al but relatively low bulk density; in these plots, SLA was lower than expected for early stands, suggesting a shift toward more conservative leaf economics under Al stress. Conversely, in plots with compact soils (high bulk density) but low Al, early-successional stands expressed a more acquisitive syndrome, with higher SLA and Amax.

Regarding seed traits, we observed heavier seeds where soils were warmer (CWM-SM: $\beta = 0.0107 \pm 0.0039$, $P = 0.006$; Figure 7.6) and richer in aluminum ($\beta = 4.59 \times 10^{-4} \pm 2.34 \times 10^{-4}$, $P = 0.050$; Figure 7.6B). Seed nitrogen content declined as bulk density increases (CWM-SN: $\beta = -1.13 \pm 0.53$, $P = 0.033$; Figure 7.6C) but increased with organic layer thickness ($\beta = 2.92 \pm 1.34$, $P = 0.029$; Figure 7.6D). Seed carbon declined with above-ground biomass (CWM-SC: $\beta = -0.153 \pm 0.055$, $P = 0.006$; Figure 7.6E), while and showed an increase with LAI ($\beta = 5.16 \pm 2.39$, $p = 0.046$; Figure 7.6G).

We found that the community-weighted mean (CWM) of the month of flowering shifted later in the calendar as aboveground biomass increased (AGB: $\beta = 1.90 \pm 0.46$ months Mg C ha^{-1}, $P < 0.001$; Figure 7.7A) and earlier as the leaf-area index increases (LAI: $\beta = -65.74 \pm 22.42$ months m^2 m^{-2}, $P = 0.003$; Figure 7.7B). Figure 7.7 illustrates the bivariate association between CWM-Flowering and each structural variable. Because these panels display ordinary least-squares fits to the raw data, the accompanying p-values differ from those reported in the GLM for the partial effects. We also observed four structural and environmental variables related to the mean month of fruit ripening. CWM-fruiting activity advanced in calendar in denser soils (BD: $\beta = 81.7 \pm 37.2$ months g cm^{-3}, $p = 0.043$), was delayed by warmer soils (Ts: $\beta = -42.3 \pm 8.4$ months $°C^{-1}$, $p < 0.001$) and shifted earlier when volumetric water content increases (Vol-moist: $\beta = -317 \pm 118$ months m^3 m^{-3}, $p = 0.007$; Figure 7.7; Table 10.12).

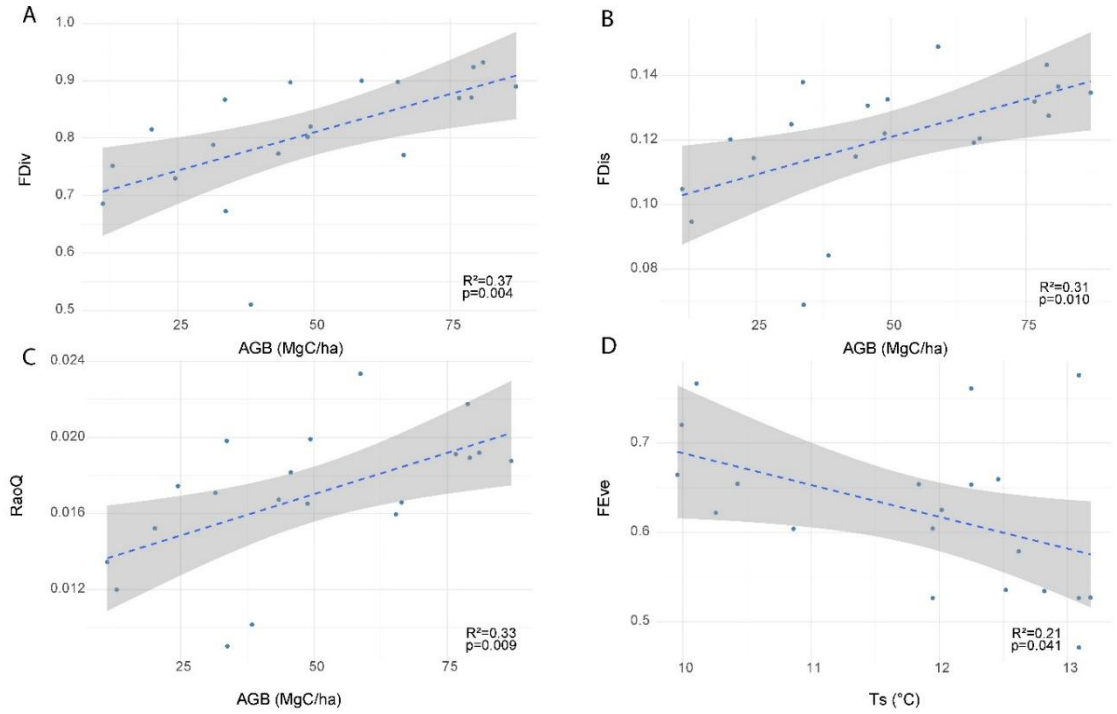

Figure 7.4. Relationships between functional-diversity metrics and key structural and microclimatic predictors derived from generalized linear models (GLMs).

Bivariate relationships between functional diversity index and key structural predictors. Points are plot values; dashed lines are ordinary least-squares fits (95 % CI shaded). Statistics in each panel refer to the simple regression; they therefore differ from the multivariate slopes and *p*-values reported in Table 10.12. The

coefficient of determination (R^2) and model p-values are displayed within each panel. (A) Functional Divergence (FDiv) increases with aboveground biomass (AGB, Mg C ha^{-1}; $\beta = 0.0027 \pm 0.0008$, $R^2 = 0.37$, $P = 0.004$). (B) Functional Dispersion (FDis) increases along the same biomass gradient ($\beta = 4.7 \times 10^{-4} \pm 1.6 \times 10^{-4}$, $R^2 = 0.31$, $P = 0.010$). (C) Rao's quadratic entropy (Rao Q) also scales positively with biomass ($\beta = 8.7 \times 10^{-5} \pm 3.0 \times 10^{-5}$, $R^2 = 0.33$, $P = 0.009$). (D) Functional Evenness (FEve) declines with increasing soil temperature (Ts, °C; $\beta = -0.038 \pm 0.016$, $R^2 = 0.21$, $P = 0.041$).

7.5 Discussion

Our study aimed to test four hypotheses regarding how reproductive and vegetative traits are organized along an acquisitive–conservative spectrum and how this spectrum shifts during succession in upper-Andean montane forests. Using three complementary matrices that together captured 64 species and 13 functional traits, we found one dominant joint axis linking seed and leaf economics (seed mass with specific leaf area and leaf dry matter content), and a second axis capturing a phenological gradient in timing and concentration of flowering and fruiting (encoded by the sine and cosine of peak month and by circular concentration), which covaried with seed-coat permeability. We found clear successional ordering of communities along these axes, monotonic gains in most diverse metrics with stand biomass, and a predictable turnover from anemochory and autochory to zoochory dispersal. Taken together, these patterns are consistent with strong abiotic filtering by soil and canopy conditions, combined with additional biotic structuring related to dispersal and regeneration niches. They provide only partial support for our prediction that functional trait composition would converge within successional stages, while also highlighting the importance of site-specific contingencies.

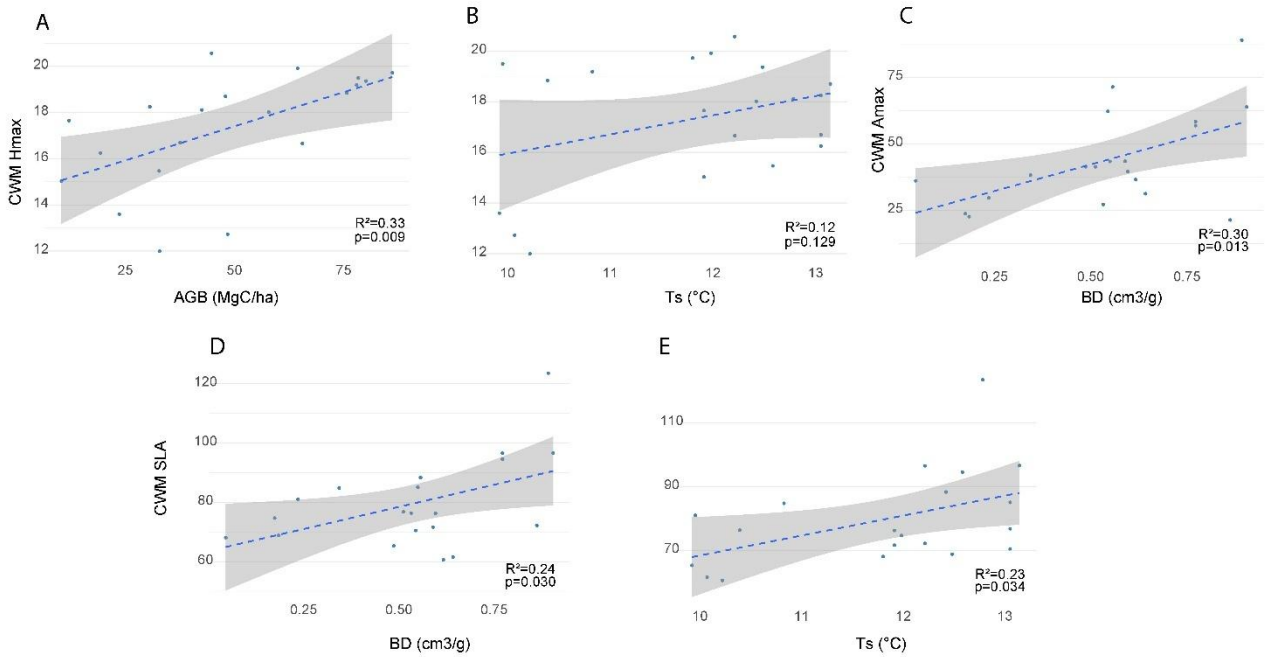

Figure 7.5. Structural and microclimatic drivers of community-weighted vegetative traits revealed by generalized linear models (GLMs).

Bivariate relationships between community-weighted vegetative traits and key structural predictors. Points are plot values; dashed lines are ordinary least-squares fits (95 % CI shaded). Statistics in each panel refer to the simple regression; they therefore differ from the multivariate slopes and *p*-values reported in Table 7.12. The coefficient of determination (R^2) and model P-values are printed within each panel: Upper row – maximum plant height: (A) CWM-Hmax versus aboveground biomass (AGB, Mg C ha^{-1}). (B) CWM-Hmax versus soil temperature (Ts, °C). (C) CWM-Hmax versus leaf area index (LAI). Lower row – specific leaf area: (D) CWM-SLA versus AGB. (E) CWM-SLA versus Ts. (F) CWM-SLA versus soil bulk density (BD, cm^3 g^{-1}).

Our first hypothesis predicted a single “fast–slow” spectrum: small, nutrient-rich seeds with acquisitive leaves (high SLA, high Amax) at one extreme, and large, low-nutrient seeds with conservative foliage at the other. In our early successional, aluminum-rich plots, RLQ Axis 1 (58% of the shared variance) ordered species along a joint seed–leaf gradient in which seed mass covaried with leaf economics: at one end, large-seeded taxa also had acquisitive leaves (high SLA and high Amax); at the other end, small-seeded taxa were associated with more conservative leaves (high LDMC and low SLA).

This pattern was in the opposite direction than proposed in Hypothesis 1, as also reported under intense light or nutrient stress (Barczyk et al., 2024), suggesting that the fast–slow spectrum shifts with local conditions., Heavier-seeded species respired faster ($\rho = 0.55$) and flowered later in the year, suggesting a lack of dormancy and more investment in reserves, both aligned with a more conservative reproductive strategy suited to survive in the shade (Graham et al., 2003; Kitajima, 1994; J. A. Myers & Kitajima, 2007). Nevertheless, these taxes combined acquisitive leaf economics (high SLA, high Amax) with low shade tolerance. High-SLA, high-Amax leaves support rapid growth when light is abundant or fluctuating, but they are generally associated with lower survival in deep shade, consistent with a light-demanding rather than truly shade-tolerant strategy (Poorter, 2009; Poorter & Bongers, 2006). In our data, these heavier-seeded species occurred mainly in forests with high above-ground biomass. By contrast, aluminum-rich, high-light early-successional forests showed conservative leaves and dense wood, consistent with selection for low-turnover tissues that safeguard hydraulic integrity under metal stress (Li et al., 2023; Santiago et al., 2018) and unlike lowland chrono sequences where acquisitive leaves often lead succession (Lohbeck, et al., 2013; Poorter et al., 2019). Agronomic work on Al-tolerant rice, which sequesters aluminum while maintaining photosynthesis (Sousa et al., 2022), offers a parallel mechanism to compare with.

Beyond light and aluminum stress, a second axis captures variation in soil water availability. Species growing in plots with higher volumetric water content have seeds with permeable coats that imbibe rapidly, whereas those in drier plots tolerate impermeable coats that postpone germination until sufficient moisture returns—a response also documented in Mediterranean and subtropical floras (Franks, 2011; Zhou et al., 2023). Our high-elevation evidence therefore shows that soil-moisture shortage, together with light and nutrient stress, reshapes the fast–slow spectrum and further loosens the usual coupling between seed and leaf traits.

Our results contradict the classical successional trajectory predicted by Hypothesis 2 because conservative foliage and lighter seeds dominated early-successional, aluminum-rich, open canopies, whereas more acquisitive leaves and heavier, reserve-rich seeds prevailed in late, shaded stands. This pattern diverges from wet-lowland chrono sequences, in which acquisitive traits dominate early stages and conservative traits emerge later (Lohbeck et al., 2013). By contrast, the prevalence of conservative traits under harsh edaphic conditions aligns with results from dry tropical systems, where intense water stress selects for dense leaves and wood even in young plots (Augusto et al., 2025; Lohbeck, Poorter,

Martínez-Ramos, et al., 2014)...A pantropical synthesis of 1,189 secondary stands likewise shows that functional trajectories can flip depending on local stressors: wood density rises early in wet forests but falls early in dry forests, converging again in late succession (Poorter et al., 2019). Our finding that aluminum, combined with high irradiance, favors conservative foliage extends this context dependence to montane environments.

The mechanistic role of aluminum is well-documented: Al^{3+} disrupts photosynthesis and promotes the formation of tougher, low-turnover tissues that protect hydraulic function (Ofoe et al., 2023). In several early-stage plots with lower soil temperatures and compact soils, the partial mitigation of aluminum stress enabled a few species to maintain healthy foliage, as indicated by high leaf dry-matter content and high wood density.

Finally, in our structurally complex late stands—characterized by low canopy openness, warmer soils, and higher volumetric water content—species produced markedly heavier seeds with higher carbon and nitrogen concentrations and flowered earlier in the year. Litter build-up and microclimatic buffering likely eased aluminum and drought stress, making these capital-intensive regeneration strategies viable (Desie et al., 2020; Zhang et al., 2022). Overall, our evidence suggests that successional trajectories pivot around whichever filter—light, moisture, or edaphic stress—is most restrictive at each stage. Classic fast-to-slow transitions prevail in chemically benign soils, whereas chemically aggressive substrates, such as our aluminum-rich soils, invert this sequence.

Our third hypothesis predicted that trait divergence, dispersion, and Rao's entropy would peak in middle-aged stands. Instead, we saw a different pattern. In the early succession stage, aluminum-rich plots exhibited a narrow range of traits; as biomass increased, divergence, dispersion, and entropy rose almost linearly. Functional evenness, however, fell on warm soils, where only a few heat-tolerant species could persist. A similar steady rise in divergence through succession has been reported in northwestern Costa Rica, where late-stage successions create many regeneration niches (Sanaphre-Villanueva et al., 2016). Andean montane studies also document an early "compression" of trait space under intense heat and metal stress (Homeier et al., 2010).

As biomass increases and shade deepens, leaves grow tougher and stems denser—LDMC and wood density both rise—so vegetative traits cluster around a more conservative profile. In contrast, seed traits enable species to utilize a broader range of seed sizes and dispersal modes to occupy the few

remaining safe sites. Thus, while the canopy locks into a narrow set of slow-growth strategies, the regeneration layer maintains diversity by partitioning establishment niches. Late-successional stands in subtropical chrono sequences exhibit the same pattern of reproductive diversification beneath dense canopies (Becknell & Powers, 2014).

Finally, our fourth hypothesis predicted a shift from anemochory and autochory to zoochory as aboveground biomass increases in late-successional forests. A PERMANOVA of 41 species confirmed that the three guilds occupy distinct regions in trait space, and the ordination showed that anemochory and autochory species are restricted to early successional forests, while zoochory species dominate late successional forests. Similar guild turnover occurs in Amazonian floodplains and other disturbed tropical forests once frugivore communities recover (Terborgh et al., 2017). By contrast, fragmented Atlantic landscapes exhibit weaker shifts because constant wind exposure allows both syndromes to coexist (Freitas et al., 2013).

Microclimate and soil chemistry operate as separate filters. Along with the full gradient, the warmer soils of late-successional forests favor the heaviest seeds. In the early cooler successional forests, however, microsites with the highest aluminum concentrations still select for the heavier seeds within an otherwise light-seeded pool. Thus, temperature drives a broad shift toward large seeds late in succession, whereas aluminum fine-tunes seed-mass differences at the start of succession, a pattern also reported by Rodrigues et al., (2019). Seed nitrogen rose where a thick soil organic layer kept soils loose but fell in compact soils, mirroring trials where nutrient-rich seeds outperform lighter ones on acidic, low-fertility substrates (Walters & Reich, 2000). These chemical advantages help large, animal-dispersed seeds out-compete others as late-successional forests cool and organic layers deepen, reinforcing the guild shift.

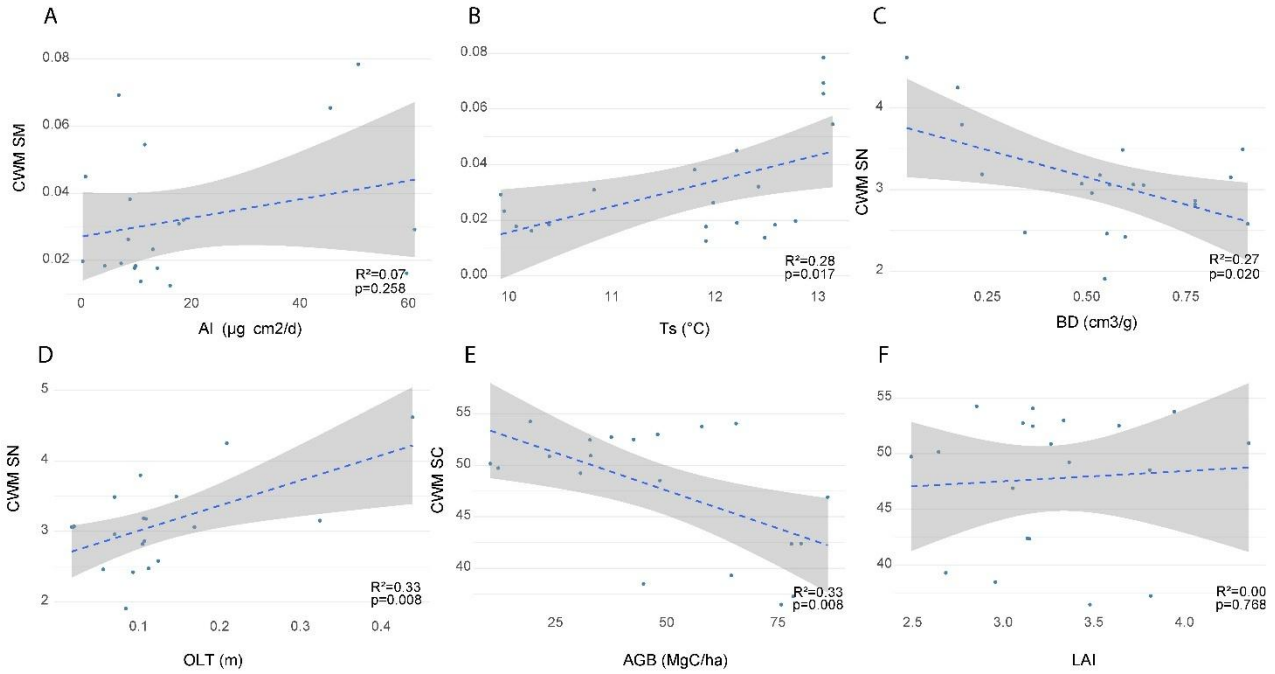

Figure 7.6. Structural and microclimatic predictors of seed-trait community-weighted means (CWMs) identified by generalized linear models (GLMs).

Bivariate relationships between seed-trait community-weighted means and key structural predictors. Points are plot values; dashed lines are ordinary least-squares fits (95 % CI shaded). Statistics in each panel refer to the simple regression; they therefore differ from the multivariate slopes and *p*-values reported in Table 10.12. Each panel reports the marginal R^2 and model P-value. Seed mass (CWM-SM) Warmer soils promote heavier seeds (soil temperature, Ts °C). B Exchangeable Aluminum (Al µg cm^{-2} day^{-1}). Seed nitrogen (CWM-SN) C Higher soil bulk density (BD g cm^{-3}) lowers seed-nitrogen content. Thicker organic layers (OLT m) increase seed nitrogen content. Seed carbon (CWM-SC) E Seed-carbon content declines as aboveground biomass rises (AGB Mg C ha^{-1}). Warmer soils tend to elevate seed carbon content. G Leaf-area index (LAI) shows no detectable influence.

Phenology tracks the same structural cues. Flowering peaks in our plots moved 1.9 months later for each Mg C ha^{-1} added, matching long-term records showing that dense crowns delay flowering under reduced light (Wright & Calderón, 2018b). Fruit ripening advances on warmer, wetter soils, as observed in Madagascar forests, where higher soil moisture accelerates community fruit production (Dunham et al.,

2018). Canopy closure, therefore, delays flowering but advances fruiting when soil water is high, tightening synchrony with the frugivores that now dominate dispersal. Taken together, the observed guild turnover, seed chemistry, and phenological shifts suggest that the patterns we detected are consistent with the predictions of Hypothesis four.

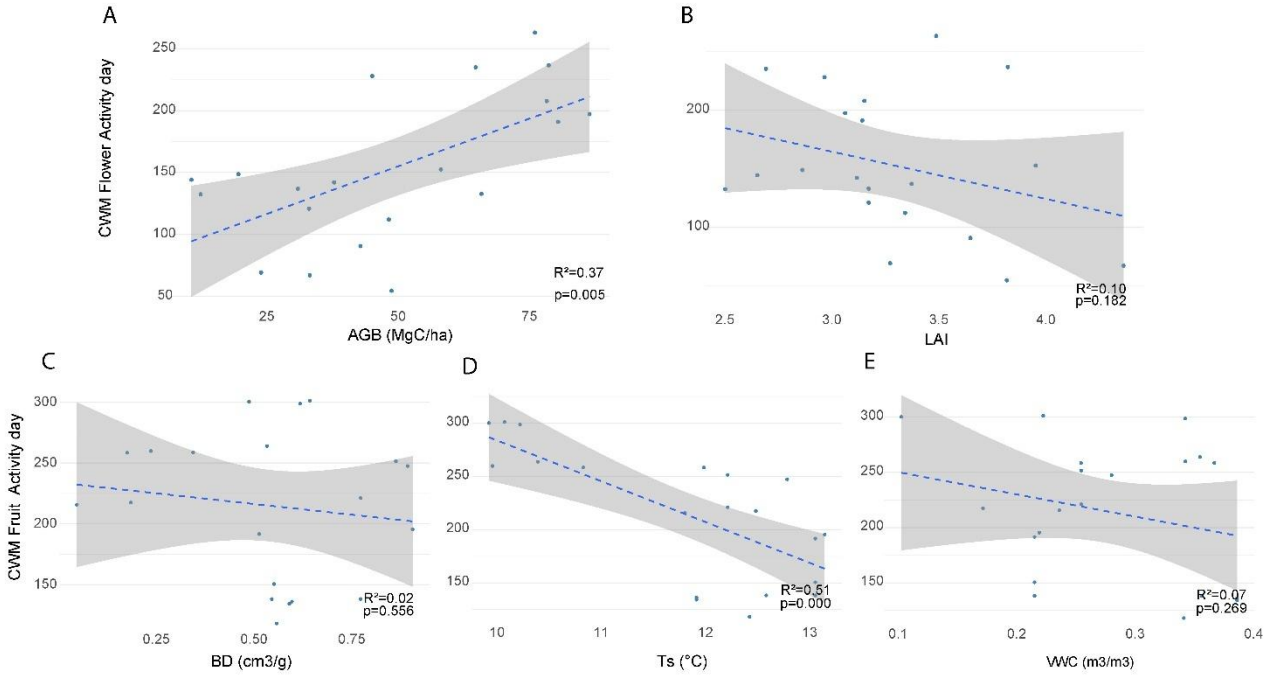

Figure 7.7. Effects of Stand Structure and Microclimate on Community-Level Phenology.

Each panel presents a generalized linear model (GLM) linking the abundance-weighted mean month of peak activity (CWM) to a single environmental predictor. Points represent individual plots; dashed lines show fitted slopes; shaded ribbons give 95 % confidence intervals. We report marginal R^2 and model P-values inside each panel. Flowering activity months: Aboveground biomass (AGB, Mg C ha^{-1}) delays peak flowering. B. Leaf-area index (LAI). Fruiting peaks: C AGB exerts a weak delaying effect. D Higher volumetric water content (VWC, m^3 m^{-3}) advances fruit-ripening activity. E Greater bulk density (BD, g cm^{-3}) postpones ripening. F Warmer surface soils (Ts, °C) advance ripening. Residual diagnostics confirm homoscedasticity, approximately standard errors, and no influential observations (Cook's D < 1, leverage < 0.30).

Our results expand the plant-economics framework by introducing two seed-based axes: (1) seed size and chemistry, and (2) seed phenology and coat permeability. These axes help explain how species cope with poor soils and limited dispersal, linking patterns observed in both lowland and mountain forests. Viewed this way, our data partly support hypothesis one but in the opposite direction, challenge hypothesis two, yet show that high aluminum and strong light flip the expected pattern, do not show the mid-successional diversity peak in hypothesis three, and align with hypothesis four.

These insights suggest a step-by-step restoration plan. First, plant aluminum-tolerant pioneer trees with dense wood and tough leaves to provide quick cover. Later, when the leaf-area index rises above about three, enrich the stand with large-seeded, animal-dispersed species to attract fruit-eating animals and restore functional diversity. Future studies should separate the effects of each factor in combined trait–environment models and run trials that adjust aluminum levels and open the canopy. Such work will improve forecasts of how upper Andean montane forests will respond to climate and land-use change.

7.6 Conclusions

This study demonstrates that seed traits, dispersal guilds, and vegetative strategies shift in tandem with canopy structure, soil aluminum, and microclimate along an upper-Andean successional gradient. Two seed axes—one linking size with chemistry and another linking phenology with coat permeability—account for most trait variation, while a single RLQ plane captures nearly 80 % of the trait–environment relationship. Open, metal-rich soils favor dense leaves and wood, along with small anemochories or autochorous seeds, whereas closed soils with high organic layers favor large zoochorous seeds. As forest stands age, metrics that quantify how different species' traits differ from one another—functional divergence, functional dispersion, and Rao's quadratic entropy—increase steadily, while functional richness, the total range of trait types present, remains constant. This pattern implies that succession does not introduce entirely new ecological strategies but instead pushes existing strategies farther apart: the breadth of trait space expands even though no additional trait categories are added.

These patterns suggest refining the plant-economics framework by showing that aluminum toxicity and strong light act as early filters, while warmer, thicker organic soil layers and recovering frugivore networks shape later communities. The growing similarity between leaves and wood, alongside the widening range of seed traits, highlights the need to consider regeneration traits—not only vegetative ones—when predicting community assembly and forest resilience.

Practical implications follow this view. Early restoration should plant pioneers with dense wood and tough leaves to give quick cover. Once the leaf-area index rises above about three, managers can enrich the canopy with large-seeded zoochorous species to attract frugivores and rebuild functional diversity. Such a phased approach aligns planting choices with the changing ecological filters that operate through succession.

Future work should conduct controlled germination trials growing seeds with contrasting traits in soil spanning a gradient of aluminum concentrations and under different light levels, to test whether the observed field patterns accurately reflect causal responses. Field experiments that adjust understory temperature, canopy openness, and soil aluminum in combination would clarify how these filters interact. Long-term records of frugivore visits, seed rain, and seedling survival could then be used to link disperser activity to trait turnover.

By showing how edaphic stress, light, and dispersal opportunity interact across succession, our study offers both a sharper lens for understanding upper Andean montane forests and concrete guidance for their recovery. Integrating seed and vegetative economics in this way will be crucial for forecasting how these ecosystems respond to climate warming and land-use change, and for ensuring that restoration investments build forests that can endure.

8 Beyond Succession: How Locality-Level Abiotic and Microclimatic Conditions Shape Seed-Bank and Seedling Communities in Upper Andean Mountain Forests

8.1 Abstract

Soil seed banks, seedlings, and adult plant communities assemble in response to multiple environmental filters; yet we lack clarity on whether successional stage or locality heterogeneity plays the dominant role in upper Andean forests. We investigated whether community assembly across different life stages is primarily shaped by forest succession or by fine-scale local variability. We hypothesized that local edaphic and microclimatic heterogeneity offsets the successional effects, because differences in soil moisture, bulk density, and temperature filter propagule germinability and persistence more strongly than changes linked to stand age, thereby producing sharper compositional turnover among localities than along the successional gradient. We surveyed four upper Andean Forest localities across early- and late-successional stands. We collected 10 15 cm-deep soil cores per plot to quantify seed-bank density and composition, and recorded seedlings in 4 subplots per plot. Data for adult trees, soil pH, organic C, bulk density, nutrients, and soil temperature were obtained from the "Rastrojos" project database for the same plots. We analyzed α-diversity metrics, partitioned Bray–Curtis β-diversity, and applied NMDS, Mantel tests, Procrustes tests, dbRDA, and negative binomial GLMs to disentangle the relative contributions of abiotic and microclimatic heterogeneity, as well as the successional stage, to seed bank and seedling community structure across upper Andean Mountain Forest plots. Alpha diversity and seed/seedling densities did not differ by forest successional stage. Instead, locality explained β-variation in seed banks, seedlings, and adults, respectively, with a high turnover. Our results showed that increased soil organic carbon content lowered seed-bank density, whereas elevated soil temperature increased seedling density. These results demonstrate that fine-scale edaphic and microclimatic heterogeneity—not the successional stage—governs the assembly of early-life stages in these upper-Andean forests. We recommend conserving locality-level heterogeneity to enhance regeneration success and maintain biodiversity in tropical montane ecosystems.

Keywords: Andean Mountain Forests; community assembly; edaphic filters; soil seed bank; successional gradient.

8.2 Introduction

Soil seed banks are critical reservoirs of viable propagules that support forest regeneration and ecological succession, allowing for vegetation recovery and biodiversity maintenance over time (Williams-Linera et al., 2016; Yang & Li, 2013; Zhang et al., 2009). In tropical and subtropical forests, these seed banks conserve genetic diversity and contain species from a wide range of successional stages—early, intermediate, and late (Anderson et al., 2012; Anju et al., 2022; Garwood, 1989; Gelviz-Gelvez et al., 2016). The taxonomic makeup of seed banks often diverges from that of the standing vegetation because dispersal, dormancy, and abiotic filters jointly determine which propagules reach, persist, and germinate in the soil, and long-distance or secondary dispersal can introduce seeds of canopy-absent species when landscape connectivity and disperser activity are high (Medeiros-Sarmento et al., 2020; Rungrojtrakool et al., 2021). Successional stage, land-use history, proximity to adult seed sources, and edaphic attributes further modulate which species persist below ground and thus shape post-disturbance recovery trajectories (Williams-Linera et al., 2016).

Studies from tropical and subtropical forest ecosystems have shown that early-successional species typically dominate soil seed banks, while many late-successional species lack persistent seed banks (Baskin & Baskin, 2014; Daïnou et al., 2011; Dalling & Brown, 2009). As a result, mature forests often exhibit significant mismatches between their seed banks and the adult vegetation (Silva et al., 2019). In some ecosystems, such as deciduous lowland tropical forests, herbaceous species can dominate the seed bank (Rico-Gray & García-Franco, 1992). In seasonally moist forests, the soil seed-bank composition more closely mirrors the current seed rain than the stand's successional stage, because seeds from nearby mature trees and mobile dispersers decouple propagule input from forest age (Dalling & Denslow, 1998). The successional stage determines which species fruit within a stand; however, this signal fades when seeds also arrive from neighboring forests, dispersal distances are short, and year-to-year fruit production fluctuates widely. Consequently, recent seed showers can dominate the below-ground pool and obscure patterns that would otherwise track forest age. Despite this decoupling, many studies report clear successional trends in richness, and numerous studies also support the hypothesis that species richness in soil seed banks and seedling communities increases with forest succession. For instance, seed-bank richness in the mid-successional stages of Karst landscapes in China was positively associated with the richness of aboveground vegetation (He et al., 2020). Likewise, research in Tibetan subalpine meadows found that species richness and germinated seed biomass increased significantly as the successional stage

advanced (Ma et al., 2013). In contrast, compositional similarity between seed banks and seedlings tends to decline with succession, reflecting recruitment filtering and shifts in the composition of adult vegetation (Bossuyt & Honnay, 2008). For example, a study in the Loire River (France) floodplain revealed a decline in similarity between seed banks and vegetation along a successional gradient (Greulich et al., 2019).

Across tropical successions, seed and seedling densities often decline as stands mature. This pattern is usually attributed to a combination of factors, including stronger negative density dependence near conspecific adults, reduced seed input per unit area, and shifts in light, litter, and soil conditions that restrict safe sites for recruitment (Paine et al., 2008). In many mature forests, background seedling densities under closed canopies are relatively low, so direct competition among seedlings can be weak (Paine et al., 2008). However, regeneration is highly patchy: canopy gaps, resource-rich microsites, and recent small-scale disturbances can sustain locally high seed and seedling densities within otherwise low-density mature stands. In a Central African rainforest, for instance, Douh et al., (2018) recorded equal seed densities in primary, secondary, and agro-forest plots, showing that fine-scale filters—light, soil moisture, nutrients, and disturbance—can override the effect of forest age. The successional stage is therefore only one axis of community assembly; spatial heterogeneity can be just as influential, or even dominant. Consistent with this view, Legendre et al., (2009) and Yang and Li, (2013) found in a subtropical Chinese forest that "pure" spatial structure (captured by spatial eigenvectors) explained more variation in tree composition than topographic variables such as elevation and slope, implicating dispersal limitation. Taken together with the synthesis by Chase and Myers, (2011), these studies suggest that much of the spatial turnover in tree communities results from stochastic demographic events and dispersal barriers rather than from the environmental gradients typically measured (i.e. succession).

At broader spatial scales, β-diversity—defined as variation in species composition among localities—frequently reflects heterogeneity in abiotic factors and is associated with greater differences in species diversity than those observed during succession. For example, elevation and mean annual precipitation were stronger predictors of beta diversity than forest successional status in a cross-ecosystem comparison (Myers et al., 2013), while analyses of tropical and temperate forests suggest that beta diversity is shaped by differing community-assembly mechanisms, often involving intraspecific aggregation and spatial clustering (Condit et al., 2002). Although forest successional status can explain some differences in species composition (e.g., early vs. late successional communities), its explanatory power is often lower than that of spatial processes (Hu et al., 2022).

Within Colombia's upper Andean mountain forests, spatial heterogeneity—here defined as the joint variation in soil properties, microclimate, and geographic distance—often compensates for successional age in structuring plant communities. Hurtado-M et al., (2021) showed that floristic dissimilarity increased with the distance separating localities. In contrast, early- and late-successional stands within a given locality differed little, suggesting that dispersal limitation, acting across edaphic and microclimatic mosaics, can offset the role of stand age. A parallel pattern emerges for other taxa: Castillo-Avila et al., (2025) found lower similarity in soil-insect assemblages between distant localities than between forests of different successional stages within the same locality, indicating that landscape-scale environmental heterogeneity is the primary driver of β-diversity across multiple groups.

We investigated how the diversity and composition of seed banks, seedlings, and adult plant communities vary with successional stage (early versus late forests) and among four localities—Tabio, Guasca, Torca-Bogotá, and Guatavita—in Colombia's upper-Andean Mountain Forests. We also assessed whether key abiotic factors—soil pH, volumetric moisture, bulk density, nutrient availability, and soil temperature—vary with respect to seed bank and seedling composition. Here, we hypothesized that (H1) species richness in both seed banks and seedlings would increase from early to late succession as seed input increases due to improving edaphic conditions that increased productivity of late forests; (H2) compositional similarity between seed banks and seedlings would decline with succession because recruitment filters and over-story composition shift as stands mature; (H3) seed banks and seedlings average densities would be lower in late-successional stages owing to stronger competition and lower light availability in the understory. Furthermore, (H4) we expected that abiotic heterogeneity among localities, particularly variation in soil moisture, bulk density, and temperature, would explain more variation in community composition than the successional stage itself. In other words, we predicted that these locality-scale environmental filters would generate sharper floristic turnover among localities than along the successional gradient (Table 1).

Table 1. Conceptual predictions for soil seed banks (SSB), seedlings (SDL), and adult trees (ADL) across four response variables—density, α-diversity (richness, evenness, Simpson), β-diversity, and composition—under two scenarios: successional stage (EF vs. LF) and local heterogeneity (among-site variation in soils, microclimate, and spatial context).

Life stage	Response variable	Successional stage (prediction)	Local heterogeneity (prediction)
Seed Bank	Density	Often lower in the late successional stage (LF) than in the early successional stage (EF).	Varies among sites; gaps and rich microsites can sustain high densities even in LF.
	α-diversity (richness, evenness, Simpson)	Often higher in LF; early banks are pioneer-biased.	Strong site effects: the stage signal can be weak or inconsistent.
	β-diversity	Early- vs late-successional stands within a site differed in composition, but species turnover among sites was larger, consistent with strong edaphic and microclimatic control of seed-bank composition.	Among-locality turnover is usually larger (edaphic and microclimatic variation).
	Composition	SSB may partly track stage; late-successional species are often scarce; mismatch with adults is common in LF.	Recent seed rain and dispersal shape composition; site effects can dominate.
Seedling	Density	Decreased from EF to LF.	Highly patchy; microsites can maintain high densities across stages.
	α-diversity (richness,	Often increases from EF to LF.	Varies by site, depending on soil moisture, bulk density, and temperature.

	evenness, Simpson)		
	β-diversity	The stage can structure turnover along the EF→LF axis.	Among-site differences usually exceed EF–LF differences.
	Composition	Similarity between SSB and SDL tends to decline with succession. More similar composition in EF than in LF	Microhabitat and dispersal shape composition; site effects are often stronger than stage.
Adult	Density	-	Between-site differences may persist, especially in EF; LF tends to be uniformly low.
	α-diversity (richness, evenness, Simpson)	May be stable or slightly higher in LF.	Expected to vary by site (soils, microclimate).
	β-diversity	Stage may explain some turnover (early vs. late stands).	Among-site heterogeneity typically predominates.
	Composition	-	-

8.3 Methods

Study Area

Our study was conducted at four localities in the Eastern Cordillera near Bogotá, Colombia: Torca (Tc, Bogotá), Tabio (Tb), Guasca (Gsc), and Guatavita (Gvt), which have elevations ranging from 2,600 to 3,200 meters above sea level. The region exhibits a bimodal rainfall regime, with wet seasons from April to June and September to November, and annual precipitation ranging from 600 to 1,200 mm. We studied upper Andean tropical mountain forests at different successional statuses, including early successional forests (EF) and late successional forests (LF; Hurtado-M et al., 2021; Figure 4.1).

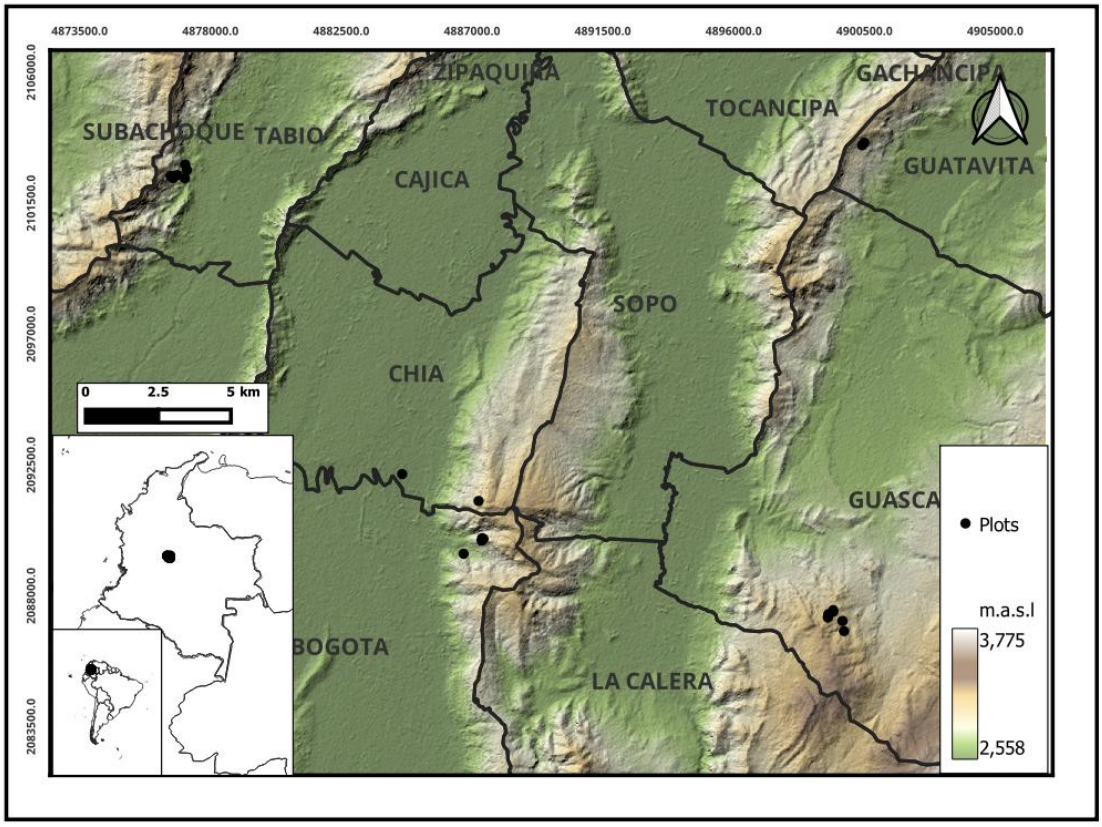

Figure 8.1. Location of the study localities and the 20 permanent plots of the Rastrojos project in the Eastern Andean Cordillera near Bogotá, Colombia.

Torca is part of the "Reserva Forestal Protectora del Río Bogotá" and the "Área de Reserva Forestal Regional de Bogotá"; the locality is primarily covered in early successional forests, with a few remnants of late successional forests and some suburban developments. Tabio is dominated by early successional forests that have regenerated following the abandonment of agro-pastoral systems. This locality has a few patches of late-successional forest and small grasslands used for cattle grazing and dairy production. Guasca is situated within the Encenillo Biological Reserve, a private conservation area formerly used for limestone mining, which features a combination of early- and late-successional forests. Guatavita is primarily a silvo-agro-pastoral landscape, characterized by patches of early successional forests, surrounded by plantations of exotic trees, grasslands for cattle, and areas of agricultural production. Our study was conducted in 20 × 20 m permanent plots, including three EF and three LF plots in each of the localities Torca, Tabio, and Guasca, and two EF plots in Guatavita, for a total of 11 EF and 9 LF plots. Each plot contained four 2 × 2 m subplots for seedling surveys (Hurtado-M et al., 2021; Table 7.13).

Soil Seed Bank Sampling and Germination

In December 2021, at the end of the rainy season, we collected ten soil cores per plot. Cores were randomly sampled due to high intra-plot heterogeneity in seed distribution (de Melo et al., 2006). Each soil core (internal diameter = 5.73 cm, depth = 15 cm, volume ≈ 387 cm^3) was transported intact to the greenhouse, where roots, litter, and tubers were carefully removed before further processing. Each soil sample was spread in individual trays (≤5 cm depth) over a substrate of 20% peat, 50% black soil, and 30% rice husk. Soil moisture was maintained at a high level using a drip irrigation system that watered the trays for 30 seconds twice daily.

We employed the seedling emergence method to detect viable seeds (Heerdt et al., 1996). Seedlings were identified as morphospecies once they produced at least two true leaves. Germination was measured every two weeks in all 200 samples and continued until each sample showed no new seedlings for two consecutive monitoring visits. Seed density was expressed as the number of individuals per square meter.

Seedling Survey

Within each 2 × 2 m subplot (n = 80), we enumerated every woody individual that stood ≥ 5 cm but < 1 m tall and had a stem diameter < 1 cm, thereby restricting the survey to true seedlings and excluding

saplings or adults. Species were identified with local field guides and taxonomic keys (Maecha Vega et al., 2012) and verified by expert botanists. Seedling density was derived from this single field census: we counted all seedlings in each 4 m² subplot and expressed abundance as individuals per m².

Adult Tree and Shrub Survey

In 2013, the Rastrojos project began establishing plots and censusing adult trees and shrubs with a basal diameter of 5 cm or greater. In this study, we used a census done in the 20 20x20 m area between 2020 and 2022. All individuals were identified to the species level, yielding 72 species. Density per plot was expressed as individuals per square meter.

Environmental Variables

To characterize soil properties, we collected ten soil cores per plot (n = 200). We measured pH using a 1:10 soil-to-water ratio (4 g of soil in 40 mL of deionized water) at 20 °C (Oksanen et al., 2020). Nutrients in the soil water solution (P, Al) were assessed by the Rastrojos project using cation and anion Plant Root Simulator (PRS) probes. Other data we used from the Rastrojos project include soil bulk density (0-30 cm), carbon percentage, and nitrogen percentage, which were measured using an elemental analyzer. Additionally, we recorded soil temperature at depths of 6 and 12 cm over a four-month period using TMS-4 dataloggers (TOMST, Czech Republic, EU), measuring it every 15 minutes. We imputed missing values using the means from plots within the same locality and successional stage (early- or late successional), ensuring that substitutions were based on ecologically comparable conditions.

Alpha Diversity Analyses

We calculated alpha diversity metrics—species richness, Shannon index, Simpson index, and Pielou's evenness—using the vegan package's diversity and *spec number* functions (Oksanen et al., 2020). Kruskal–Wallis and Dunn's tests assessed differences among forest successional status, localities, and their interactions (Dinno, 2015; Lantz, 2013).

Community Composition and Environmental Relationships

To compare species composition in SSB, SDL, and ADL, we generated Bray–Curtis dissimilarity matrices (Ricotta & Podani, 2017) using the *vegdist* package (Oksanen et al., 2020) and evaluated correlations across stages with Mantel tests (M. Anderson & Walsh, 2013; Spearman, 999 permutations). We used

Procrustes analysis and the protest function to test for structural congruence among NMDS ordinations (Smith, 2017; *metaMDS*) of the three life stages. We employed distance-based redundancy analysis (dbRDA; McArdle & Anderson, 2001) with the cascade function to investigate the impact of environmental predictors on the composition of SSB and SDL. Predictors were standardized, and significant variables ($p < 0.05$) were retained following permutation tests (ANOVA, 999 permutations). We applied PERMANOVA (M. Anderson & Walsh, 2013; *adonis2*) and dispersion tests (M. Anderson, 2006; *betadisper*) to assess group differences and compositional variability across forest status and localities. We decomposed Sørensen β-diversity into its two additive components—species turnover (Simpson dissimilarity, *β_SIM)* and nestedness (*β_SNE*)—and then used each metric to compare community differentiation among successional stages.

We identified the most parsimonious abiotic drivers of soil-seed bank (SSB) and seedling (SDL) composition by coupling ordination-based screening with information-theoretic model selection. Each community matrix (SSB, SDL) was first ordinated with three-dimensional NMDS (Bray–Curtis distance), and all numeric environmental variables were fitted as vectors onto the ordination with 999 permutations; only vectors with marginal significance ($p \leq 0.06$) were kept, resulting in three predictors for SSB (soil organic carbon, soil temperature, pH) and three for SDL (bulk density, temperature, canopy cover). These candidates were centered, scaled, and tested for collinearity (pairwise $|r| < 0.7$; VIF < 3), then entered into distance-based redundancy analyses, for which global, term-wise, and axis-wise significance was confirmed by 999-permutation ANOVA.

Density Analyses

We calculated density as the number of individuals per square meter for seeds (SSB per core), seedlings (SDL per subplot), and adults (ADL per plot). We used Kruskal-Wallis tests to assess differences across forest successional status and locality (Lantz, 2013), followed by Dunn's post hoc tests with a Bonferroni correction where appropriate (Dinno, 2015) for their interactions. Cross-stage comparisons used average plot-level densities. All analyses were conducted in R 4.4.3 (R Core Team, 2024).

Generalized Linear Modeling and Model Selection

We used generalized linear models (GLMs; Neuhaus & McCulloch, 2011) to assess the effects of environmental variables on SSB and SDL abundance. We computed three complementary response

variables. Total abundance measures absolute propagule pressure at the plot scale; mean abundance per sampling unit reflects local intensity independent of plot size; and density enables cross-study comparisons. Although densities are linearly related when every plot has the same number and area of samples, minor losses of cores/subplots and the different statistical properties of counts versus averages justify modelling all three. We retained density for cross-plot comparisons and chose the distribution (Gaussian vs. negative binomial) that best fitted the residual structure of each metric (Komori et al., 2016). Candidate predictors were first screened using an NMDS + *envfit* procedure; only vectors that were significant ($p < 0.05$) and explained at least 15% of the ordination variance were retained. These results yielded three variables for the seed bank (soil organic carbon [C], soil temperature at a 6 cm depth [Ts], and pH) and three for seedlings (bulk density [BD], Ts, and canopy cover). Variance-inflation factors confirmed that collinearity was negligible for SDL (VIF ≈ 1.0–1.1) and moderate but acceptable for SSB (VIF = 2.0–8.0, tolerance > 0.12). All predictors were z-standardized (mean = 0, SD = 1) before entering the generalized linear models. Placing variables on this standard, dimensionless scale allows for direct comparison of effect sizes and prevents those with large numeric ranges, such as soil organic carbon percentage, from disproportionately influencing the model estimates. Gaussian models were fitted using *glm*, while negative binomial models were fitted with *glm.nb* from the MASS package (Ripley et al., 2025). We compared model performance using AIC and pseudo-R^2 metrics from the performance package (Nakagawa & Schielzeth, 2013). We selected the most parsimonious models using the dredge function from *MuMIn* and extracted the coefficients. All models and outputs were generated in R 4.4.3 and exported for reproducibility (R Core Team, 2024).

Sampling balance and inference scope

The final dataset comprised 11 early-successional (EF) and nine late-successional (LF) plots; Guatavita contributed 2 EF plots and none LF. To minimize confounding between successional stage and locality and to limit bias from the uneven design, we: (i) modeled/ tested stage while controlling for locality (two-factor designs throughout); (ii) for multivariate analyses (PERMANOVA/dbRDA), constrained permutations within locality and inspected multivariate dispersion with *betadisper* before interpreting location or succession effects; (iii) for univariate responses (densities, α-diversity), used rank-based tests (Kruskal–Wallis with Dunn–Bonferroni) that are robust to unequal group sizes; (iv) avoided interpreting stage × locality interactions where cells were empty, and, when an analysis required both stages within each locality, restricted inference to Torca, Tabio, and Guasca, treating Guatavita as EF-only context.

8.4 Results

Alpha Diversity Patterns Across Forest Successional Status and Localities

Taxonomic richness was high across the upper Andean plots in both life-history stages. The seed bank contained 105 morphospecies, of which 79 were assigned to species or infraspecific ranks, and 26 could only be resolved to genus level. The seedling layer harbored 92 morphospecies; 54 were identified as species and seven as genera, with the remainder retained as morphospecies owing to limited diagnostic material. We recorded 72 adult-tree species, all identified to species level, spanning 38 families and 57 genera.

No significant differences in alpha diversity were observed between EF and LF for any life stage (Figure 8.2**Error! Reference source not found.**A-D; Table 10.17). For adult communities, richness ($p = 0.446$), Shannon ($p = 0.650$), Simpson ($p = 0.762$), and evenness ($p = 0.939$) were not significantly different from one another. Similarly, seedling and seed bank communities showed no significant differences in forest successional status (all $p > 0.1$). However, locality-level comparisons revealed significant variation in seedling ($p = 0.006$) and seed bank ($p = 0.049$) richness, though other indices remained consistent (Figure 8.2).

Beta Diversity Across Forest Successional Status and Localities

Permanova indicated that species composition did not differ significantly between forest successional status for any life stage (Table 10.18). In contrast, locality effects were significant: seed bank ($R^2 = 0.222$, $F = 1.52$, $p = 0.006$; Table 10.18), seedlings ($R^2 = 0.35$, $F = 2.88$, $p = 0.001$; Table 10.18), and adults ($R^2 = 0.41$, $F = 3.71$, $p = 0.001$; Table 10.18).

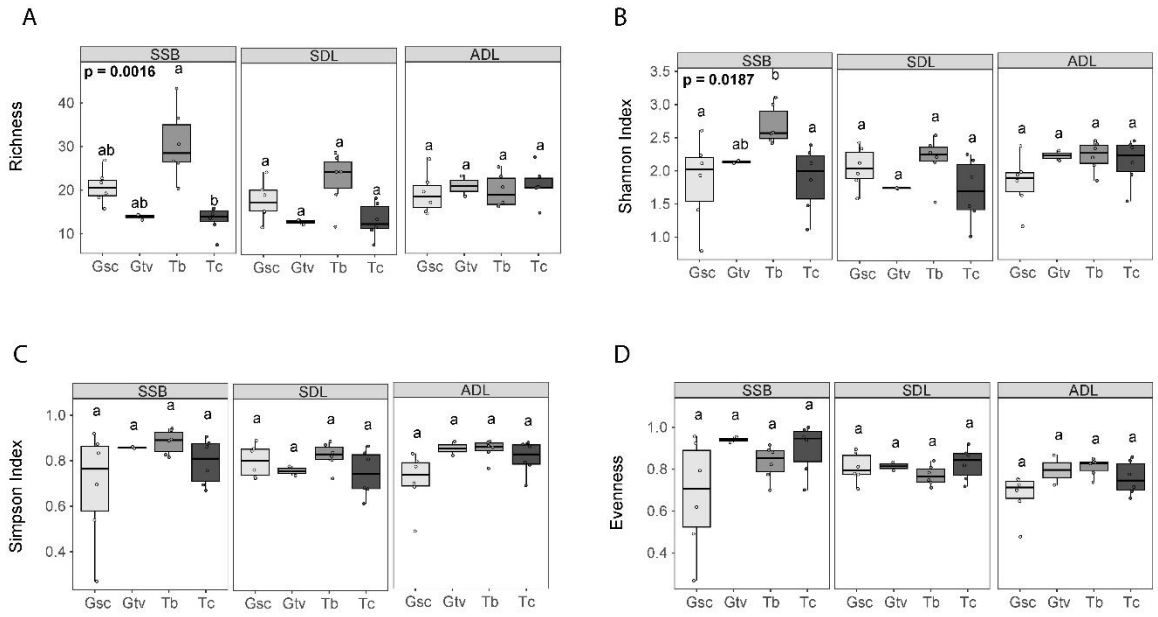

Figure 8.2. Alpha diversity indices (species richness, Shannon, Simpson, and Evenness) between forest types (early vs. late successional forest) and plant community stages (adults, seedlings, and seed bank).

Boxplots represent the distribution of diverse values for each index. Letters above the boxes indicate pairwise comparisons; identical letters denote non-significant differences ($p > 0.05$). None of the diversity indices showed significant variation between forest types for any life stage, suggesting structural similarity in alpha diversity across successional stages.

Sørensen dissimilarity indices indicated high beta diversity: seeds = 0.92, seedlings = 0.92, adults = 0.89. Turnover was the dominant component (~87%), while nestedness contributed minimally (<5%), indicating that species replacement, not richness differences, drove compositional variation (Table 10.18).

Density Patterns Across Life Stages and Forest Successional Status

Soil Seed Bank (SSB) density did not differ between forest succession status ($\chi^2 = 0.20$, $p = 0.653$; Table 10.14; Figure 8.3A) but varied significantly among localities ($\chi^2 = 48.5$, $p < 0.001$; Figure 8.3B), with Tabio showing the highest values. Interaction effects between forest succession status and localities were also

significant ($\chi^2 = 68.7$, $p < 0.001$), with EF plots in Guasca having significantly higher seed densities than LF plots in the same locality (Figure 8.3B).

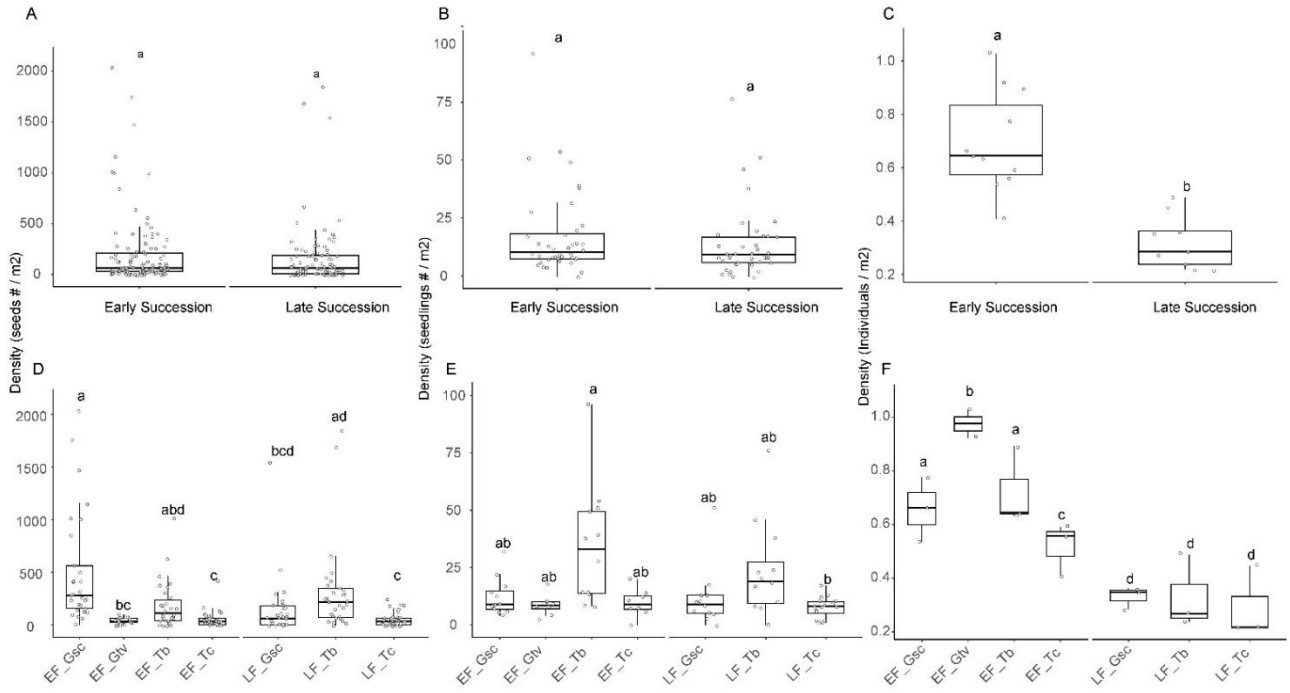

Figure 8.3. Density of soil seed bank (SSB), seedlings (SDL), and adult (ADL) woody individuals along with successional and spatial gradients in upper-Andean Mountain forests.

(A, B) Soil Seed Bank (SSB). Panel A compares late-successional forest (LF) versus early-successional forest (EF); panel B resolves the same contrast by locality combinations (LF-Gsc, EF-Gsc, EF-Gtv, LF-Tb, EF-Tb, LF-Tc, EF-Tc). (C, D) Seedlings (SDL). Panel C illustrates the density differences between LF and EF, and Panel D expands these comparisons by combining localities. (E, F) Adults (ADL). Panel E contrasts late-successional forest (LF) with early-successional forest (EF); panel F depicts forest-type × locality combinations (e.g., LF-Gsc, EF-Gsc, etc.). In every panel, points denote geometric means and error bars represent 95 % confidence intervals. Distinct letters above bars indicate statistically significant differences among groups, as determined by Dunn's post-hoc test with the Bonferroni correction ($p < 0.05$). Locality abbreviations: Gsc = Guasca; Gtv = Guatavita; Tb = Tabio; Tc = Torca (Bogotá).

Seedling (SDL) density also did not differ between forest types ($\chi^2 = 1.36$, $p = 0.243$; Table 10.15; Figure 8.3C) but varied significantly across localities ($\chi^2 = 19.6$, $p < 0.001$; Figure 8.3D). Tabio had significantly higher seedling density than Guasca and Torca. The forest successional status × locality interaction was significant ($\chi^2 = 21.0$, $p = 0.001$), though few contrasts remained significant after post hoc correction (Figure 8.3).

Adult tree density was significantly higher in EF than in LF ($\chi^2 = 13.0$, $p = 0.000$; Table 10.16; Figure 8.3E). No significant differences were detected among localities ($\chi^2 = 6.19$, $p = 0.103$). Interaction effects were significant ($\chi^2 = 15.8$, $p = 0.015$; Figure 8.3F), though pairwise comparisons did not yield significant results. Also, the Dunn test was not significant among localities and interactions (Table 10.16).

Cross-Stage Compositional Correlations

Mantel tests showed significant correlations, albeit weak, in species β composition among stages: seed bank vs. seedlings ($r = 0.174$, $p = 0.024$; Table 10.19), seed bank vs. adults ($r = 0.369$, $p = 0.001$; Table 10.19), and seedlings vs. adults ($r = 0.326$, $p = 0.002$; Table 10.19). Procrustes analyses confirmed these relationships, with the highest congruence between seedlings and adults (correlation = 0.565, $p = 0.002$; Table 10.19), followed by seed banks and adults (correlation = 0.549, $p = 0.002$; Table 10.19). NMDS ordinations supported these results, showing an increase in spatial structure with ontogeny (stress: seeds = 0.128, seedlings = 0.122, adults = 0.079; Table 10.19, Figure 8.4).

Environmental Drivers of Community Composition

Multivariate and univariate analyses converged on a concise suite of abiotic drivers for the β community and abundance of the earliest life-history stages. Envfit screening of the NMDS ordinations identified three significant vectors for soil-seed bank composition—soil organic carbon (C%), soil temperature (Ts °C), and pH —and three for seedlings—bulk density (BD), Ts, and canopy openness (Table 10.20). Distance-based redundancy analyses corroborated these results: a dbRDA model containing C, Ts, and pH explained seed-bank composition ($F = 1.55$, $p = 0.001$), whereas BD, Ts, and canopy openness jointly structured the seedling assemblage ($F = 2.76$, $p = 0.001$; Table 10.21, Figure 8.55A - B). Negative binomial GLMs identified the same variables as key determinants of plot-level abundance (Table 8.1, Table 10.22). For seeds, the model intercept was 3.869 ± 0.165 (SE), and soil carbon had a negative effect ($\beta = –0.804 \pm 0.171$, $z = –4.70$, $p < 0.001$), resulting in a pseudo-R^2 of 0.77. For seedlings, the intercept was 4.087 ±

0.152, and soil temperature showed a positive, though weaker, influence on abundance ($\beta = 0.312 \pm 0.157$, $z = 1.99$, $p = 0.046$), with a pseudo-R^2 of 0.45. Bulk density and canopy openness did not attain significance in the seedling GLM after accounting for covariation with temperature, mirroring their reduced marginal contributions in the dbRDA.

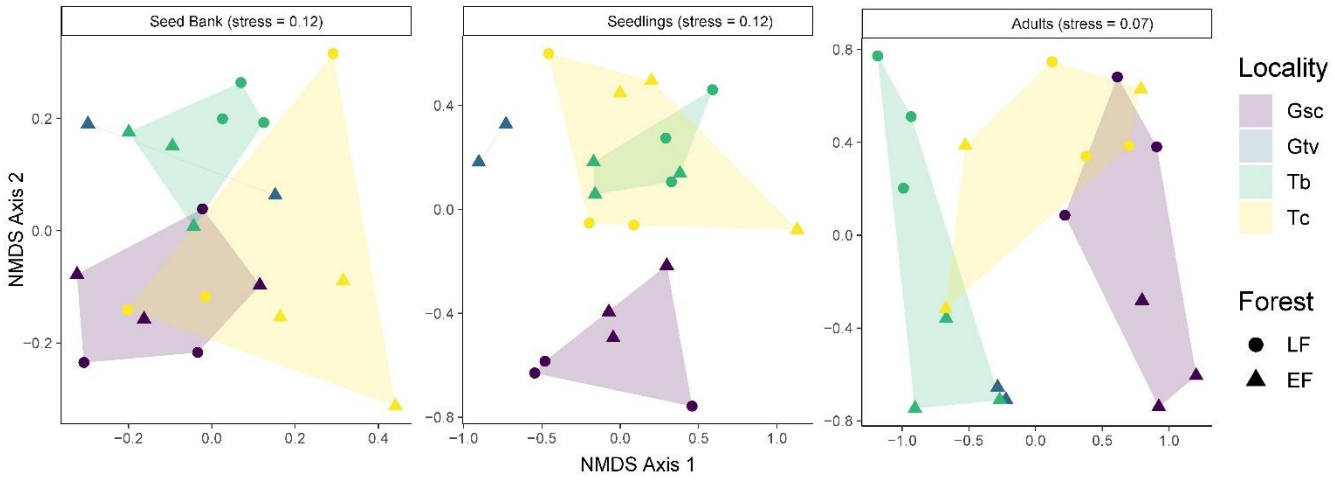

Figure 8.4. Non-metric multidimensional scaling (NMDS) ordination plots showing the compositional dissimilarity of plant communities across three life stages.

Germinated Soil Seed Bank (SSB), Seedlings (SDL), and Adults (ADL). Each panel corresponds to a specific life stage, and points represent plots grouped by locality (Gsc = Guasca, Gtv = Guatavita, Tb = Tabor, Tc = Torca) and forest type (LF = Late Successional Forest, EF = Early Successional Forest). The ordinations were based on Bray–Curtis dissimilarity of species composition. Stress values were < 0.13 in all cases, indicating a good fit of the ordination.

8.5 Discussion

Taken together, our results only partially support the proposed hypotheses. Contrary to hypothesis 1, species richness in the soil seed bank and seedling communities did not differ across early- and late-successional stands, indicating that successional forests alone do not dictate local α-diversity. Hypothesis two—which predicted a progressive decoupling of seed-bank and seedling composition with stand maturation—also found little traction: community dissimilarity was driven far more by locality identity

than by forest age. Although hypothesis three anticipated lower seed and seedling abundances in late forests, negative-binomial models instead revealed stage-specific edaphic controls (soil carbon for seeds, temperature for seedlings) that transcend successional boundaries. By contrast, the fourth hypothesis was strongly supported: locality-scale heterogeneity in soil chemistry, bulk density, soil temperature, and canopy structure explained a significantly larger share of variance in composition and abundance than did the successional stage.

The lack of significant differences in alpha diversity across successional stages challenges assumptions that early- or late-successional forests are inherently more diverse. While some studies report higher diversity in pioneer-dominated early forests due to rapid colonization (Dalling & Denslow, 1998), our findings align with those that show that environmental filtering and spatial heterogeneity often dominate over successional trends (Chazdon et al., 2007). Similar patterns have been reported for upper-montane Andean (Hurtado-M et al., 2021) and Central American cloud forests, where strong edaphic and microclimatic controls yield weak or inconsistent stage differences in alpha diversity when local heterogeneity is high (Marca-Zevallos et al., 2022) This results suggest that we should not assume diversity is tightly linked to successional stage; instead, we should evaluate it in light of functional traits, dispersal strategies, and microenvironmental constraints (Moles et al., 2006). The significant variation in SSB and SDL alpha diversity between localities suggests that fine-scale local environmental variability may be more critical for biodiversity conservation than restoring forest cover alone.

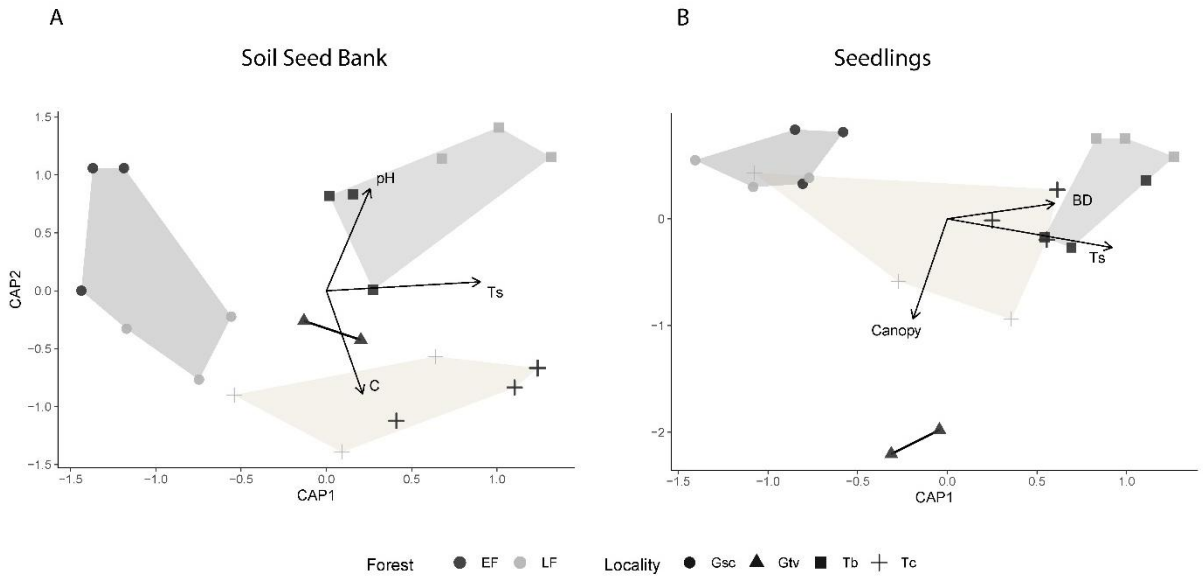

Figure 8.5. Distance-based redundancy analysis (dbRDA) ordination.

A. the soil seed bank (SSB) community based on Bray–Curtis dissimilarity. The plot shows the relationships between species composition and the significant environmental variables: soil carbon content (C), pH, and soil temperature (Ts). B Distance-based redundancy analysis (dbRDA) ordination for the seedling (SDL) community based on Bray–Curtis dissimilarity. The ordination illustrates the influence of the significant environmental variables — bulk density (BD), soil temperature (Ts), and canopy cover percentage — on species composition. Points represent individual plots, colored by forest type (LF = Late successional Forest, EF = Early successional Forest) and shaped by the locality (Gsc = Guasca, Gtv = Guatavita, Tb = Tabio, Tc = Torca). Arrows indicate the direction and strength of the fitted environmental vectors. Only significant variables ($p < 0.05$) are shown.

Similarly, forest successional status failed to explain community dissimilarity, while locality identity accounted for substantial variance, reflecting the overriding influence of local abiotic factors on community assembly. The increasing locality effect from seeds to seedlings to adults is consistent with ontogenetic filtering: regional seed rain and stored seeds generate a relatively homogenized seed bank with low match to the standing flora; seedlings are then filtered by microenvironment and biotic interactions; adults represent the cumulative outcome of survival, density dependence, and disturbance history, which strengthens site-specific composition. Low seed–vegetation similarity in forests is expected because soil seed banks are typically dominated by pioneers and generalists and integrate inputs from

outside the plot (edges/matrix). This pattern has been widely reported for forests and tropical systems (Hopfensperger, 2007). Our results are consistent with studies in Neotropical forests, which demonstrate that environmental parameters, such as topography, soil depth, and subcanopy architecture, influence species composition (Baldeck et al., 2013).

The considerable variation in seed and seedling densities within and among localities further highlights how microsite heterogeneity drives intense selection pressures and divergent recruitment outcomes (Dalling et al., 1997; Grubb, 1977). Consistent with global mountain floras, high β-diversity across life stages—driven primarily by species turnover rather than nestedness—reflects fine-grained spatial structuring underpinned by dispersal limitation and habitat filtering: neighboring localities often share only 3–25 % of their species despite belonging to the same regional pool (Allen et al., 1991; Coelho et al., 2018; McFadden et al., 2019). Steep elevational gradients, dispersal barriers, and sharp shifts in temperature, moisture, and soil properties reinforce endemism and low floristic similarity (De Mattos et al., 2021; López-Angulo et al., 2018), and turnover dominance persists even in heavily modified upper-Andean forests (Calbi et al., 2021; Rubiano et al., 2017), indicating that the original fine-grained spatial structuring characteristic of mountain ecosystems endures (Báez, Fadrique, et al., 2022) and arguing for landscape-scale conservation to safeguard mountain β-diversity (Hurtado-M et al., 2021).

Our ordination-based screening and distance-based redundancy analyses (Figure 8.5A; Table 10.21) show that soil organic carbon, pH, and temperature strongly filter seed-bank β composition, whereas canopy openness and bulk density predominantly structure seedling communities. Corresponding negative-binomial GLMs (Table 8.1) confirm these stage-specific drivers: soil carbon limits seed-bank abundance, and warmer soils enhance seedling abundance. Together, these results demonstrate that local edaphic and microclimatic heterogeneity—not successional age—governs both compositional turnover and abundance during early ontogenetic stages (Martini et al., 2024; Morellato et al., 2016; Zalamea et al., 2015; Zhang et al., 2009).

We observed moderate β compositional overlap between seedling and adult communities but weak correspondence with soil seed banks, supporting the ontogenetic filtering hypothesis in which only a subset of species transitions successfully through successive life stages (Auffret et al., 2024; Baraloto et al., 2005; Souza et al., 2021). Early stages respond acutely to local environmental filters, while adult

composition reflects longer-term historical and spatial processes, highlighting that relying solely on adult vegetation to infer regeneration dynamics may misrepresent underlying community processes.

Table 8.1. Coefficients of the best negative binomial model selected by AIC for SSB and SDL.

Final models were selected using dredge (MuMIn package) based on AIC. For SSB, the best model included only carbon content (C) as a significant predictor; for SDL, soil temperature (Ts) was retained as a significant predictor. Asterisks indicate significance levels: *p < 0.001, p < 0.01, p < 0.05.

Response	Model (complete formula)	Distribution/link (θ)	Coefficients (β ± SE) [z, P]	AIC	Residual deviance (df)
SSB abundance	~ C	NB/log (θ = 1.945)	Intercept: 3.8687 ± 0.1648 [23.481, P < 2e−16]; **C**: −0.8041 ± 0.1710 [−4.702, P = 2.57×10⁻⁶]	197.29	21.300 (18)
SSB abundance	~ succession	NB/log (θ = 1.086)	Intercept: 4.1631 ± 0.2918 [14.268, P < 2e−16]; **LF**: −0.1104 ± 0.4352 [−0.254, P = 0.800]	210.78	22.602 (18)
SDL abundance	~ Ts	NB/log (θ = 2.250)	Intercept: 4.0866 ± 0.1520 [26.886, P < 2e−16]; **Ts**: 0.3120 ± 0.1565 [1.993, P = 0.0463]	204.11	21.349 (18)
SDL abundance	~ succession	NB/log (θ = 1.878)	Intercept: 4.1660 ± 0.2232 [18.667, P < 2e−16]; **LF**: −0.0661 ± 0.3329 [−0.199, P = 0.843]	208.04	21.589 (18)

These patterns find parallels across biomes: episodic hydrological extremes structure seed banks in Neotropical savannas (Sousa et al., 2017), and stochastic rainfall drives soil seed bank composition in Mediterranean shrublands (Del Vecchio et al., 2021). Our data also suggest that soil seed banks serve as ecological reservoirs, maintaining temporal continuity of species pools despite limited congruence with aboveground layers (Anju et al., 2022; Auffret et al., 2024; Plue et al., 2021). However, large-seeded, late-successional taxa often exhibit low persistence due to rapid germination and predation (Moles & Westoby, 2003), skewing the stored pool toward small-seeded, disturbance-adapted species.

Beyond species richness, Soil seed banks also harbor functional and phylogenetic diversity, providing additional layers of ecological insurance against recruitment failure and environmental stochasticity (Baskin & Baskin, 2014). However, they are typically depauperate in large-seeded or recalcitrant species (e.g., Dalling & Brown, 2009), a bias that any restoration plan must offset through targeted enrichment planting. In degraded landscapes, leveraging remnant seed banks for natural

regeneration therefore offers a cost-effective, ecologically congruent strategy—provided that managers complement natural recruitment with supplemental introductions of those missing, large-seeded taxa to maintain community integrity.

8.6 Conclusion

Our study shows that locality, reflecting edaphic and microclimatic heterogeneity, consistently exerts a more substantial influence on plant community composition than forest successional stage, and that successional status has no detectable effect on β-diversity. Stage-specific environmental filters also align with life-stage responses: soil organic carbon, pH, and soil temperature align with seed-bank patterns, while bulk density, canopy openness, and warmer soils align with seedling structure and abundance. Together, these results indicate that fine-scale environmental variation, rather than forest stage alone, shapes early life-stage communities and the spatial turnover observed in upper Andean forests. Conservation and restoration should therefore prioritize locality-level heterogeneity and key soil conditions to sustain high β-diversity and regeneration potential. Future work that tracks seed banks across seasons and links propagule and seedling traits to microhabitat filters will further clarify how local processes maintain biodiversity in tropical mountain ecosystems.

9 General conclusions

This study shows how reproductive ecology and community assembly are influenced by successional forests (e.g., aboveground biomass) and edaphic conditions in Upper-Andean Mountain Forests. My general objectives were to determine whether seed traits and flower and fruit phenology extend the predictive reach of the leaf-and-wood fast–slow spectrum, and to test how local micro-environmental conditions and forest successional status influence early-life community patterns. We integrate a year-long phenological census of 66 woody species, multi-trait measurements for 64 species, and complete inventories of seeds, seedlings, and adults across twenty permanent plots spanning early- to late-successional forests at four Andean localities near Bogotá, Colombia.

My thesis, therefore, makes three contributions to the understanding of the ecology of forests in this biodiversity hotspot. It shows that 1) flowers, seed and fruits are available all year-round but also that phenology varies with forest succession and climate conditions, 2) documents a conservative leaf-wood-syndrome in early stands with subsequent regeneration-trait divergence in late successional forests, and 3) quantifies how locality-specific edaphic and microclimatic conditions (soil organic carbon, temperature, pH, canopy openness, and bulk density) govern species turnover and abundance across seed banks and seedlings.

By bringing together detailed soil and climatic records with measured seed trait combinations, this dissertation clarifies how temperature, light, and moisture cues interact with species' functional strategies and local edaphic filters. The resulting models link specific climate variables—such as cool temperatures and low solar radiation—to shifts in flowering, fruiting, and seed traits, and show that aluminum concentration, canopy openness, and bulk density constrain or release functional diversity. Because each component of the framework is quantified, managers can determine how different climate scenarios, soil amendments, or canopy interventions will affect recruitment success and trait composition. Thus, the study also supplies a practical basis for forecasting which species and trait syndromes are likely to thrive under anticipated warming, altered rainfall, or ongoing land-use change. In turn, these forecasts can inform targeted restoration actions—such as the timing of seed collection to coincide with phenological peaks, selecting species with traits that match local conditions, or mitigating aluminum toxicity—to accelerate both biodiversity recovery and carbon sequestration in tropical mountain forests that would act as a buffer against rapidly expanding urban centers.

Vegetative- and reproductive-trait analyses confirm that succession structures functional assembly, but the pattern is more nuanced than a simple early-fast-to-late-slow sequence. Early-successional forests, defined by open canopies, thin organic layers, and elevated exchangeable aluminum, display community-level conservative vegetative traits, as indicated by low Functional Dispersion and low Rao's Quadratic Entropy. These plots are dominated by dense wood, high LDMC, low SLA, and reduced Amax. Seed-trait space, however, is compressed around small, anemochorous and autochorous species of low mass, reflecting strong abiotic filtering by aluminum and high irradiance plots. As aboveground biomass accumulates and canopies close in late-successional forests, functional diversity in the regeneration layer increases (late-stage FDis; Rao; FRic): zoochorous species with large, nutrient-rich seeds (higher N concentrations) now coexist with small, wind-dispersed seeds. RLQ and GLM results reconcile these patterns by showing that aluminum concentration and canopy openness compress functional diversity in early successional forests, whereas warmer soils and greater biomass relax these constraints, allowing broader niche regeneration in mature forests.

Community diversity in the early stages of regeneration (from germinated seeds to seedlings) does not differ between early and late successional forests for any early life stage; however, it varies significantly among localities for seedlings and seed banks. Beta diversity remains high for seeds, seedlings, and adults, deriving almost entirely from turnover rather than from nestedness, underscoring strong species replacement across space. We found that the Permanova analysis detects no compositional variance attributable to forest successional status; however, locality explains 22% of seed-bank, 35% of seedling, and 41% of adult variation, which is attributed to differences in edaphic and microclimatic conditions. These environmental drivers differ by life stage (germinated seeds and seedlings). I found that, through the analysis of Envfit and dbRDA, soil organic carbon, pH, and soil surface temperature were linked to seed-bank abundance, whereas bulk density, canopy openness, and soil temperature structure seedling assemblages. Negative-binomial GLMs show that higher soil organic carbon and colder soils reduce seed densities, while warmer soils boost seedling abundance. Cross-stage Mantel and Procrustes tests reveal modest but significant congruence among NMDS ordinations, supporting the progression from seed bank to adults. Stress values decline with ontogeny, indicating a growing spatial signal as cohorts mature.

Collectively, these outcomes challenge two assumptions. First, forest successional status alone cannot predict community composition or functional diversity in upper-Andean Mountain forests; fine-

scale edaphic and microclimatic heterogeneity are important predictors of community assembly. Second, vegetative fast–slow trait spectra fail to capture the full breadth of community dynamics. In late-successional forests, the data indicate that seed traits and reproductive phenology do not covary with foliar and woody attributes, suggesting an orthogonal axis of functional variation.

My dissertation presents the first assessment of regenerative functional traits in upper-Andean forests of Colombia's Eastern Cordillera, which also act as peri-urban ecosystems that supply key services to Bogotá and nearby cities. The consistent findings across traits, phenology, and community composition provide support for the overall results. Several factors, however, limit the conclusions that can be drawn from my study.

Phenology was monitored for only one year, and future work should expand the temporal scope of this study by tracking phenology, traits, and communities across multiple ENSO cycles. Doing so would enable researchers to distinguish between short-term El Niño and La Niña signals and longer climatic trends. Adding genomic data will help distinguish the influence of shared ancestry from that of local niche conditions, while combining parentage analysis with seed-rain traps will map actual dispersal routes. At the experimental level, field trials can test the effect of soil aluminum in solution, adjust canopy openness, and supplement seed banks to test cause-and-effect links and provide more precise guidance for restoration. Within this expanded framework, two questions emerge for phenology: Will the early- and late-successional forest flowering peaks we documented shift during strong ENSO events, and if multi-year records are collected, will colder temperatures remain a strong driver of flowering activity across successional stages?

For traits, our data prompt two lines of inquiry that could also be addressed through experimentation and increased spatial and temporal sampling. First, if aluminum levels are reduced in early successional forests, will leaf, wood, and seed traits move toward more acquisitive values, or will conservative strategies persist? Second, to what extent do vertebrate dispersers sustain the divergence in seed traits seen in late successional forests, and how might changes in the disperser community alter these trait–environment links? Finally, the seed-bank results raise two practical questions. Does adding seeds from late successional to early forest increase the functional diversity of both the seed bank and emerging seedlings, and how quickly does seed-bank composition respond when the canopy suddenly opens or

closes? Addressing these questions will deepen our understanding of the processes that govern regeneration and functional diversity in upper-Andean forests.

10 Supplementary material

10.1 Chapter: Reproductive Schedules vary with succession: Evidence from Flowering and Fruit Peaks in Andean Mountain Forests

Table 10.1. Geographical coordinates estimated age since abandonment (years), of the early (E) and late-successional (L) plots located in the four study localities: Guatavita (Gua), Guasca (Gu), Torca (To), and Tabio (Ta) (Cundinamarca, Colombia).

Locality-Successional stage	Plot	Geographical coordinates		Estimated age (years)
		Latitude (N)	Longitude (W)	
Guatavita-E	P1	4° 56' 9,716"	73° 53' 54,237"	10-25
Guatavita-E	P2	4° 56' 12,618"	73° 53' 51,825"	10-25
Guasca- L	P3	4° 47' 20,318"	73° 54' 31,812"	<60
Guasca-E	P4	4° 47' 28,667"	73° 54' 25,886"	20-25
Guasca-L	P5	4° 47' 24,124"	73° 54' 31,332"	<60
Guasca-E	P6	4° 47' 26,609"	73° 54' 25,904"	20-25
Tabio-E	P7	4° 55' 40,858"	74° 6' 29,194"	20-25
Tabio-E	P8	4° 55' 47,149"	74° 6' 31,021"	20-25
Tabio-L	P9	4° 55' 33,961"	74° 6' 47,225"	<70
Tabio-L	P10	4° 55' 31,683"	74° 6' 31,579"	<70
Torca-L	P11	4° 48' 48,674"	74° 0' 58,527"	<70

Locality-Successional stage	Plot	Geographical coordinates		Estimated age (years)
		Latitude (N)	Longitude (W)	
Torca-L	P12	4° 48' 47,937"	74° 0' 56,997"	<70
Torca-E	P13	4° 48' 31,216"	74° 1' 19,178"	10-20
Torca-E	P14	4° 48' 45,912"	74° 0' 58,852"	10-20
Guasca-E	P15	4° 47' 16.5"	73° 54' 15.4"	20-25
Guasca-L	P16	4° 47' 05,2"	73° 54' 13,8"	<60
Torca-L	P17	4° 49' 30,41¨	74° 01' 02,49¨	<70
Torca-E	P18	4° 50' 00,4¨	74° 01'08,8¨	10-20
Tabio-L	P19	4° 55' 31.79"	74° 06'44.42"	<70
Tabio-E	P20	4° 55' 35.03"	74° 06'40.15"	20-25

Table 10.2. Family, genus, and species were evaluated in the phenology study across the 20 permanent plots of the Rastrojos Project, providing information on the growth form and the number of individuals in both forest stages, as per the Leipzig Catalog of Vascular Plants (LCVP; Freiberg et al., 2020).

Family	Genus	Species	Growth-Form	Individuals in the Forest stage	
				Late	Early
Adoxaceae	Viburnum	Viburnum triphyllum	Arboreal	10	16
Aquifoliaceae	Ilex	Ilex kunthiana	Tree	3	14

Family	Genus	Species	Growth-Form	Individuals in the Forest stage	
				Late	Early
Araliaceae	Oreopanax	Oreopanax bogotensis	Tree	2	1
		Oreopanax incisus	Tree	6	8
Asteraceae	Ageratina	Ageratina asclepiadea	Shrubs		1
		Ageratina fastigiata	Shrubs		5
		Ageratina glyptophlebia	Shrubs		5
	Baccharis	Baccharis macrantha	Shrubs		5
	Barnadesia	Barnadesia spinosa	Shrubs	1	
	Critoniopsis	Critoniopsis bogotana	Tree	9	3
	Linochilus	Linochilus rosmarinifolius	Tree		12
	Pentacalia	Monticalia pulchella	Shrubs	2	3
	Verbesina	Verbesina arborea	Tree	6	
Betulaceae	Alnus	Alnus acuminata	Tree		5
Boraginaceae	Varronia	Varronia cylindrostachya	Tree	6	5
Caricaceae	Vasconcellea	Vasconcellea pubescens	Tree	1	
Celastraceae	Maytenus	Maytenus laxiflora	Tree		10
Clethraceae	Clethra	Clethra fimbriata	Tree		10

Family	Genus	Species	Growth-Form	Individuals in the Forest stage	
				Late	Early
		Clethra mexicana	Tree	2	
Clusiaceae	Clusia	Clusia multiflora	Tree	6	1
Cunoniaceae	Weinmannia	Weinmannia tomentosa	Tree	9	10
Elaeocarpaceae	Vallea	Vallea stipularis	Tree	2	22
Ericaceae	Bejaria	Bejaria resinosa	Shrubs	5	4
	Cavendishia	Cavendishia bracteata	Shrubs	1	14
		Cavendishia nitida	Shrubs	3	2
	Macleania	Macleania rupestris	Shrubs	1	28
Escalloniaceae	Escallonia	Escallonia resinosa	Tree	2	
Euphorbiaceae	Croton	Croton bogotanus	Tree	5	
Fabaceae	Ulex	Ulex europaeus	Shrubs		5
Gentianaceae	Macrocarpaea	Macrocarpaea glabra	Shrubs	5	
Lauraceae	Aiouea	Aiouea dubia	Tree	3	
	Ocotea	Ocotea calophylla	Tree	4	
Loranthaceae	Gaiadendron	Gaiadendron punctatum	Tree		5
Melastomataceae	Bucquetia	Bucquetia glutinosa	Shrubs	1	

Family	Genus	Species	Growth-Form	Individuals in the Forest stage	
				Late	Early
	Miconia	Miconia elaeoides	Tree	2	
		Miconia ligustrina	Shrubs	5	12
		Miconia squamulosa	Shrubs	2	24
Meliaceae	Cedrela	Cedrela montana	Tree	6	
Myricaceae	Morella	Morella parvifolia	Shrubs		18
		Morella pubescens	Tree	2	5
Myrtaceae	Myrcianthes	Myrcianthes leucoxyla	Tree	4	15
Papaveraceae	Bocconia	Bocconia frutescens	Tree	1	
Piperaceae	Piper	Piper bogotense	Shrubs	11	
Primulaceae	Cybianthus	Cybianthus iteoides	Shrubs	1	
	Myrsine	Myrsine coriaceae	Tree	9	3
		Myrsine dependens	Tree		3
		Myrsine latifolia	Tree	3	20
Rhamnaceae	Frangula	Frangula goudotiana	Tree	10	3
		Frangula sphaerosperma	Tree		4
Rosaceae	Hesperomeles	Hesperomeles goudotiana	Tree	5	16

Family	Genus	Species	Growth-Form	Individuals in the Forest stage	
				Late	Early
	Prunus	Prunus buxifolia	Tree	3	
Rubiaceae	Palicourea	Palicourea angustifolia	Shrubs	2	3
		Palicourea demissa	Shrubs	2	
		Palicourea paniculata	Shrubs	7	5
		Palicourea boqueronensis	Shrubs		5
Salicaceae	Abatia	Abatia parviflora	Shrubs	1	
	Xylosma	Xylosma spiculifera	Tree	3	7
Solanaceae	Cestrum	Cestrum cuneifolium	Tree	3	
	Sessea	Sessea corymbiflora	Shrubs		1
	Solanum	Solanum cornipholium	Tree	3	
Symplocaceae	Symplocos	Symplocos theoformis	Tree		10
Thymelaceae	Daphnopsis	Daphnopsis caracasana	Shrubs		5
Verbenaceae	Citharexylum	Citharexylum sulcatum	Tree		3
	Duranta	Duranta mutissi	Shrubs	4	
	Lippia	Lippia hirsuta	Tree	2	
Winteraceae	Drimys	Drimys granadensis	Tree	9	1

Table 10.3. Comparison of the circular data distribution in early and late successional forest stages with Rao's Tests for Homogeneity and Test for Equality of Dispersions: For the circular data in Activity and intensity of phenophase, including the p-value for each statistic.

Phenophase	Rao's Tests for Homogeneity	p-value	Test for Equality of Dispersions:	p-value
Flower Activity	6.78329	< 0.01	0.37928	>0.10
Unripe Fruit activity	0.01998	>0.10	0.01345	>0.10
Ripe Fruit activity	3.23879	> 0.05	0.66559	>0.10
Flower intensity	3.64148	> 0.05	0.79565	>0.10
Unripe fruit intensity	0.01201	<0.10	2.32944	>0.10
Ripe fruit intensity	0.01201	<0.10	2.32944	>0.10

Table 10.4. The performance of climate models explaining reproductive Activity and intensity.

The table ranks generalized additive models (GAMs) that relate monthly climate descriptors to two response metrics—Activity (proportion of individuals expressing a given phenophase) and intensity (mean crown percentage occupied by the phenophase) for flowers, unripe fruits, and ripe fruits. For each single-predictor model, we report the Akaike Information Criterion (AIC) and the proportion of deviance explained (Dev Expl). Lower AIC values denote better model support, whereas higher Dev Expl values indicate greater explanatory power (with a maximum value of 1.00). Climate predictors are the monthly mean precipitation (Mean Prec), air temperature (Mean Temp), solar radiation (Mean SR), wind speed (Mean WS), and cloudiness (Mean Cld), plus their first quartile values (Temp Q1, SR Q1, WS Q1) calculated from daily averages. The Full model includes all six predictors simultaneously and serves as a target for explanatory capacity. All climate measurements are average daily values aggregated to the monthly scale.

Activity	Model	AIC	Dev Expl	Intensity	Model	AIC	Dev Expl
Flower	Mean Prec	92.22	0.19	Flower	SR Q1	54.91	0.76
	Mean Temp	91.38	0.11		Mean WS	68.18	0.18
	Temp Q1	90.02	0.20		Full	56.31	0.77
	SR Q1	91.25	0.13				
	WS Q1	92.87	0.04				
	Mean Cld	92.30	0.04				
	Full	-223.56	1.00				
Unripe Fruit	Mean Prec	96.19	0.24	Unripe Fruit	Mean Temp	71.98	0.38
	Mean Temp	91.28	0.43		Temp Q1	68.39	0.41
	Temp Q1	86.25	0.63		SR Q1	68.40	0.41
	Mean SR	96.12	0.34		Mean Cld	69.90	0.34
	WS Q1	96.66	0.12		Full	55.83	0.88
	Mean Cld	90.29	0.48				
	Full	84.86	0.87				
Ripe Fruit	Mean Prec	100.73	0.16	Ripe Fruit	SR Q1	49.84	0.47
	Mean Temp	98.43	0.30				
	Temp Q1	87.63	0.72				

Activity	Model	AIC	Dev Expl	Intensity	Model	AIC	Dev Expl
	SR Q1	89.59	0.87				
	WS Q1	102.46	0.03				
	Mean Cld	95.96	0.43				
	Full	-344.43	1.00				

A: Phenological Activity (Individual Percentage)

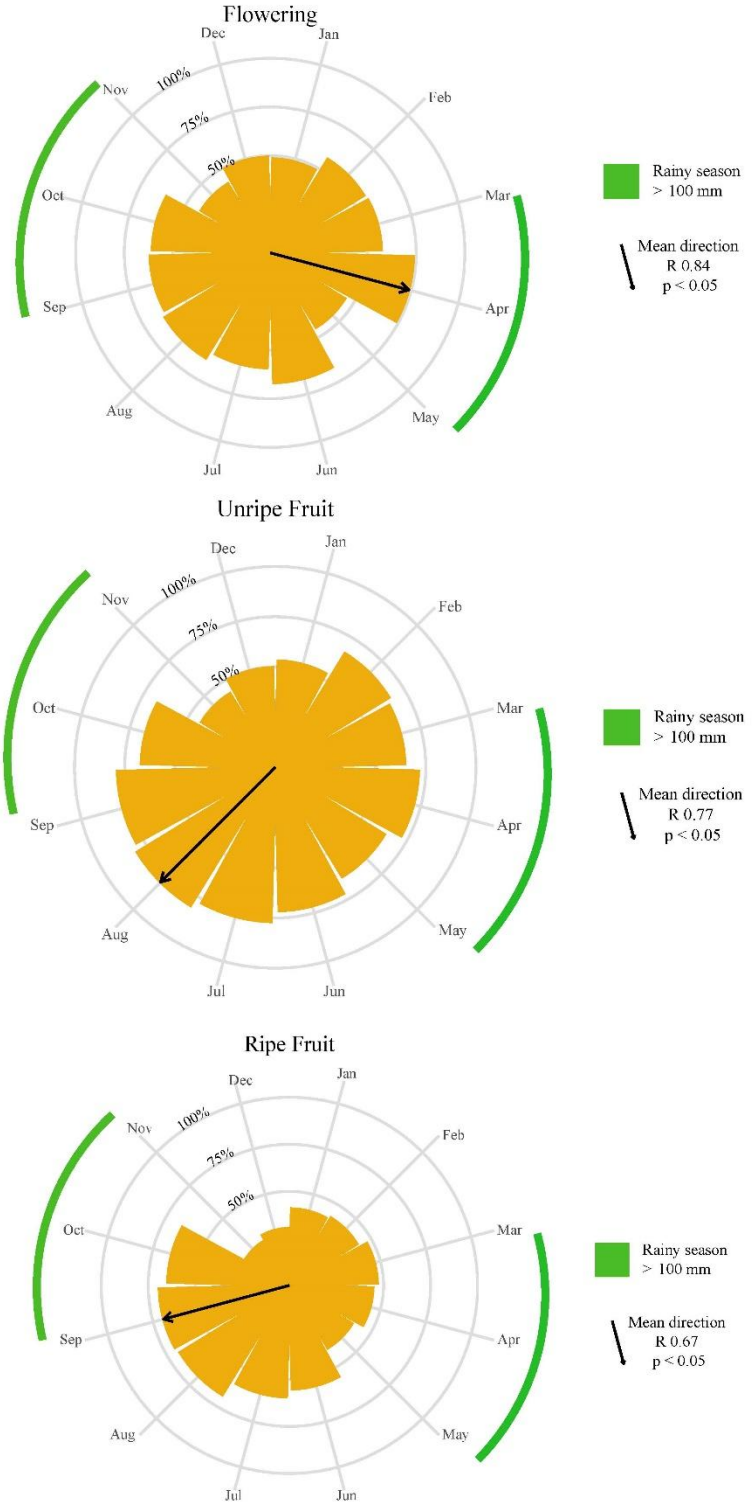

B: Phenological Intensity (FI)

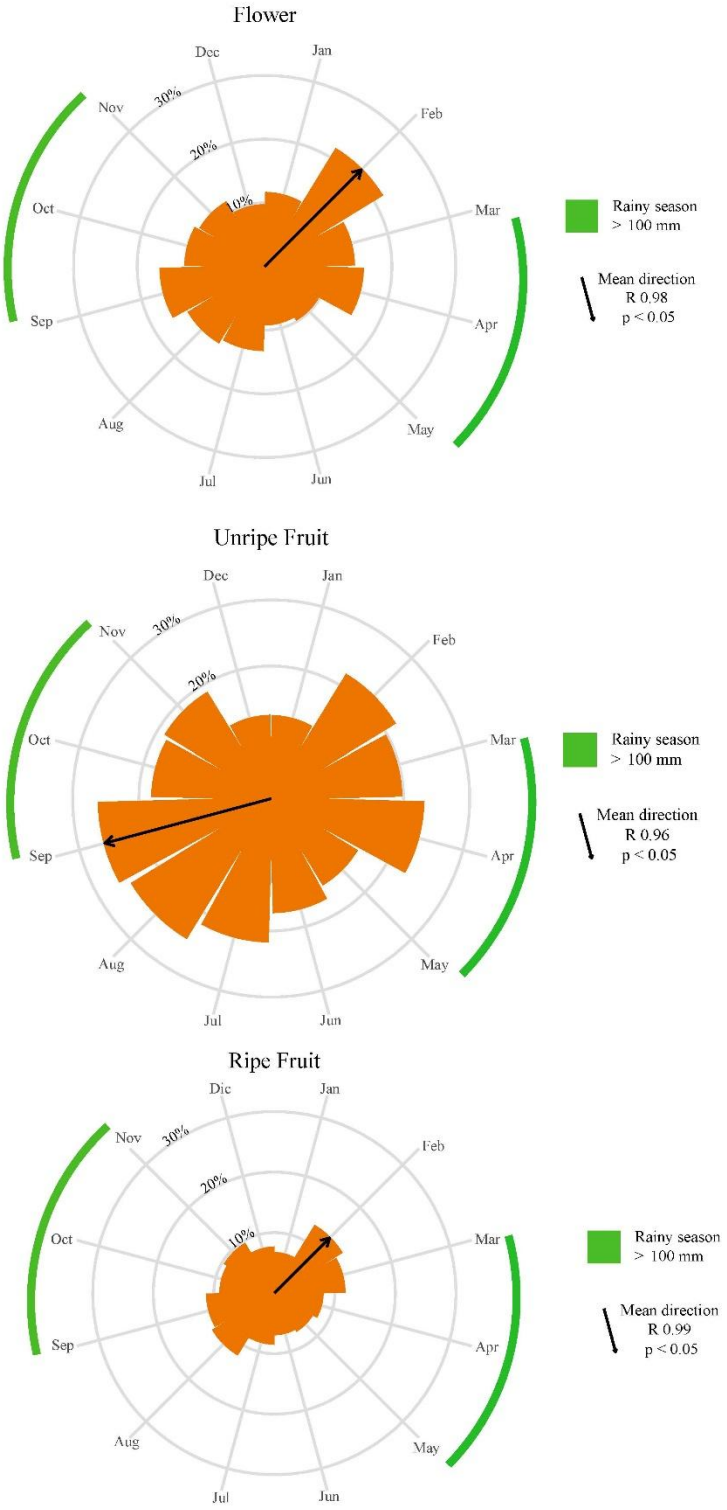

Figure 10.1. Phenological activity and intensity in the upper Andean Mountain forests.

A) Percentage of individuals in flowering, unripe, or ripe fruit during 2021-2022 in Upper Andean Mountain Tropical Forests. The circles represent the months of the year. The yellow bars represent the % of individuals in each phenophase. The arrow and its direction represent the Rayleigh Test for uniformity and the p-value. The two green semi-circles represent the two rainy seasons evaluated from 30 years of precipitation data for the study zone. (B). Phenological Intensity: Percentage of intensity in flowering, unripe, or ripe fruit during 2021-2022 using the Fournier Index in Upper Andean Mountain Tropical Forests. The circles represent the months of the year; The orange bars represent the % of intensity in each phenophase. The arrow and its direction represent the Rayleigh Test for uniformity and the p-value. The two green semi-circles represent the two rainy seasons evaluated from 30 years of precipitation data for the study zone.

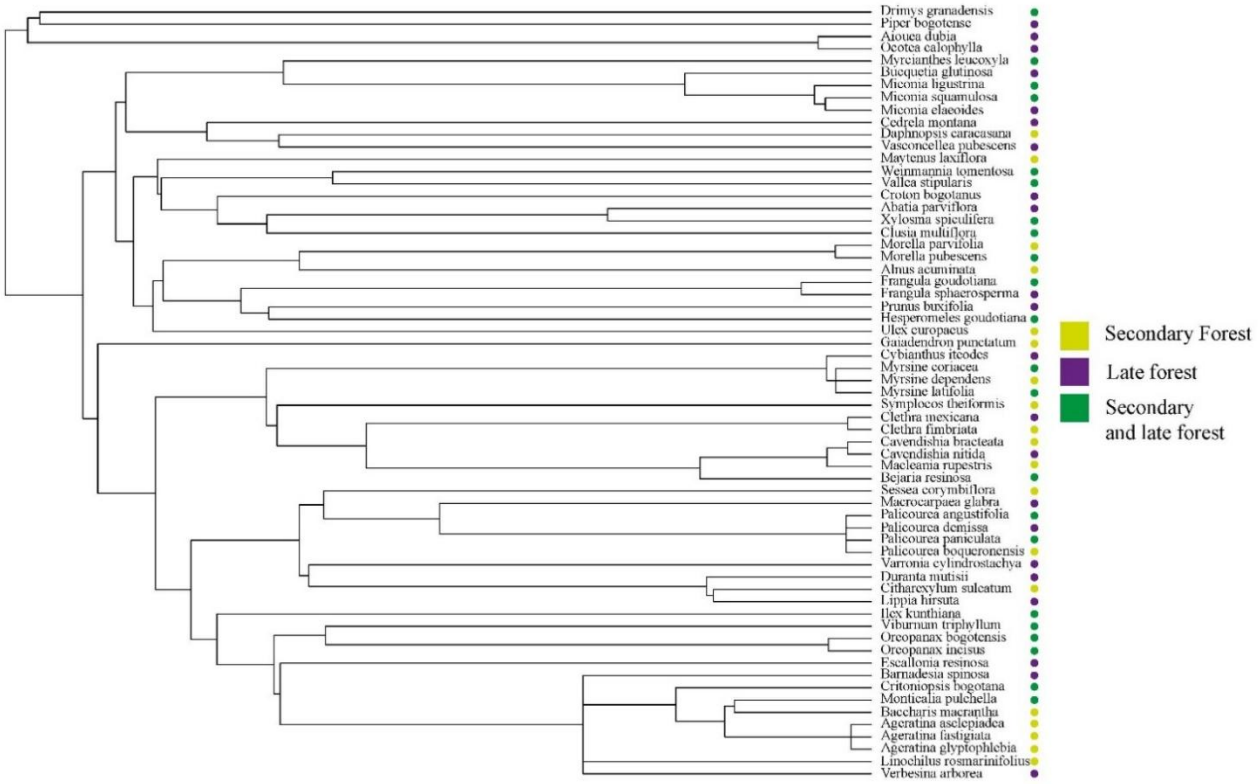

Figure 10.2. Phylogenetic reconstruction hypothesis of the community of species.

We reconstructed the phylogenetic hypothesis of our community using the V.PhyloMaker2 package in R. This package extracted the phylogeny of seeded plants from Smith and Brown (2018) based on divergence time (Jin and Qian, 2022).

10.2 Chapter: Integrating Vegetative and Regenerative Trait Axes Across Successional Gradients in Upper Andean Mountain Forests

Table 10.5. This table presents the coverage of functional trait datasets for 64 woody species in the Upper Andean Mountain Forest community.

We use ✓ to indicate when a species has a complete set of nine seed traits (seed mass SM gr; seed nitrogen and carbon content SN – SC %; seed coat permeability SP %; seed respiration SR µmol CO2 kg-1 s-1; dispersion mode DM; flowering and fruit sine and cosine (Flco, Flsin; Frco, Frsin), and a complete set of five plant traits—leaf dry matter content LDMC g g-1; leaf mass per area LMA g m-2; wood density WD g cm-3; light-saturated assimilation rate Amax µmol CO2 g-1 s-1; and maximum height Hmax m. Species that satisfy both trait suites appear in the "Combined" column (SM, SN, SC, DM, Flco, Flsin, Frco, Frsin, LDMC, LMA, WD, Amax, Hmax). In total, 18 species provide all ten seed traits, 61 species provide all five plant traits, and 41 species provide 12 seed and plant traits.

Species	Code	Seed	Plant	Conjunct
Abatia parviflora	Abapar	–	✓	–
Ageratina asclepiadea	Ageasc	–	✓	–
Ageratina fastigiata	Agefas	–	✓	✓
Ageratina glyptophlebia	Agegly	–	✓	✓
Aiouea dubia	Aiodub	–	–	–
Alnus acuminata	Alnacu	✓	✓	✓
Baccharis macrantha	Bacmac	–	✓	✓

Species	Code	Seed	Plant	Conjunct
Barnadesia spinosa	Barspi	–	✓	–
Bejaria resinosa	Bejres	–	✓	✓
Bucquetia glutinosa	Bucglu	–	✓	–
Cavendishia bracteata	Cavbra	–	✓	✓
Cavendishia nitida	Cavnit	–	✓	✓
Cedrela montana	Cedmon	✓	✓	✓
Citharexylum sulcatum	Citsul	–	✓	✓
Clethra fimbriata	Clefim	–	✓	✓
Clethra mexicana	Clelan	–	✓	–
Clusia multiflora	Clumul	–	✓	✓
Critoniopsis bogotana	Cribog	–	✓	✓
Croton bogotanus	Crobog	✓	✓	✓
Cybianthus iteoides	Cybite	–	✓	–
Daphnopsis caracasana	Dapcar	✓	✓	✓
Drimys granadensis	Drigra	–	✓	–
Duranta mutisii	Durmut	–	✓	–

Species	Code	Seed	Plant	Conjunct
Escallonia resinosa	Escdis	–	✓	–
Frangula goudotiana	Fragou	✓	✓	✓
Frangula sphaerosperma	Frasph	✓	✓	✓
Gaiadendron punctatum	Gaipun	–	✓	✓
Hedyosmum sp1	Hedsp1	–	✓	–
Hesperomeles goudotiana	Hesgou	✓	✓	✓
Ilex kunthiana	Ilekun	✓	✓	✓
Linochilus rosmarinifolius	Linros	–	✓	✓
Lippia hirsuta	Liphir	–	✓	–
Macleania rupestris	Macrup	✓	✓	✓
Macrocarpaea glabra	Macgla	–	✓	✓
Maytenus laxiflora	Maylax	–	✓	–
Miconia elaeoides	Micela	–	✓	–
Miconia ligustrina	Miclig	–	✓	✓
Miconia squamulosa	Micsqu	✓	✓	✓
Morella parvifolia	Morpar	–	✓	✓

Species	Code	Seed	Plant	Conjunct
Morella pubescens	Morpub	–	✓	✓
Myrcianthes leucoxyla	Myrleu	✓	✓	✓
Myrsine coriacea	Myrcor	–	✓	–
Myrsine dependens	Myrdep	–	✓	✓
Myrsine latifolia	Myrlat	–	✓	✓
Ocotea calophylla	Ococal	–	✓	–
Oreopanax bogotensis	Orebog	–	✓	–
Oreopanax incisus	Oreinc	✓	✓	✓
Palicourea angustifolia	Palang	✓	✓	✓
Palicourea boqueronensis	Psyboq	–	✓	✓
Palicourea demissa	Paldem	–	✓	✓
Palicourea paniculata	Pallin	–	✓	✓
Piper bogotense	Pipbog	✓	✓	✓
Prunus buxifolia	Prubux	–	✓	✓
Sessea corymbiflora	Sescor	–	✓	–
Solanum cornifolium	Solcor	✓	–	–

Species	Code	Seed	Plant	Conjunct
Symplocos theiformis	Symthe	–	✓	✓
Ulex europaeus	Uleeur	✓	✓	✓
Vallea stipularis	Valsti	–	✓	–
Varronia cylindrostachya	Varcyl	–	✓	–
Vasconcellea pubescens	Vaspub	–	–	–
Verbesina arborea	Verarb	–	✓	–
Viburnum triphyllum	Vibtri	✓	✓	✓
Weinmannia tomentosa	Weitom	–	✓	✓
Xylosma spiculifera	Xylspi	✓	✓	✓
Totals (n species)		18	61	41
Community pool (n = 64)				

Table 10.6. Completeness of the functional-trait matrix used in the community-level analyses.

The table summarizes data coverage for the 12 focal traits measured across the 64 woody species recorded in the upper Andean Mountain Forest study plots. The first panel reports the number and proportion of species for which a full suite of traits—specific leaf area (SLA), leaf dry-matter content (LDMC), maximum height (Hmax), maximum photosynthetic rate (Amax), wood density (WD), seed mass (SM), seed nitrogen content (SN), seed carbon content (SC), and circular phenological position of reproductive peaks (flower- and fruit-peak sine and cosine)—is available. The second panel details the percentage of missing observations for each trait across the entire species pool. Trait coverage is complete for vegetative dimensions (SLA, LDMC, H max) and exceeds 95 % for

A max and WD, while reproductive and seed-nutrient traits exhibit larger data gaps, with 9–31 % missing-value proportions.

Dataset coverage	**Value**
Species with a complete set of 12 traits	41 / 64 (64.1 %)
which are represented in the abundance matrix	41 / 64 (64.1 %)
Trait	**Missing values (%)(n = 64 species)**
Specific leaf area (SLA)	0.0
Leaf dry-matter content (LDMC)	0.0
Maximum height (H_{max})	0.0
Maximum photosynthetic rate (A_{max})	4.7
Wood density (WD)	1.6
Seed mass (SM)	23.4
Seed nitrogen (SN)	31.2
Seed carbon (SC)	31.2

Table 10.7. Sensitivity analysis of community weighted means (CWMs) and functional diversity (FD) metrics to the choice of abundance estimator (importance values vs. percent canopy cover).

Values are expressed as the percentage change relative to the baseline percent cover. Median absolute percentage change is reported for CWMs across all plots. Median absolute changes in CWMs were uniformly negligible (0 %), indicating that switching from percent canopy cover to importance values had no practical effect on trait means.

Trait (CWM)	Median
Specific leaf area (SLA)	0 %
Maximum photosynthetic rate (Amax)	0 %
Leaf dry-matter content (LDMC)	0 %
Maximum height (Hmax)	0 %
Seed mass (SM)	0 %
Seed nitrogen (SN)	0 %
Seed carbon (SC)	0 %
Wood density (WD)	0 %
Flowering peak (sine)	0 %
Flowering peak (cosine)	0 %
Fruit peak (sine)	0 %
Fruit peak (cosine)	0 %

Table 10.8. Summary of PERMANOVA and homogeneity of multivariate dispersion (PERMDISP) analyses for the 41 species matrix of 12 traits (seven seed traits and five leaf-wood traits) testing for the grouping in dispersion mode.

PERMANOVA was used to test for differences in community composition (Grower dissimilarities) among dispersion mode groups, and PERMDISP assessed whether within-group dispersion differed. PERMANOVA was based on 999 permutations; significant P-values (< 0.05) indicate group differences in community composition.

Statistically significant P-values (α = 0.05) are shown in bold. Abbreviations: PERMDISP = beta dispersion (multivariate homogeneity of dispersions). Dash (-) indicates values not applicable to the corresponding term.

Analysis	Term	Df	Sum of Squares	R^2	Mean Square	F	P-value
PERMANOVA	Model	2.00	0.44	0.26	–	6.75	0.00
	Residual	38.00	1.24	0.74	–	–	–
PERMDISP	Groups	2.00	0.01	–	0.00	2.54	0.09
	Residuals	38.00	0.07	–	0.00	–	–

Table 10.9. The top five variables driving variability across the first five FMAD axes.

Values represent the percentage contribution of each variable to axes 1 through 5. SP% % denotes seed permeability; Dispersion mode; Frsin and Flsin denote the sine-transformed angles of fruiting and flowering peaks, respectively; and SR (µmol CO_2 kg^{-1} s^{-1}) corresponds to seed respiration rate.

Variable	Dim. 1 (%)	Dim. 2 (%)	Dim. 3 (%)	Dim. 4 (%)	Dim. 5 (%)
SP %	23.45	0.92	0.87	0.98	3.93
Dispersion mode	22.05	24.60	17.34	19.94	3.66
Frsin	14.95	0.37	0.01	23.35	0.83
Flsin	10.53	10.45	0.50	12.53	7.18
SR µmol Co2 kg s	10.19	2.99	7.21	26.95	0.39

Table 10.10. **S**ummary statistics for the RLQ ordination linking environment (R-table), species composition (L-table), and functional traits (Q-table) across the 20 upper-Andean Forest plots**.**

The first block reports eigenvalues, projected inertia, and cumulative inertia for the two retained axes. The second block lists the cross-table decomposition, including the covariance between R and Q scores, their respective standard deviations (σR, σQ), and the environment–trait correlation on each axis. "Partial inertia" shows the variance captured by the R and Q tables, while "coinertia ratios" express that variance relative to its theoretical maximum. The final block presents Monte Carlo permutation tests (999 permutations, model types sensu ade4). Model 2 holds species scores fixed and randomizes traits across environments, whereas Model 4 randomizes the complete RLQ structure. Observed coinertia, standardized z-scores, and one-tailed P-values (greater alternative) assess whether the realized coupling exceeds chance expectations. Axes 1–2 together capture 78.4 % of the co-structure, and only Model 4 shows a significant global association (P = 0.001).

Component	Metric	Axis 1	Axis 2	Notes
Eigenstructure	Eigenvalue	1.823	0.641	Total inertia = 3.141
	Projected inertia (%)	58.0 %	20.4 %	Axes 1–2 capture 78.4 % of the co-structure
	Cumulative inertia (%)	58.0 %	78.4 %	—
Cross-table decomposition	Covariance	1.350	0.801	—
	σR (environment)	1.248	1.443	The standard deviation of environmental scores
	σQ (traits)	1.438	1.246	The standard deviation of trait scores
	R–Q correlation	0.752	0.446	Strength of environmental–trait match
Partial inertia	InertiaR	1.557	3.638*	*Total of remaining axes
	InertiaQ	2.069	3.621*	—
Coinertia ratios	R (R-table)	0.703	0.835*	Ratio = inertia/maximum
	Q (Q-table)	0.918	0.893*	—
Monte-Carlo tests (999 permutations)		Observed coinertia	Std. z	*P* (greater)
	Model 2 (environment–traits, species fixed)	3.141	0.66	0.266
	Model 4 (complete RLQ structure)	3.141	5.33	0.001

Table 10.11. Functional diversity metrics per plot.

Values correspond to the twenty upper-Andean Forest plots (P1–P20). Functional richness (FRic) is scaled for readability (×10⁻⁴). FEve, FDiv, FDis, and Rao's quadratic entropy (RaoQ) are unitless indices that describe the regularity, divergence, dispersion, and overall variance of trait distributions in multidimensional space. Metrics were computed from thirteen functional traits after abundance weighting. Together, they provide a plot-level overview of the functional structure along the successional gradient analyzed in this study.

Plot	Succession	FRic (×10⁻⁴)	FEve	FDiv	FDis	RaoQ
P1	Early	2.81	0.526	0.752	0.095	0.0120
P2	Early	1.26	0.604	0.686	0.105	0.0134
P3	Late	3.62	0.720	0.924	0.127	0.0189
P4	Early	2.51	0.622	0.673	0.069	0.0090
P5	Late	5.98	0.604	0.871	0.143	0.0218
P6	Early	3.27	0.665	0.730	0.114	0.0174
P7	Early	4.04	0.471	0.788	0.125	0.0171
P8	Early	0.89	0.776	0.815	0.120	0.0152
P9	Late	4.85	0.659	0.900	0.149	0.0233
P10	Late	3.46	0.527	0.802	0.122	0.0165
P11	Late	2.65	0.654	0.890	0.135	0.0188
P12	Late	2.49	0.625	0.898	0.119	0.0160
P13	Early	5.39	0.579	0.867	0.138	0.0198

Plot	Succession	FRic (×10⁻⁴)	FEve	FDiv	FDis	RaoQ
P14	Late	3.19	0.536	0.932	0.137	0.0192
P15	Early	1.41	0.767	0.820	0.133	0.0199
P16	Late	2.08	0.654	0.870	0.132	0.0191
P17	Late	1.51	0.761	0.897	0.131	0.0182
P18	Early	4.44	0.654	0.771	0.120	0.0166
P19	Late	2.74	0.534	0.773	0.115	0.0167
P20	Early	2.23	0.527	0.510	0.084	0.0102

Table 10.12. Generalized linear models (GLMs) link functional-diversity metrics and community-weighted means (CWMs) to environmental predictors across 20 upper-Andean Forest plots.

For each response variable, we list each retained predictor, its coefficient (β ± SE), and the corresponding P-value. "Max Cook's D" and "Max Leverage" have the highest influence and leverage values among all observations in that model; none exceeded conventional thresholds (Cook's D > 1, leverage > 0.30), confirming the robustness of the fits. † Predictors appear in order of decreasing |z|. Units: AGB = Mg C ha^{-1}; VWC = m^3 m^{-3}; BD = g cm^{-3}; Ts = °C; LAI; OLT = m; Al = µg cm^{-2} day^{-1}.

Response (CWM or FD metric)	Predictors retained†	β ± SE	P	Max Cook's D	Max Leverage
FRic	Intercept only	$3.04 \times 10^{-4} \pm 3.09 \times 10^{-5}$	<0.001	0.26	0.11
FEve	Ts	–0.038 ± 0.016	0.031	0.24	0.12
FDiv	AGB	0.0027 ± 0.0008	0.004	0.21	0.09

Response (CWM or FD metric)	Predictors retained†	β ± SE	P	Max Cook's D	Max Leverage
FDis	AGB	$4.66 \times 10^{-4} \pm 1.63 \times 10^{-4}$	0.010	0.23	0.10
RaoQ	AGB	$8.69 \times 10^{-5} \pm 2.95 \times 10^{-5}$	0.009	0.22	0.11
CWM-SLA	AGB; BD; Ts; Al	0.291 ± 0.143; 35.9 ± 14.8; 5.32 ± 2.57; –0.319 ± 0.158	0.041; 0.015; 0.038; 0.044	0.29	0.14
CWM-Hmax	AGB; Ts; LAI	0.0706 ± 0.0219; 0.901 ± 0.408; –1.77 ± 0.94	0.001; 0.027; 0.060	0.25	0.13
CWM-Amax	BD; Ts	32.1 ± 16.2; 8.09 ± 3.95	0.048; 0.041	0.27	0.12
CWM-SM	Al; Ts	$4.59 \times 10^{-4} \pm 2.19 \times 10^{-4}$; 0.0107 ± 0.0039	0.050; 0.006	0.28	0.14
CWM-SN	BD; OLT	–1.13 ± 0.53; 2.92 ± 1.34	0.033; 0.029	0.26	0.12
CWM-SC	AGB; LAI; Ts	–0.153 ± 0.055; 5.16 ± 2.59; 2.13 ± 1.14	0.006; 0.046; 0.062	0.24	0.11
CWM-Flower month	AGB; LAI; VWC	1.90 ± 0.46; –65.7 ± 22.4; 237 ± 125	<0.001; 0.003; 0.057	0.28	0.13
CWM-Fruit month	AGB; VWC; BD; Ts	0.857 ± 0.441; –317 ± 118; 81.7 ± 40.5; –42.3 ± 8.4	0.052; 0.007; 0.043; <0.001	0.29	0.15

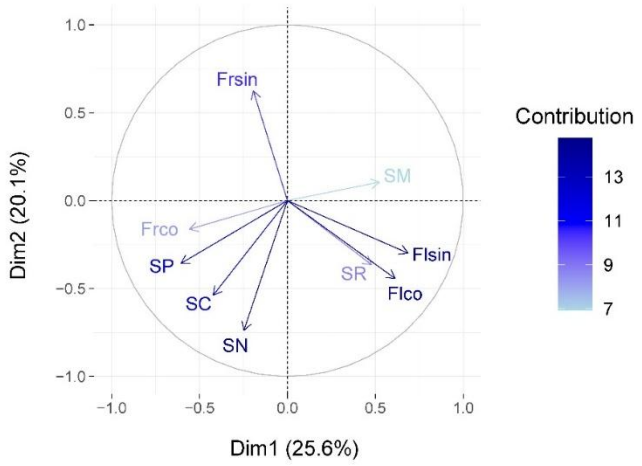

Figure 10.3. The PCA biplot shows nine standardized seed traits for 18 species on the first two principal components, which explain 25.6 % (PC1) and 20.1 % (PC2) of the total variance.

Each trait as an arrow pointing toward higher values: seed mass (SM, g), seed nitrogen content (SN, %), seed carbon content (SC, %), seed permeability (SP, %), seed respiration rate (SR, μmol CO_2 kg^{-1} s^{-1}), flowering cosine (Flco), flowering sine (Flsin), fruiting cosine (Frco) and fruiting sine (Frsin). We apply a light-to-dark blue gradient to the arrows to show each trait's contribution to the axes, with darker blue indicating a more substantial contribution.

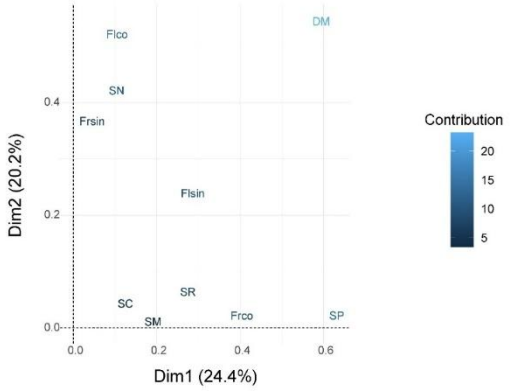

Figure 10.4. Factor map from the Factor Analysis of Mixed Data (FAMD): summarizes seed and phenological traits of a set of 18 species.

We plot Dimension 1 (24.4% of the total variation) on the horizontal axis and Dimension 2 (20.2%) on the vertical axis; together, they explain 44.6% of the trait variation. Each label marks one trait: seed mass (SM, g), seed nitrogen (SN, %), seed carbon (SC, %), seed permeability (SP, %), seed respiration (SR µmol Kg-1 s-1), dispersal mode (DM), flowering timing cosine (Flco) and sine (Flsin), and fruiting timing cosine (Frco) and sine (Frsin). Traits farther from the origin drive the pattern along these axes most strongly. The color scale indicates the percentage contribution of each trait to the total inertia; warmer tones correspond to higher contributions.

10.3 Chapter: Beyond Succession: How Locality-Level Abiotic and Microclimatic Conditions Shape Seed-Bank and Seedling Communities in Upper Andean Mountain Forests

Table 10.13. Geographical coordinates estimated age since abandonment (years), and biomass (kg CO^2/ha) of the early (E) and late-successional (L) plots located in the four study localities.

Guatavita (Gua), Guasca (Gu), Torca (To), and Tabio (Ta) at Cundinamarca, Colombia. Forest types are categorized as late-successional forests (LF) and early-successional forests (EF). Localities include Gsc: Guasca, Gtv: Guatavita, Tb: Tabio, and Tc: Torca (Bogotá).

Local-Successional stage	Plot	Geographical coordinates		Estimated age (years)
		Latitude (N)	Longitude (W)	
Guatavita-E	**P1**	**4° 56' 9,716"**	**73° 53' 54,237"**	**30-50**
Guatavita-E	**P2**	**4° 56' 12,618"**	**73° 53' 51,825"**	**30-50**
Guasca-L	P3	4° 47' 20,318"	73° 54' 31,812"	<60
Guasca-E	P4	4° 47' 28,667"	73° 54' 25,886"	20-25
Guasca-L	P5	4° 47' 24,124"	73° 54' 31,332"	<60

Local-Successional stage	Plot	Geographical coordinates		Estimated age (years)
		Latitude (N)	Longitude (W)	
Guatavita-E	**P1**	**4° 56' 9,716"**	**73° 53' 54,237"**	**30-50**
Guatavita-E	**P2**	**4° 56' 12,618"**	**73° 53' 51,825"**	**30-50**
Guasca-E	P6	4° 47' 26,609"	73° 54' 25,904"	20-25
Tabio-E	P7	4° 55' 40,858"	74° 6' 29,194"	20-25
Tabio-E	P8	4° 55' 47,149"	74° 6' 31,021"	20-25
Tabio-L	P9	4° 55' 33,961"	74° 6' 47,225"	<70
Tabio-L	P10	4° 55' 31,683"	74° 6' 31,579"	<70
Torca-L	P11	4° 48' 48,674"	74° 0' 58,527"	<70
Torca-L	P12	4° 48' 47,937"	74° 0' 56,997"	<70
Torca-E	P13	4° 48' 31,216"	74° 1' 19,178"	10-20
Torca-L	P14	4° 48' 45,912"	74° 0' 58,852"	10-20
Guasca-E	P15	4° 47' 16.5"	73° 54' 15.4"	20-25
Guasca-L	P16	4° 47' 05,2"	73° 54' 13,8"	<60
Torca-L	P17	4° 49' 30,41¨	74° 01' 02,49¨	<70
Torca-E	P18	4° 50' 00,4¨	74° 01'08,8¨	10-20
Tabio-L	P19	4° 55' 31.79"	74° 06'44.42"	<70

Local-Successional stage	Plot	Geographical coordinates		Estimated age (years)
		Latitude (N)	Longitude (W)	
Guatavita-E	**P1**	**4° 56' 9,716"**	**73° 53' 54,237"**	**30-50**
Guatavita-E	**P2**	**4° 56' 12,618"**	**73° 53' 51,825"**	**30-50**
Tabio-E	P20	4° 55' 35.03"	74° 06'40.15"	20-25

Table 10.14. Results of Kruskal-Wallis and Dunn's posthoc tests for seed bank density across forest types (LF vs. EF), localities, and forest successional status × locality combinations.

Kruskal-Wallis results include test statistics and degrees of freedom. Dunn's pairwise comparisons were adjusted using the Bonferroni correction. Significance codes: ns = not significant; p < 0.05 = *, < 0.01 = **, < 0.001 = ***, < 0.0001 = ****. Forests' successional status is categorized as late successional (LF) and early successional forest (EF). Localities include Gsc: Guasca, Gtv: Guatavita, Tb: Tabio, and Tc: Torca (Bogotá).

Analysis	Comparison	Sample Size	Test Statistic	df	p-value	Adjusted p-value	Significance	n1	n2
Kruskal-Wallis (Type Forest)	-	200.	0.20	1.000	0.653	-	ns		
Dunn Test (Locality)	Gsc vs Gtv		-3.87	-	0.00	0.001	***	59	20
	Gsc vs. Tb		0.12	-	0.90	1.00	ns	59	60
	Gsc vs. Tc		-5.408	-	0.000	0.000	****	59	61
	Gtv vs. Tb		3.976	-	0.000	0.000	***	20	60

Analysis	Comparison	Sample Size	Test Statistic	df	p-value	Adjusted p-value	Significance	n1	n2
	Gtv vs. Tc		0.063	-	0.950	1.000	ns	20	61
	Tb vs Tc		-5.556	-	0.000	0.000	****	60	61
Dunn Test (Forest x Locality)	LF.Gsc vs EF.Gsc		4.242	-	0.000	0.000	***	30	29
	LF.Gsc vs EF.Gtv		-1.596	-	0.111	1.000	ns	30	20
	LF.Gsc vs. LF.Tb		2.926	-	0.003	0.072	ns	30	30
	LF.Gsc vs. EF.Tb		1.456	-	0.145	1.000	ns	30	30
	OF.Gsc vs. LF.Tc		-1.611	-	0.107	1.000	ns	30	30
	LF.Gsc vs. EF.Tc		-1.843	-	0.065	1.000	ns	30	31
	EF.Gsc vs EF.Gtv		-5.386	-	0.000	0.000	****	29	20
	EF.Gsc vs. LF.Tb		-1.341	-	0.180	1.000	ns	29	30
	EF.Gsc vs. EF.Tb		-2.798	-	0.005	0.108	ns	29	30
	EF.Gsc vs. LF.Tc		-5.839	-	0.000	0.000	****	29	30

Analysis	Comparison	Sample Size	Test Statistic	df	p-value	Adjusted p-value	Significance	n1	n2
	EF.Gsc vs. EF.Tc		-6.103	-	0.000	0.000	****	29	31
	EF.Gtv vs LF.Tb		4.213	-	0.000	0.001	***	20	30
	EF.Gtv vs EF.Tb		2.899	-	0.004	0.079	ns	20	30
	EF.Gtv vs LF.Tc		0.155	-	0.877	1.000	ns	20	30
	EF.Gtv vs EF.Tc		-0.039	-	0.969	1.000	ns	20	31
	LF.Tb vs EF.Tb		-1.470	-	0.142	1.000	ns	30	30
	LF.Tb vs LF.Tc		-4.537	-	0.000	0.000	***	30	30
	LF.Tb vs EF.Tc		-4.793	-	0.000	0.000	****	30	31
	EF.Tb vs LF.Tc		-3.067	-	0.002	0.045	*	30	30
	EF.Tb vs EF.Tc		-3.311	-	0.001	0.020	*	30	31
	LF.Tc vs EF.Tc		-0.219	-	0.827	1.000	ns	30	31

Table 10.15. Results of Kruskal-Wallis and Dunn's post-hoc tests for seedling density (SDL) across forest successional status, localities, and forest × localities combinations.

Dunn's pairwise comparisons used Bonferroni-adjusted p-values. Significance codes: ns = not significant; p < 0.05 = *, < 0.01 = **, < 0.001 = ***, < 0.0001 = ****. Forests' successional status is categorized as late (LF) and early successional (EF). Localities include Gsc: Guasca, Gtv: Guatavita, Tb: Tabio, and Tc: Torca (Bogotá).

Analysis	Comparison	Sample Size	Test Statistic	df	p-value	Adjusted p-value	Significance	n1	n2
Kruskal-Wallis (Type Forest)	-	80.00	1.36	1.00	0.24	-	ns		
Dunn Test (Locality)	Gsc vs Gtv		-0.41	-	0.68	1.00	ns	24	8
	Gsc vs. Tb		3.21	-	0.00	0.01	**	24	24
	Gsc vs. Tc		-0.87	-	0.38	1.00	ns	24	24
	Gtv vs. Tb		2.68	-	0.01	0.04	*	8	24
	Gtv vs. Tc		-0.21	-	0.84	1.00	ns	8	24
	Tb vs Tc		-4.08	-	0.00	0.00	***	24	24
Dunn Test (Forest x Locality)	LF.Gsc vs EF.Gsc		0.50	-	0.62	1.00	ns	12	12
	LF.Gsc vs EF.Gtv		-0.14	-	0.89	1.00	ns	12	8
	LF.Gsc vs. LF.Tb		2.06	-	0.04	0.82	ns	12	12
	LF.Gsc vs. EF.Tb		2.97	-	0.00	0.06	ns	12	12

Analysis	Comparison	Sample Size	Test Statistic	df	p-value	Adjusted p-value	Significance	n1	n2
	LF.Gsc vs. LF.Tc		-0.63	-	0.53	1.00	ns	12	16
	LF.Gsc vs. EF.Tc		0.06	-	0.95	1.00	ns	12	8
	EF.Gsc vs EF.Gtv		-0.59	-	0.55	1.00	ns	12	8
	EF.Gsc vs. LF.Tb		1.56	-	0.12	1.00	ns	12	12
	EF.Gsc vs. EF.Tb		2.47	-	0.01	0.28	ns	12	12
	EF.Gsc vs. LF.Tc		-1.16	-	0.24	1.00	ns	12	16
	EF.Gsc vs. LF.Tc		-0.39	-	0.70	1.00	ns	12	8
	EF.Gtv vs LF.Tb		1.99	-	0.05	0.98	ns	8	12
	EF.Gtv vs EF.Tb		2.80	-	0.01	0.11	ns	8	12
	EF.Gtv vs LF.Tc		-0.40	-	0.69	1.00	ns	8	16
	EF.Gtv vs EF.Tc		0.19	-	0.85	1.00	ns	8	8
	LF.Tb vs EF.Tb		0.91	-	0.36	1.00	ns	12	12
	LF.Tb vs LF.Tc		-2.83	-	0.00	0.10	ns	12	16

Analysis	Comparison	Sample Size	Test Statistic	df	p-value	Adjusted p-value	Significance	n1	n2
	LF.Tb vs EF.Tc		-1.78	-	0.07	1.00	ns	12	8
	EF.Tb vs LF.Tc		-3.80	-	0.00	0.00	**	12	16
	EF.Tb vs EF.Tc		-2.59	-	0.01	0.20	ns	12	8
	LF.Tc vs EF.Tc		0.62	-	0.54	1.00	ns	16	8

Table 10.16. Results of Kruskal-Wallis and Dunn's post-hoc tests for adult density (ADL) across forest types, locality, and forest type × locality combinations.

Dunn's pairwise comparisons used Bonferroni-adjusted p-values. Significance codes: ns = not significant; p < 0.05 = *, < 0.01 = **, < 0.001 = ***, < 0.0001 = ****. Forest successional status is categorized as late (LF) and early successional forest (EF). Localities include Gsc: Guasca, Gtv: Guatavita, Tb: Tabio, and Tc: Torca (Bogotá).

Analysis	Comparison	Sample Size	Test Statistic	df	p-value	Adjusted p-value	Significance	n1	n2
Kruskal-Wallis (Type Forest)	-	20	13.032	1	0.000306	-	*		
Kruskal-Wallis (Locality)	-	20	6.185	3	0.103	-	ns		
Kruskal-Wallis (Forest — Locality)	-	20	15.797	6	0.0149	-	*		
Dunn Test (Forest — Locality)	LF.Gsc vs EF.Gsc		1.794845335	-	0.072678345	1	ns	3	3

Analysis	Comparison	Sample Size	Test Statistic	df	p-value	Adjusted p-value	Significance	n1	n2
	LF.Gsc vs EF.Gtv		2.500654542	-	0.012396403	0.260324471	ns	3	2
	LF.Gsc vs. LF.Tb		-0.069032513	-	0.94496374	1	ns	3	3
	LF.Gsc vs. EF.Tb		2.001942874	-	0.045290876	0.951108393	ns	3	3
	LF.Gsc vs. LF.Tc		-0.414195077	-	0.678731247	1	ns	3	3
	LF.Gsc vs. EF.Tc		1.035487693	-	0.300441211	1	ns	3	3
	EF.Gsc vs EF.Gtv		0.895296071	-	0.37062884	1	ns	3	2
	EF.Gsc vs. LF.Tb		-1.863877848	-	0.06233886	1	ns	3	3
	EF.Gsc vs. EF.Tb		0.207097539	-	0.835933684	1	ns	3	3
	EF.Gsc vs. LF.Tc		-2.209040412	-	0.02717183	0.570608433	ns	3	3
	EF.Gsc vs. LF.Tc		-0.759357642	-	0.447638645	1	ns	3	3
	EF.Gtv vs LF.Tb		-2.562399098	-	0.010395179	0.218298756	ns	2	3

Analysis	Comparison	Sample Size	Test Statistic	df	p-value	Adjusted p-value	Significance	n1	n2
	EF.Gtv vs EF.Tb		-0.710062401	-	0.477665441	1	ns	2	3
	EF.Gtv vs LF.Tc		-2.871121881	-	0.004090178	0.085893735	ns	2	3
	EF.Gtv vs EF.Tc		-1.574486193	-	0.115375091	1	ns	2	3
	LF.Tb vs EF.Tb		2.070975387	-	0.038361096	0.805583022	ns	3	3
	LF.Tb vs LF.Tc		-0.345162564	-	0.729972161	1	ns	3	3
	LF.Tb vs EF.Tc		1.104520206	-	0.269367543	1	ns	3	3
	EF.Tb vs LF.Tc		-2.416137951	-	0.015686117	0.32940846	ns	3	3
	EF.Tb vs EF.Tc		-0.96645518	-	0.333816464	1	ns	3	3
	LF.Tc vs EF.Tc		1.449682771	-	0.147147003	1	ns	3	3

Table 10.17 Summary of alpha diversity comparisons by forest type and locality across life stages.

We evaluated differences in four alpha diversity indices (species richness, Shannon diversity, Simpson diversity, and evenness) across forest types (early-successional vs. late-successional) and study localities (Gsc, Gtv, Tb, Tc) for three plant community stages (adults, seedlings, and seed bank). Kruskal-Wallis tests were applied to assess

overall differences. When significant effects were detected ($p < 0.05$), we conducted post hoc pairwise comparisons using Dunn's test. P-values for each Kruskal-Wallis test are reported. Significant differences are shown in bold. The absence of significance suggests a similar alpha diversity structure across forest types or localities for the respective index and community stages.

Life Stage	Index	Forest Type (p)	Locality (p)	Significant Differences
Adults	Richness	0.4466	0.5982	None
	Shannon	0.6501	0.508	None
	Simpson	0.7624	0.2839	None
	Evenness	0.9397	0.3687	None
Seedlings	Richness	0.6209	0.0067	Locality only (richness)
	Shannon	0.8206	0.0728	None
	Simpson	0.8206	0.4676	None
	Evenness	0.5453	0.1178	None
Seed Bank	Richness	0.1028	0.049	Locality only (richness)
	Shannon	0.1123	0.4955	None
	Simpson	0.0962	0.7798	None
	Evenness	1	0.1237	None

Table 10.18. Summary of multivariate analyses of community composition for soil seed bank (SSB), seedlings (SDL), and adult plants (ADL) across forest types and localities.

Community	NMDS Stress	β-Sorensen	Turnover	Nestedness	Permanova Forest (R^2)	Permanova Forest (F)	p (Forest)	PERMANOVA Locality (R^2)	F (Locality)	p (Locality)
SSB	0.128	0.918	0.874	0.043	0.063	1.22	0.180	0.222	1.52	0.009
SDL	0.122	0.916	0.874	0.042	0.048	0.91	0.573	0.350	2.87	0.001
ADL	0.079	0.890	0.862	0.027	0.111	2.25	0.041	0.410	3.70	0.001

Table 10.19**.** Results of Mantel and Procrustes tests comparing dissimilarity matrices between community stages (SSB: soil seed bank; SDL: seedlings; ADL: adults).

Mantel and Procrustes correlation coefficients have associated significance values based on 999 permutations.

Comparison	Test	Statistic (r / corr.)	Significance (p)	Interpretation
SSB vs. SDL	Mantel	0.1744	0.019	Significant weak correlation
SSB vs. ADL	Mantel	0.3694	0.001	Significant moderate correlation
SDL vs. ADL	Mantel	0.3259	0.001	Significant moderate correlation
SSB vs. SDL	Procrustes	0.4267	0.122	Not significant
SSB vs. ADL	Procrustes	0.5492	0.004	Significant moderate correlation
SDL vs. ADL	Procrustes	0.5642	0.006	Significant moderate correlation

Table 10.20. Significant environmental vectors fitted onto the NMDS ordination of SSB and SDL communities.

Results of vector fitting (envfit) of environmental variables onto NMDS ordinations for SSB and SDL communities. Values indicate correlation strength (r^2) and significance (p) based on 999 permutations. Only variables with $p < 0.05$ in either community are shown. Asterisks denote significance levels: *$p < 0.001$, $p < 0.01$, $p < 0.05$.

Variable	r^2 (SSB)	*p* (SSB)	r^2 (SDL)	*p* (SDL)	Significance
BD	0.106	0.406	0.366	0.028 *	SDL only
pH	0.326	0.048 *	0.078	0.496	SSB only
Ts	0.315	0.039 *	0.679	0.001 ***	Both
T_air	0.311	0.047 *	0.621	0.001 ***	Both
Canopy	0.052	0.628	0.312	0.046 *	SDL only
C	0.370	0.023 *	0.010	0.919	SSB only
Others	–	> 0.1	–	> 0.1	Not significant

Table 10.21 Distance-based redundancy analysis (dbRDA) results for soil seed bank (SSB) and seedling (SDL) communities—**r**esults of dbRDA models based on Bray–Curtis dissimilarity using 999 permutations.

The global F and p-value indicate the significance of the overall model. Environmental predictors were tested sequentially, and constrained ordination axes (CAP) were tested individually. Asterisks denote significance levels: *$p < 0.001$, $p < 0.01$, $p < 0.05$.

Community	Global dbRDA (F)	Global *p*	Significant Variables (p < 0.05)	Significant CAP Axes
SSB	1.392	0.004 **	pH (0.007 **), C (0.028 *)	CAP1 (0.044 *)

Community	Global dbRDA (F)	Global *p*	Significant Variables (p < 0.05)	Significant CAP Axes
SDL	2.301	0.001 ***	BD (0.001 ***), Ts (0.001 ***), Canopy (0.024 *)	CAP1 (0.001 ***), CAP2 (0.002 **), CAP3 (0.029 *)

Table 10.22 Comparison of generalized linear models (GLMs) for soil seed bank (SSB) and seedling (SDL) abundance.

Comparison of models explaining variation in total and average abundance for SSB and SDL using two distributions (Gaussian for mean abundance per subsample and negative binomial for total count). The best model within each group (based on the lowest AIC) was selected for model averaging and variable importance evaluation.

Community	Model	Distribution	AIC	Pseudo-R^2
SSB	Gaussian (mean)	Gaussian	131.00	0.392
SSB	Negative Binomial	Negative binomial	199.00	0.770
SDL	Gaussian (mean)	Gaussian	161.00	0.272
SDL	Negative Binomial	Negative binomial	205.00	0.448

11 Literature

Adamescu, G. S., Plumptre, A. J., Abernethy, K. A., Polansky, L., Bush, E. R., Chapman, C. A., Shoo, L. P., Fayolle, A., Janmaat, K. R. L., Robbins, M. M., Ndangalasi, H. J., Cordeiro, N. J., Gilby, I. C., Wittig, R. M., Breuer, T., Hockemba, M. B. N., Sanz, C. M., Morgan, D. B., Pusey, A. E., … Beale, C. M. (2018). Annual cycles are the most common reproductive strategy in African tropical tree communities. *Biotropica*, *50*(3), 418–430. https://doi.org/10.1111/btp.12561

Agostinelli, C. (2022). *Package ‘ CircStats .’* CRAN.

Alice Boyle, W., & Bronstein, J. L. (2012). Phenology of tropical understory trees: Patterns and correlates. *Revista de Biologia Tropical*, *60*(4), 1415–1429. https://doi.org/10.15517/rbt.v60i4.2050

Allen, R., Peet, R., & Baker, W. (1991). Gradient analysis of latitudinal variation in southern Rocky Mountain forests. *Journal of Biogeography*, *18*, 123–139. https://doi.org/10.2307/2845287

Álvarez-Buylla, E., & Martínez-Ramos, M. (1990). Seed bank versus seed rain in the regeneration of a tropical pioneer tree. *Oecologia*, *84*, 314–325. https://doi.org/10.1007/BF00329755

Anderson, M. (2006). Distance-Based Tests for Homogeneity of Multivariate Dispersions. *Biometrics*, *62*. https://doi.org/10.1111/j.1541-0420.2005.00440.x

Anderson, M., & Walsh, D. (2013). PERMANOVA, ANOSIM, and the Mantel test in the face of heterogeneous dispersions: What null hypothesis are you testing? *Ecological Monographs*, *83*, 557–574. https://doi.org/10.1890/12-2010.1

Anderson, T. M., Schütz, M., & Risch, A. C. (2012). Seed germination cues and the importance of the soil seed bank across an environmental gradient in the Serengeti. *Oikos*, *121*(2), 306–312. https://doi.org/10.1111/j.1600-0706.2011.19803.x

Anju, M. V, Warrier, R. R., & Kunhikannan, C. (2022). Significance of Soil Seed Bank in Forest Vegetation—A Review. *Seeds*, *1*(3), 181–197. https://doi.org/10.3390/seeds1030016

Armenteras, D., Rodríguez, N., Retana, J., & Morales, M. (2011). Understanding deforestation in montane and lowland forests of the Colombian Andes. *Regional Environmental Change*, *11*(3), 693–705. https://doi.org/10.1007/s10113-010-0200-y

Auffret, A. G., Ladouceur, E., Haussmann, N. S., Daouti, E., Elumeeva, T. G., Kačergytė, I., Knape, J., Kotowska, D., Low, M., Onipchenko, V. G., Paquet, M., Rubene, D., & Plue, J. (2024). A global database of soil seed bank richness, density, and abundance. *Ecology*, *June*, 2023–2024. https://doi.org/10.1002/ecy.4438

Augusto, L., Borelle, R., Boča, A., Bon, L., Orazio, C., Bakker, M. R., Auge, H., Bernier, F., Cantero, A.,

Correia, A. H., Schrijver, A., Eisenhauer, N., Fotelli, M. N., Gâteblé, G., Godbold, D. L., Gundale, M. J., Jactel, H., Koricheva, J., Larsson, M., … Charru, M. (2025). Widespread slow growth of acquisitive tree species. *Nature*, *640*(February 2024). https://doi.org/10.1038/s41586-025-08692-x

Baccini, A., Walker, W., Carvalho, L., Farina, M., & Houghton, R. A. (2019). Response to Comment on "Tropical forests are a net carbon source based on aboveground measurements of gain and loss." *Science*, *363*(6423), 1–11. https://doi.org/10.1126/science.aat1205

Báez, S., Cayuela, L., Macía, M. J., Álvarez-Dávila, E., Apaza-Quevedo, A., Arnelas, I., Baca-Cortes, N., Bañares de Dios, G., Bauters, M., Ben Saadi, C., Blundo, C., Cabrera, M., Castaño, F., Cayola, L., de Aledo, J. G., Espinosa, C. I., Fadrique, B., Farfán-Rios, W., Fuentes, A., … Homeier, J. (2022). FunAndes – A functional trait database of Andean plants. *Scientific Data*, *9*(1), 1–9. https://doi.org/10.1038/s41597-022-01626-6

Báez, S., Fadrique, B., Feeley, K., & Homeier, J. (2022). Changes in tree functional composition across topographic gradients and through time in a tropical montane forest. *PLoS ONE*, *17*(4 April), 1–20. https://doi.org/10.1371/journal.pone.0263508

Baldeck, C. A., Harms, K. E., Yavitt, J. B., John, R., Turner, B. L., Valencia, R., Navarrete, H., Davies, S. J., Chuyong, G. B., Kenfack, D., Thomas, D. W., Madawala, S., Gunatilleke, N., Gunatilleke, S., Bunyavejchewin, S., Kiratiprayoon, S., Yaacob, A., Nur Supardi, M. N., & Dalling, J. W. (2013). Soil resources and topography shape local tree community structure in tropical forests. *Proceedings of the Royal Society B: Biological Sciences*, *280*(1753). https://doi.org/10.1098/rspb.2012.2532

Baraloto, C., Forget, P. M., & Goldberg, D. E. (2005). Seed mass, seedling size and neotropical tree seedling establishment. *Journal of Ecology*, *93*(6), 1156–1166. https://doi.org/10.1111/j.1365-2745.2005.01041.x

Barczyk, M. K., Acosta-Rojas, D. C., Iván Espinosa, C., Homeier, J., Tinoco, B. A., Velescu, A., Wilcke, W., Schleuning, M., & Neuschulz, E. L. (2024). Environmental conditions differently shape leaf, seed and seedling trait composition between and within elevations of tropical montane forests. *Oikos*, 1–13. https://doi.org/10.1111/oik.10421

Bartoń, K. (2010). MuMIn: Multi-Model Inference. In *CRAN: Contributed Packages*.

https://doi.org/10.32614/CRAN.package.MuMIn

Baskin, C. C., & Baskin, J. M. (2014). *Seeds Ecology, Biogeography, and Evolution of dormancy and Germination* (C. C. Baskin & J. M. Baskin (eds.); 2nd Editio). Elsevier Inc.

Basnett, S., Nagaraju, S., Ravikanth, G., & Devy, S. (2019). Influence of phylogeny and abiotic factors varies across early and late reproductive phenology of Himalayan Rhododendrons. *Ecosphere*. https://doi.org/10.1002/ECS2.2581

Becknell, J. M., & Powers, J. S. (2014). Stand age and soils as drivers of plant functional traits and aboveground biomass in secondary tropical dry forest. *Canadian Journal of Forest Research*, *44*(6), 604–613. https://doi.org/10.1139/cjfr-2013-0331

Benavidez, A., Tallei, E., & Schaaf, A. (2023). Reproductive phenology of timber tree species in the Yungas Piedmont Forest of Argentina. *Darwiniana, Nueva Serie*. https://doi.org/10.14522/darwiniana.2023.111.1098

Bernard-Verdier, M., Navas, M. L., Vellend, M., Violle, C., Fayolle, A., & Garnier, E. (2012). Community assembly along a soil depth gradient: Contrasting patterns of plant trait convergence and divergence in a Mediterranean rangeland. *Journal of Ecology*, *100*(6), 1422–1433. https://doi.org/10.1111/1365-2745.12003

Borchert, R., Calle, Z., Strahler, A. H., Baertschi, A., Magill, R. E., Broadhead, J. S., Kamau, J., Njoroge, J., & Muthuri, C. (2015). Insolation and photoperiodic control of tree development near the equator. *New Phytologist*, *205*(1), 7–13. https://doi.org/10.1111/nph.12981

Bossuyt, B., & Honnay, O. (2008). Can the seed bank be used for ecological restoration? An overview of seed bank characteristics in European communities. *Journal of Vegetation Science*, *19*(6), 875–884. https://doi.org/10.3170/2008-8-18462

Boukili, V. K., & Chazdon, R. L. (2017). Environmental filtering, local site factors and landscape context drive changes in functional trait composition during tropical forest succession. *Perspectives in Plant Ecology, Evolution and Systematics*, *24*, 37–47. https://doi.org/10.1016/j.ppees.2016.11.003

Brito, V., Brito, V., Maia, F., Maia, F., Silveira, F., Fracasso, C., Lemos-Filho, J., Fernandes, G.,

Fernandes, G., Goldenberg, R., Morellato, L., Sazima, M., & Staggemeier, V. (2017). Reproductive phenology of Melastomataceae species with contrasting reproductive systems: contemporary and historical drivers. *Plant Biology*, *19 5*, 806–817. https://doi.org/10.1111/plb.12591

Brokaw, N. V. L. (1985). Gap-Phase Regeneration in a Tropical Forest. *Ecology*, *66*(3), 682–687. https://doi.org/10.2307/1940529

Bu, H. Y., Jia, P., Qi, W., Liu, K., Xu, D. H., Ge, W. J., & Wang, X. J. (2018). The effects of phylogeny, life-history traits and altitude on the carbon, nitrogen, and phosphorus contents of seeds across 203 species from an alpine meadow. *Plant Ecology*, *219*(6), 737–748. https://doi.org/10.1007/s11258-018-0830-6

Butler, C., Razgour, O., Peh, K., Morris, R., Soh, M., & Mata-Guel, E. (2023). Impacts of anthropogenic climate change on tropical montane forests: an appraisal of the evidence. *Biological Reviews*, *98*. https://doi.org/10.1111/brv.12950

Calbi, M., Fajardo-Gutiérrez, F., Posada, J. M., Lücking, R., Brokamp, G., & Borsch, T. (2021). Seeing the wood despite the trees: Exploring human disturbance impact on plant diversity, community structure, and standing biomass in fragmented high Andean forests. *Ecology and Evolution*, *11*(5), 2110–2172. https://doi.org/10.1002/ece3.7182

Campbell, G. S., & Norman, J. M. (1998). An Introduction to Environmental Biophysics. In *Journal of Environmental Quality* (Vol. 6, Issue 4). Springer New York. https://doi.org/10.1007/978-1-4612-1626-1

Cao, X., Yang, P., Engel, B., & Li, P. (2018). The effects of rainfall and irrigation on cherry root water uptake under drip irrigation. *Agricultural Water Management*, *197*, 9–18. https://doi.org/10.1016/J.AGWAT.2017.10.021

Cardoso, F. C. G., Zwiener, V. P., & Marques, M. C. M. (2018). Tree phenology along a successional gradient of tropical Atlantic Forest. *Journal of Plant Ecology*, *12*(2), 272–280. https://doi.org/10.1093/jpe/rty020

Castellanos-Castro, C., & Newton, A. C. (2015). Environmental Heterogeneity Influences Successional Trajectories in Colombian Seasonally Dry Tropical Forests. *Biotropica*, *47*(6), 660–671.

https://doi.org/10.1111/btp.12245

Castillo-Avila, C., Castillo-Figueroa, D., & Posada, J. M. (2025). Drivers of soil fauna communities along a successional gradient in upper andean tropical forests. In *Soil Biology and Biochemistry* (Vol. 202, Issue September 2024). Elsevier Ltd. https://doi.org/10.1016/j.soilbio.2024.109692

Castillo-Figueroa, D., González-Melo, A., & Posada, J. M. (2023). Wood density is related to aboveground biomass and productivity along a successional gradient in upper Andean tropical forests. *Frontiers in Plant Science*, *14*(November), 1–16. https://doi.org/10.3389/fpls.2023.1276424

Chacoff, N., Lomáscolo, S., Tylianakis, J., Vázquez, D., Perry, G., & Peralta, G. (2020). Trait matching and phenological overlap increase the spatio-temporal stability and functionality of plant-pollinator interactions. *Ecology Letters*. https://doi.org/10.1111/ele.13510

Chapman, C. A., Valenta, K., Bonnell, T. R., Brown, K. A., & Chapman, L. J. (2018). Solar radiation and ENSO predict fruiting phenology patterns in a 15-year record from Kibale National Park, Uganda. *Biotropica*, *50*(3), 384–395. https://doi.org/10.1111/btp.12559

Chase, J. M., & Myers, J. A. (2011). Disentangling the importance of ecological niches from stochastic processes across scales. *Philosophical Transactions of the Royal Society B: Biological Sciences*, *366*(1576), 2351–2363. https://doi.org/10.1098/rstb.2011.0063

Chave, J., Muller-Landau, H. C., Baker, T. R., Easdale, T., Ter Steege, H., & Webb, C. O. (2006). REGIONAL AND PHYLOGENETIC VARIATION OF WOOD DENSITY ACROSS 2456 NEOTROPICAL TREE SPECIES. *Ecological Applications*, *16*(6), 2356–2367. https://doi.org/doi/abs/10.1890/1051-0761%282006%29016%5B2356%3ARAPVOW%5D2.0.CO%3B2

Chazdon, R. L. (2003). Tropical forest recovery: Legacies of human impact and natural disturbances. *Perspectives in Plant Ecology, Evolution and Systematics*, *6*(1–2), 51–71. https://doi.org/10.1078/1433-8319-00042

Chazdon, R. L. (2008). Chance and Determinism in Tropical Forest Succession. In W. P. Carson & S. A. Schnitzer (Eds.), *Tropical Forest Community Ecology* (pp. 384–408). Wiley-Blackwell.

Chazdon, R. L., Broadbent, E. N., Rozendaal, D. M. A., Bongers, F., Zambrano, A. M. A., Aide, T. M., Balvanera, P., Becknell, J. M., Boukili, V., Brancalion, P. H. S., Craven, D., Almeida-Cortez, J. S., Cabral, G. A. L., de Jong, B., Denslow, J. S., Dent, D. H., DeWalt, S. J., Dupuy, J. M., Durán, S. M., … Poorter, L. (2016). Carbon sequestration potential of second-growth forest regeneration in the Latin American tropics. *Science Advances*, *2*(5), e1501639. https://doi.org/10.1126/sciadv.1501639

Chazdon, R. L., Letcher, S. G., Van Breugel, M., Martínez-Ramos, M., Bongers, F., & Finegan, B. (2007). Rates of change in tree communities of secondary Neotropical forests following major disturbances. *Philosophical Transactions of the Royal Society B: Biological Sciences*, *362*(1478), 273–289. https://doi.org/10.1098/rstb.2006.1990

Christmann, T., Palomeque, X., Armenteras, D., Wilson, S. J., Malhi, Y., & Oliveras Menor, I. (2023). Disrupted montane forest recovery hinders biodiversity conservation in the tropical Andes. *Global Ecology and Biogeography*, *32*(5), 793–808. https://doi.org/10.1111/geb.13666

Clerici, N., Rubiano, K., Abd-Elrahman, A., Hoestettler, J. M. P., & Escobedo, F. J. (2016). Estimating aboveground biomass and carbon stocks in periurban Andean secondary forests using very high resolution imagery. *Forests*, *7*(7). https://doi.org/10.3390/f7070138

Coelho, M., Carneiro, M., Branco, C., Borges, R., & Fernandes, G. (2018). Species turnover drives β-diversity patterns across multiple spatial scales of plant-galling interactions in mountaintop grasslands. *PLoS ONE*, *13*. https://doi.org/10.1371/journal.pone.0195565

Collins, S., Palmer, M., & Cardinale, B. (2002). Species diversity enhances ecosystem functioning through interspecific facilitation. *Nature*, *415*, 426–429. https://doi.org/10.1038/415426a

Comita, L. S., Queenborough, S. A., Murphy, S. J., Eck, J. L., Xu, K., Krishnadas, M., Beckman, N., & Zhu, Y. (2014). Testing predictions of the Janzen-Connell hypothesis: a meta-analysis of experimental evidence for distance- and density-dependent seed and seedling survival. *Journal of Ecology*, *102*(4), 845–856. https://doi.org/10.1111/1365-2745.12232

Condit, R., Pitman, N., Leigh, E. G., Chave, J., Terborgh, J., Foster, R. B., Núñez, P. V., Aguilar, S., Valencia, R., Villa, G., Muller-Landau, H. C., Losos, E., & Hubbell, S. P. (2002). Beta-diversity in tropical forest trees. *Science*, *295*(5555), 666–669. https://doi.org/10.1126/science.1066854

Cornelissen, J. H. C., Lavorel, S., Garnier, E., Díaz, S., Buchmann, N., Gurvich, D. E., Reich, P. B., ter Steege, H., Morgan, H. D., Heijden, van der M. G. A., Pausas, J. G., & Poorter, H. (2003). A handbook of protocols for standardised and easy measurements of plant functional traits worldwide. Aust. J. Bot. 51, 335-380. *Aust. J. Bot.*, *51*, 335–380. https://doi.org/10.1071/BT02124

Corredor-Londoño, G.-A., Beltran, J., Torres-González, A., & Sardi-Saavedra, A. (2020). Phenological synchrony and seasonality of tree species in a fragmented landscape in the Colombian Andes. *Revista de Biología Tropical*. https://doi.org/10.15517/RBT.V68I3.39277

Craven, D., Hall, J. S., Berlyn, G. P., Ashton, M. S., & van Breugel, M. (2015). Changing gears during succession: shifting functional strategies in young tropical secondary forests. *Oecologia*, *179*(1), 293–305. https://doi.org/10.1007/s00442-015-3339-x

Csecserits, A., Halassy, M., Lhotsky, B., Rédei, T., Somay, L., & Botta-Dukát, Z. (2021). Changing assembly rules during secondary succession: evidence for non-random patterns. *Basic and Applied Ecology*, *52*, 46–56. https://doi.org/10.1016/j.baae.2021.02.009

Daïnou, K., Bauduin, A., Bourland, N., Gillet, J. F., Fétéké, F., & Doucet, J. L. (2011). Soil seed bank characteristics in cameroonian rainforests and implications for post-logging forest recovery. *Ecological Engineering*, *37*(10), 1499–1506. https://doi.org/10.1016/j.ecoleng.2011.05.004

Dalling, J., & Hubbell, S. (2002). Seed size, growth rate and gap microsite conditions as determinants of recruitment success for pioneer species. *Journal of Ecology*, *90*. https://doi.org/10.1046/j.1365-2745.2002.00695.x

Dalling, J. W., & Brown, T. A. (2009). Long-term persistence of pioneer species in tropical rain forest soil seed banks. *American Naturalist*, *173*(4), 531–535. https://doi.org/10.1086/597221

Dalling, J. W., & Denslow, J. S. (1998). Soil seed bank composition along a forest chronosequence in seasonally moist tropical forest, Panama. *Journal of Vegetation Science*, *9*(5), 669–678. https://doi.org/10.2307/3237285

Dalling, J. W., & Hubbell, S. P. (2002). Seed size, growth rate and gap microsite conditions as determinants of recruitment success for pioneer species. *Journal of Ecology*, *90*(3), 557–568. https://doi.org/10.1046/j.1365-2745.2002.00695.x

Dalling, J. W., Swaine, M. D., & Garwood, N. C. (1997). Soil seed bank community dynamics in seasonally moist lowland tropical forest, Panama. *Journal of Tropical Ecology*, *13*(5), 659–680. https://doi.org/10.1017/S0266467400010853

Davies, T. J., Wolkovich, E. M., Kraft, N. J. B., Salamin, N., Allen, J. M., Ault, T. R., Betancourt, J. L., Bolmgren, K., Cleland, E. E., Cook, B. I., Crimmins, T. M., Mazer, S. J., Mccabe, G. J., Pau, S., Regetz, J., Schwartz, M. D., & Travers, S. E. (2013). Phylogenetic conservatism in plant phenology. *Journal of Ecology*, *101*(6), 1520–1530. https://doi.org/10.1111/1365-2745.12154

De Mattos, J., Morellato, L., & Batalha, M. (2021). Plant communities in tropical ancient mountains: how are they spatially and evolutionary structured? *Botanical Journal of the Linnean Society*. https://doi.org/10.1093/BOTLINNEAN/BOAB017

de Melo, F. P. L., Dirzo, R., & Tabarelli, M. (2006). Biased seed rain in forest edges: Evidence from the Brazilian Atlantic forest. *Biological Conservation*, *132*(1), 50–60. https://doi.org/10.1016/j.biocon.2006.03.015

De Sousa, A., AbdElgawad, H., Fidalgo, F., Teixeira, J., Matos, M., Tamagnini, P., Fernandes, R., Figueiredo, F., Azenha, M., Teles, L., Korany, S., Alsherif, E., Selim, S., Beemster, G., & Asard, H. (2022). Subcellular compartmentalization of aluminum reduced its hazardous impact on rye photosynthesis. *Environmental Pollution*, 120313. https://doi.org/10.1016/j.envpol.2022.120313

De Souza, E. B., Bao, F., Damasceno Junior, G. A., & Pott, A. (2021). Differences between species in seed bank and vegetation helps to hold functional diversity in a floodable Neotropical savanna. *Journal of Plant Ecology*, *14*(4), 605–615. https://doi.org/10.1093/jpe/rtab014

Del Vecchio, S., Mattana, E., Ulian, T., & Buffa, G. (2021). Functional seed traits and germination patterns predict species coexistence in Northeast Mediterranean foredune communities. *Annals of Botany*, *127*(3), 361–370. https://doi.org/10.1093/aob/mcaa186

Desie, E., Vancampenhout, K., Nyssen, B., Van Den Berg, L., Weijters, M., Van Duinen, G.-J., Ouden, D., Van Meerbeek, K., & Muys, B. (2020). Litter quality and the law of the most limiting: Opportunities for restoring nutrient cycles in acidified forest soils. *The Science of the Total Environment*, *699*, 134383. https://doi.org/10.1016/j.scitotenv.2019.134383

Díaz, S., Kattge, J., Cornelissen, J. H. C., Wright, I. J., Lavorel, S., Dray, S., Reu, B., Kleyer, M., Wirth, C., Colin Prentice, I., Garnier, E., Bönisch, G., Westoby, M., Poorter, H., Reich, P. B., Moles, A. T., Dickie, J., Gillison, A. N., Zanne, A. E., … Gorné, L. D. (2016). The global spectrum of plant form and function. *Nature*, *529*(7585), 167–171. https://doi.org/10.1038/nature16489

Dinno, A. (2015). Nonparametric Pairwise Multiple Comparisons in Independent Groups using Dunn's Test. *The Stata Journal*, *15*(1), 292–300. https://doi.org/10.1177/1536867X1501500117

Dolédec, S., Chessel, D., Braak, C., & Champely, S. (1996). Matching species traits to environmental variables: a new three-table ordination method. *Environmental and Ecological Statistics*, *3*, 143–166. https://doi.org/10.1007/BF02427859

Douh, C., Daïnou, K., Joël Loumeto, J., Moutsambote, J. M., Fayolle, A., Tosso, F., Forni, E., Gourlet-Fleury, S., & Doucet, J. L. (2018). Soil seed bank characteristics in two central African forest types and implications for forest restoration. *Forest Ecology and Management*, *409*(September 2017), 766–776. https://doi.org/10.1016/j.foreco.2017.12.012

Dray, S., Choler, P., Dolédec, S., Peres-Neto, P., Thuiller, W., Pavoine, S., & Ter Braak, C. (2014). Combining the fourth-corner and the RLQ methods for assessing trait responses to environmental variation. *Ecology*, *95 1*, 14–21. https://doi.org/10.1890/13-0196.1

Du, Y., Mao, L., Queenborough, S., Freckleton, R., & Chen, B. (2015). Phylogenetic constraints and trait correlates of flowering phenology in the angiosperm flora of China. *Global Ecology and Biogeography*, *24*, 928–938. https://doi.org/10.1111/GEB.12303

Dunham, A. E., Razafindratsima, O. H., Rakotonirina, P., & Wright, P. C. (2018). Fruiting phenology is linked to rainfall variability in a tropical rain forest. *Biotropica*, *50*(3), 396–404. https://doi.org/10.1111/btp.12564

E-Vojtkó, A., Junker, R. R., de Bello, F., & Götzenberger, L. (2022). Floral and reproductive traits are an independent dimension within the plant economic spectrum of temperate Central Europe. *The New Phytologist*, *1*. https://doi.org/10.1111/nph.18386

Egler, F. E. (1954). Vegetation science concepts I. Initial floristic composition, a factor in old-field vegetation development with 2 figs. *Vegetatio*, *4*(6), 412–417. https://doi.org/10.1007/BF00275587

Ellison, A., Denslow, J., & Loiselle, B. (1993). SEED AND SEEDLING ECOLOGY OF NEOTROPICAL MELASTOMATACEAE. *Ecology*, *74*, 1733–1749. https://doi.org/10.2307/1939932

Etter, A., & van Wyngaarden, W. (2000). Patterns of Landscape Transformation in Colombia, with Emphasis in the Andean Region. *AMBIO: A Journal of the Human Environment*, *29*(7), 432–439. https://doi.org/10.1579/0044-7447-29.7.432

Faccion, G., Alves, A. M., Espírito-Santo, M., Silva, J., Sánchez-Azofeifa, A., & Ferreira, K. (2021). Intra- and interspecific variations on plant functional traits along a successional gradient in a Brazilian tropical dry forest. *Flora*, *279*, 151815. https://doi.org/10.1016/J.FLORA.2021.151815

Fazlioglu, F., Keskin, G., Akçin, Ö. E., & Özbucak, T. (2021). Mining and quarrying activities tend to favor stress-tolerant plants. *Ecological Indicators*, *127*, 107759. https://doi.org/10.1016/J.ECOLIND.2021.107759

Foster, S. (1986). On the adaptive value of large seeds for tropical moist forest trees: A review and synthesis. *The Botanical Review*, *52*, 260–299. https://doi.org/10.1007/BF02860997

Fournier, L. A. (1974). Un método cuantitativo para la medición de características fenológicas en árboles. *Turrialba*.

Franks, S. J. (2011). Plasticity and evolution in drought avoidance and escape in the annual plant Brassica rapa. *New Phytologist*, *190*(1), 249–257. https://doi.org/10.1111/j.1469-8137.2010.03603.x

Freiberg, M., Winter, M., Gentile, A., Zizka, A., Muellner-Riehl, A. N., Weigelt, A., & Wirth, C. (2020). LCVP, The Leipzig catalogue of vascular plants, a new taxonomic reference list for all known vascular plants. *Scientific Data*, *7*(1), 1–7. https://doi.org/10.1038/s41597-020-00702-z

Freitas, C., Dambros, C., & Camargo, J. (2013). Changes in seed rain across Atlantic Forest fragments in Northeast Brazil. *Acta Oecologica-International Journal of Ecology*, *53*, 49–55. https://doi.org/10.1016/J.ACTAO.2013.08.005

Funk, J. L., Larson, J. E., Ames, G. M., Butterfield, B. J., Cavender-Bares, J., Firn, J., Laughlin, D. C., Sutton-Grier, A. E., Williams, L., & Wright, J. (2017). Revisiting the Holy Grail: Using plant

functional traits to understand ecological processes. *Biological Reviews*, *92*(2), 1156–1173. https://doi.org/10.1111/brv.12275

García, J. G., Carollo, I. M., & Picado, J. (2016). Presenting the frame of the unit circle. *Journal of Pure and Applied Algebra*, *220*, 976–1001. https://doi.org/10.1016/J.JPAA.2015.08.004

Garwood, N. C. (1983). Seed Germination in a Seasonal Tropical Forest in Panama : A Community Study. *Ecological Monographs*, *53*(2), 159–181.

Garwood, N. C. (1989). Tropical Soil Seed Banks : A Review. In A. Leck, V. T. Parker, & R. L. Simpson (Eds.), *Ecology of Soil Seed Banks* (pp. 149–209). ACADEMIC PRESS, INC. https://doi.org/https://doi.org/10.1016/b978-0-12-440405-2.50014-2

Gelviz-Gelvez, S. M., Lufs, R. Sa. M., Leonel, L. T., & Felipe, B. A. (2016). The andean forest soil seed bank in two successional stages in Northeastern Colombia. *Botanical Sciences*, *94*(4), 713–727. https://doi.org/10.17129/botsci.666

Gomes, F. M., Oliveira, C. C. De, Rocha Miranda, R. Da, Costa, R. C. Da, & Loiola, M. I. B. (2019). Relationships between soil seed bank composition and standing vegetation along chronosequences in a tropical dry forest in north-eastern Brazil. *Journal of Tropical Ecology*, *35*(4), 173–184. https://doi.org/10.1017/S0266467419000130

González, O., & Loiselle, B. (2016). Species interactions in an Andean bird–flowering plant network: phenology is more important than abundance or morphology. *PeerJ*, *4*. https://doi.org/10.7717/peerj.2789

Graham, E. A., Mulkey, S. S., Kitajima, K., Phillips, N. G., & Wright, S. J. (2003). Cloud cover limits net CO2 uptake and growth of a rainforest tree during tropical rainy seasons. *Proceedings of the National Academy of Sciences of the United States of America*, *100*(2), 572–576. https://doi.org/10.1073/pnas.0133045100

Greulich, S., Chevalier, R., & Villar, M. (2019). Soil seed banks in the floodplain of a large river: A test of hypotheses on seed bank composition in relation to flooding and established vegetation. *Journal of Vegetation Science*. https://doi.org/10.1111/JVS.12762

Gross, N., Bagousse-Pinguet, Y., Liancourt, P., Berdugo, M., Gotelli, N., & Maestre, F. (2017). Functional trait diversity maximizes ecosystem multifunctionality. *Nature Ecology & Evolution*, *1 5*, 132. https://doi.org/10.1038/s41559-017-0132

Grubb, P. J. (1977). The Maintenance of species richness in plant communities: The importance of the regeneration niche. *Biological Reviews*, *52*(1), 107–145. https://doi.org/10.1111/j.1469-185X.1977.tb01347.x

Guzmán, M. N. N., Beltrán, L. C., Rodriguez, C. H., & Roa-Fuentes, L. L. (2023). Functional seed traits as predictors of germination and seedling growth for species with potential for restoration in Caquetá, Colombia. *Trees - Structure and Function*, *37*(3), 947–961. https://doi.org/10.1007/s00468-023-02396-3

Hai, N., Tan, N. T., Bao, T., Petritan, A., Mai, T., Hiền, C. T. T., Anh, P. T., Hưng, V. T., & Petriṭan, I. (2020). Changes in Community Composition of Tropical Evergreen Forests during Succession in Ta Dung National Park, Central Highlands of Vietnam. *Forests*. https://doi.org/10.3390/f11121358

Hawes, J., Vieira, I., Magnago, L., Berenguer, E., Ferreira, J., Aragão, L., Cardoso, A., Lees, A., Lennox, G., Tobias, J., Waldron, A., & Barlow, J. (2020). A large-scale assessment of plant dispersal mode and seed traits across human-modified Amazonian forests. *Journal of Ecology*, *108*, 1373–1385. https://doi.org/10.1111/1365-2745.13358

He, X., Yuan, L., Wang, Z. H., Zhou, Z., & Wan, L. (2020). A study of soil seed banks across one complete chronosequence of secondary succession in a karst landscape. *PeerJ*, *8*. https://doi.org/10.7717/peerj.10226

Heerdt, G. N. J. Ter, Verweij, G. L., Bekker, R. M., & Bakker, J. P. (1996). An Improved Method for Seed-Bank Analysis: Seedling Emergence After Removing the Soil by Sieving. *Functional Ecology*, *10*(1), 144. https://doi.org/10.2307/2390273

Homeier, J, Breckle, S., Günter, S., Rollenbeck, R., & Leuschner, C. (2010). Tree Diversity, Forest Structure and Productivity along Altitudinal and Topographical Gradients in a Species-Rich Ecuadorian Montane Rain Forest. *Biotropica*, *42*. https://doi.org/10.1111/j.1744-7429.2009.00547.x

Homeier, J, Seeler, T., Pierick, K., & Leuschner, C. (2021). Leaf trait variation in species-rich tropical

Andean forests. *Scientific Reports*, *11*. https://doi.org/10.1038/s41598-021-89190-8

Homeier, Jürgen, Seeler, T., Pierick, K., & Leuschner, C. (2021). Leaf trait variation in species-rich tropical Andean forests. *Scientific Reports*, *11*(1). https://doi.org/10.1038/s41598-021-89190-8

Hopfensperger, K. N. (2007). A review of similarity between seed bank and standing vegetation across ecosystems. *Oikos*, *116*(9), 1438–1448. https://doi.org/10.1111/j.2007.0030-1299.15818.x

Hu, D., Jiang, L., Hou, Z., Zhang, J., Wang, H., & Lv, G. (2022). Environmental filtration and dispersal limitation explain different aspects of beta diversity in desert plant communities. *Global Ecology and Conservation*, *33*(October 2021), e01956. https://doi.org/10.1016/j.gecco.2021.e01956

Huang, C., Xu, Y., & Zang, R. (2021). Variation Patterns of Functional Trait Moments Along Geographical Gradients and Their Environmental Determinants in the Subtropical Evergreen Broadleaved Forests. *Frontiers in Plant Science*, *12*(July), 1–12. https://doi.org/10.3389/fpls.2021.686965

Hurtado-M, A. B., Echeverry-Galvis, M. Á., Salgado-Negret, B., Muñoz, J. C., Posada, J. M., & Norden, N. (2021). Little trace of floristic homogenization in peri-urban Andean secondary forests despite high anthropogenic transformation. *Journal of Ecology*, *109*(3), 1468–1478. https://doi.org/10.1111/1365-2745.13570

Hurtado-M, A. B., Muñoz, J. C., Echeverry-Galvis, M. Á., & Norden, N. (2022). Successional forests in Colombia: an opportunity for recovery of transformed landscapes. *Caldasia*, *44*(2), 332–344. https://doi.org/10.15446/caldasia.v44n2.82255

Huxley, J., White, C., Humphries, H., Weber, S., & Spasojevic, M. (2023). Plant functional traits are dynamic predictors of ecosystem functioning in variable environments. *Journal of Ecology*, *111*, 2597–2613. https://doi.org/10.1111/1365-2745.14197

Iwasaki, N., Hori, K., & Ikuta, Y. (2019). Xylem plays an important role in regulating the leaf water potential and fruit quality of Meiwa kumquat (Fortunella crassifolia Swingle) trees under drought conditions. *Agricultural Water Management*. https://doi.org/10.1016/J.AGWAT.2018.12.026

Jin, Y., & Qian, H. (2022). V.PhyloMaker2: An updated and enlarged R package that can generate very

large phylogenies for vascular plants. *Plant Diversity*, *44*(4), 335–339. https://doi.org/10.1016/j.pld.2022.05.005

Kaur, M., Tak, Y., Bhatia, S., Asthir, B., Lorenzo, J., & Amarowicz, R. (2021). Crosstalk during the Carbon–Nitrogen Cycle That Interlinks the Biosynthesis, Mobilization and Accumulation of Seed Storage Reserves. *International Journal of Molecular Sciences*, *22*. https://doi.org/10.3390/ijms222112032

Kearney, M. R., Isaac, A. P., & Porter, W. P. (2014). Microclim: Global estimates of hourly microclimate based on long-term monthly climate averages. *Scientific Data*, *1*, 1–9. https://doi.org/10.1038/sdata.2014.6

Kitajima, K. (1994). Relative importance of photosynthetic traits and allocation patterns as correlates of seedling shade tolerance of 13 tropical trees. *Oecologia*, *98*(3–4), 419–428. https://doi.org/10.1007/BF00324232

Komori, O., Eguchi, S., Ikeda, S., Okamura, H., Ichinokawa, M., & Nakayama, S. (2016). An asymmetric logistic regression model for ecological data. *Methods in Ecology and Evolution*, *7*. https://doi.org/10.1111/2041-210X.12473

Kuzee, M., & Wijdeven, S. (2000). Seed Availability as a Limiting Factor in Forest Recovery Processes in Costa Rica. *Restoration Ecology*, *8*. https://doi.org/10.1046/j.1526-100x.2000.80056.x

La Spada, P., Dominguez, E., Continella, A., Heredia, A., & Gentile, A. (2024). Factors influencing fruit cracking: an environmental and agronomic perspective. In *Frontiers in Plant Science* (Vol. 15, Issue February, pp. 1–6). https://doi.org/10.3389/fpls.2024.1343452

Lantz, B. (2013). The impact of sample non-normality on ANOVA and alternative methods. *British Journal of Mathematical and Statistical Psychology*, *66*(2), 224–244. https://doi.org/10.1111/j.2044-8317.2012.02047.x

Larson, J. E., & Funk, J. L. (2016). Regeneration: an overlooked aspect of trait-based plant community assembly models. *Journal of Ecology*, *104*(5), 1284–1298. https://doi.org/10.1111/1365-2745.12613

Lasky, J. R., Uriarte, M., & Muscarella, R. (2016). Synchrony, compensatory dynamics, and the functional

trait basis of phenological diversity in a tropical dry forest tree community: Effects of rainfall seasonality. *Environmental Research Letters*, *11*(11). https://doi.org/10.1088/1748-9326/11/11/115003

Lavorel, S., & Garnier, E. (2002). Predicting changes in community composition and ecosystem functioning from plant traits: revisiting the Holy Grail. *Functional Ecology*, *16*, 545–556. https://doi.org/10.1046/J.1365-2435.2002.00664.X

Lê, S., Josse, J., & Husson, F. (2008). FactoMineR: An R Package for Multivariate Analysis. *Journal of Statistical Software*, *25*(1), 1–18. https://doi.org/10.18637/jss.v025.i01

Legendre, P., & Legendre, L. (2012a). *Multidimensional quantitative data* (pp. 143–194). https://doi.org/10.1016/B978-0-444-53868-0.50004-6

Legendre, P., & Legendre, L. (2012b). *Numerical Ecology* (P. Legendre & L. Legendre (eds.); Volume 24). Elsevier. https://doi.org/10.1016/B978-0-12-409548-9.10595-0

Legendre, P., Mi, X., Ren, H., Ma, K., Yu, M., Sun, I.-F., & He, F. (2009). Partitioning beta diversity in a subtropical broad-leaved forest of China. *Ecological Society of Amerrica*, *90*(3), 663–674.

Leishman, M. R., Wright, I. J., Moles, A. T., & Westoby, M. (2000). The Evolution Ecology of Seed size. In CABI Publishing (Ed.), *Seeds. The Ecology of Regeneration in Plant Communities* (Second, p. 423). CABI Publishing.

Li, H., Zhang, X., Hou, X., & Du, T. (2021). Developmental and water deficit-induced changes in hydraulic properties and xylem anatomy of tomato fruit and pedicel. *Journal of Experimental Botany*. https://doi.org/10.1093/jxb/erab001

Li, S., Lu, S., Wang, J., Chen, Z., Zhang, Y., Duan, J., Liu, P., Wang, X., & Guo, J. (2023). Responses of Physiological, Morphological and Anatomical Traits to Abiotic Stress in Woody Plants. *Forests*. https://doi.org/10.3390/f14091784

Liu, M., Yibo, Wang, X., & Xu, L. (2021). Plant Community Assembly Mechanisms of a Subalpine Meadow Community along Different Successional Time☆. *Rangeland Ecology and Management*, *77*, 118–125. https://doi.org/10.1016/j.rama.2021.04.006

Lohbeck, M., Lebrija-Trejos, E., Martínez-Ramos, M., Meave, J., Poorter, L., & Bongers, F. (2015). Functional Trait Strategies of Trees in Dry and Wet Tropical Forests Are Similar but Differ in Their Consequences for Succession. *PLoS ONE*, *10*. https://doi.org/10.1371/journal.pone.0123741

Lohbeck, M., Lohbeck, M., Poorter, L., Lebrija-Trejos, E., Lebrija-Trejos, E., Lebrija-Trejos, E., Martínez-Ramos, M., Meave, J., Paz, H., Pérez-García, E., Romero-Pérez, I., Tauro, A., & Bongers, F. (2013). Successional changes in functional composition contrast for dry and wet tropical forest. *Ecology*, *94 6*, 1211–1216. https://doi.org/10.1890/12-1850.1

Lohbeck, M., Poorter, L., Lebrija-Trejos, E., Martinez-Ramos, M., Meave, J. A., Paz, H., Pérez-García, E. A., Romero-Pérez, I. E., Tauro, A., & Bongers, F. (2013). Successional changes in functional composition contrast for dry and wet tropical forest. *Ecology*, *94*(6), 1211–1216.

Lohbeck, M., Poorter, L., Martínez-Ramos, M., Rodriguez-Velázquez, J., van Breugel, M., & Bongers, F. (2014). Changing drivers of species dominance during tropical forest succession. *Functional Ecology*, *28*(4), 1052–1058. https://doi.org/10.1111/1365-2435.12240

Lohbeck, M., Poorter, L., Martínez-Ramos, M., Rodríguez-Velázquez, J., Breugel, M., & Bongers, F. (2014). Changing drivers of species dominance during tropical forest succession. *Functional Ecology*, *28*, 1052–1058. https://doi.org/10.1111/1365-2435.12240

López-Angulo, J., Pescador, D., Sánchez, A., Mihoc, M., Cavieres, L., & Escudero, A. (2018). Determinants of high mountain plant diversity in the Chilean Andes: From regional to local spatial scales. *PLoS ONE*, *13*. https://doi.org/10.1371/journal.pone.0200216

Lorer, E., Verheyen, K., Blondeel, H., De Pauw, K., Sanczuk, P., De Frenne, P., & Landuyt, D. (2024). Forest understorey flowering phenology responses to experimental warming and illumination. *New Phytologist*, *241*(4), 1476–1491. https://doi.org/10.1111/nph.19425

Luna-Nieves, A., González, E., Cortés-Flores, J., Ibarra-Manríquez, G., Maldonado-Romo, A., & Meave, J. (2022). Interplay of environmental cues and wood density in the vegetative and reproductive phenology of seasonally dry tropical forest trees. *Biotropica*, *54*, 500–514. https://doi.org/10.1111/btp.13072

Lund, U., Agostinelli, C., Arai, H., Gagliardi, A., Portugués-García, E., Giunchi, D., Irisson, J.-O.,

Pocernich, M., & Rotolo, F. (2024). *Circular Statistics*. CRAN.

Ma, M., Zhou, X., Qi, W., Liu, K., Jia, P., & Du, G. (2013). Seasonal dynamics of the plant community and soil seed bank along a successional gradient in a subalpine meadow on the Tibetan Plateau. *PLoS ONE*, *8*(11). https://doi.org/10.1371/journal.pone.0080220

Maecha Vega, G. E., Ovalle Escobar, A., Camelo Salamanca, D., Rozo Fernández, A., & Barrero Barrero, D. (2012). *Vegetación del territorio CAR, 450 especies de sus llanuras y montañas* (A. Ovalle Escobar (ed.); Segunda ed). Corporación Autónima Regional de Cundinamarca.

Malizia, A., Blundo, C., Carilla, J., Acosta, O. O., Cuesta, F., Duque, A., Aguirre, N., Aguirre, Z., Ataroff, M., Baez, S., Calderón-Loor, M., Cayola, L., Cayuela, L., Ceballos, S., Cedillo, H., Ríos, W. F., Feeley, K. J., Fuentes, A. F., Gámez Álvarez, L. E., … Young, K. R. (2020). Elevation and latitude drives structure and tree species composition in Andean forests: Results from a large-scale plot network. *PLoS ONE*, *15*(4), 1–18. https://doi.org/10.1371/journal.pone.0231553

Marca-Zevallos, M., Moulatlet, G., Sousa, T., Schietti, J., Coelho, L., Ramos, J., De Andrade Lima Filho, D., Amaral, I., De Almeida Matos, F. D., Rincón, L., Revilla, J. D. C., Pansonato, M., Gribel, R., Barbosa, E., Miranda, I., Bonates, L., Guevara, J., Salomão, R., Ferreira, L., … Costa, F. (2022). Local hydrological conditions influence tree diversity and composition across the Amazon basin. *Ecography*. https://doi.org/10.1111/ecog.06125

Martini, F., Buechling, A., Bače, R., Hofmeister, J., Janda, P., Matula, R., & Svoboda, M. (2024). Biotic and abiotic effects on tree regeneration vary by life stage in European primary forests. *Oikos*. https://doi.org/10.1111/oik.10755

Maza, B., Rodes-Blanco, M., & Rojas, E. (2022). Aboveground Biomass Along an Elevation Gradient in an Evergreen Andean–Amazonian Forest in Ecuador. *Frontiers in Forests and Global Change*, *5*. https://doi.org/10.3389/ffgc.2022.738585

McFadden, I., Sandel, B., Tsirogiannis, C., Morueta-Holme, N., Svenning, J., Enquist, B., & Kraft, N. (2019). Temperature shapes opposing latitudinal gradients of plant taxonomic and phylogenetic β diversity. *Ecology Letters*, *22 7*, 1126–1135. https://doi.org/10.1111/ele.13269

Medeiros-Sarmento, P., Ferreira, L., & Gastauer, M. (2020). Natural regeneration triggers compositional

and functional shifts in soil seed banks. *The Science of the Total Environment*, *753*, 141934. https://doi.org/10.1016/j.scitotenv.2020.141934

Mitchard, E. T. A. (2018). The tropical forest carbon cycle and climate change. In *Nature* (Vol. 559, Issue 7715, pp. 527–534). https://doi.org/10.1038/s41586-018-0300-2

Moles, A. T., & Westoby, M. (2003). Latitude, seed predation and seed mass. *Journal of Biogeography*, *30*(1), 105–128. https://doi.org/10.1046/j.1365-2699.2003.00781.x

Moles, Angela T., & Westoby, M. (2004). Seedling survival and seed size: a synthesis of the literature. *Journal of Ecology*, *92*, 3372–3383. https://doi.org/10.1111/j.0022-0477.2004.00884.x

Moles, Angela T, Westoby, M., & Eroksson, O. (2006). Seed Size and Plant Strategy across the Whole Life Cycle. *Oi*, *113*(1), 91–105.

Morellato, L. P. C., Alberton, B., Alvarado, S. T., Borges, B., Buisson, E., Camargo, M. G. G., Cancian, L. F., Carstensen, D. W., Escobar, D. F. E., Leite, P. T. P., Mendoza, I., Rocha, N. M. W. B., Soares, N. C., Silva, T. S. F., Staggemeier, V. G., Streher, A. S., Vargas, B. C., & Peres, C. A. (2016). Linking plant phenology to conservation biology. *Biological Conservation*, *195*, 60–72. https://doi.org/10.1016/j.biocon.2015.12.033

Morellato, P. C., Camargo, M. G. G., D'essa Neves, F., Luize, B. G., Mantovani, A., & Hudson, I. L. (2010). The Influence of Sampling Method, Sample Size, and Frequency of Observations on Plant Phenological Patterns and Interpretation in Tropical Forest Trees. In *Phenological Research* (pp. 99–121). https://doi.org/10.1007/978-90-481-3335-2

Morellato, P. C., Camargo, M. G. G., & Gressler, E. (2013). A Review of Plant Phenology in South and Central America. In M. D. Schwartz (Ed.), *Phenology: An Integrative Environmental Science* (pp. 91–113). Springer. https://doi.org/10.1007/978-94-007-6925-0

Morellato, P. C., Talora, D. C., Takahasi, A., Bencke, C. C., Romera, E. C., & Zipparro, V. B. (2000). Phenology of Atlantic Rain Forest Trees: A Comparative Study1. *Biotropica*, *32*(4b), 811–823. https://doi.org/10.1646/0006-3606(2000)032[0811:poarft]2.0.co;2

Myers, J. A., Chase, J. M., Jiménez, I., Jørgensen, P. M., Araujo-Murakami, A., Paniagua-Zambrana, N.,

& Seidel, R. (2013). Beta-diversity in temperate and tropical forests reflects dissimilar mechanisms of community assembly. *Ecology Letters*, *16*(2), 151–157. https://doi.org/10.1111/ele.12021

Myers, J. A., & Kitajima, K. (2007). Carbohydrate storage enhances seedling shade and stress tolerance in a neotropical forest. *Journal of Ecology*, *95*(2), 383–395. https://doi.org/10.1111/j.1365-2745.2006.01207.x

Myers, N., Mittermeier, R. A., Mittermeier, C. ., da Fonseca, G. A. ., & Kent, J. (2000). Biodiversity hotspots for conservation priorities. *Nature*, *403: 853*, 853.

Nakagawa, S., & Schielzeth, H. (2013). A general and simple method for obtaining R2 from generalized linear mixed-effects models. *Methods in Ecology and Evolution*, *4*. https://doi.org/10.1111/j.2041-210x.2012.00261.x

Nations, F. and A. O. of the U. (2020). Global Forest Resources Assessment 2020. In *FAO*. FAO. https://doi.org/10.4060/ca8753en

Neuhaus, J., & McCulloch, C. (2011). Generalized linear models. *Wiley Interdisciplinary Reviews: Computational Statistics*, *3*. https://doi.org/10.1002/wics.175

Norden, N., Angarita, H. A., Bongers, F., Martínez-Ramos, M., Cerda, I. G. D. La, Van Breugel, M., Lebrija-Trejos, E., Meave, J. A., Vandermeer, J., Williamson, G. B., Finegan, B., Mesquita, R., & Chazdon, R. L. (2015). Successional dynamics in Neotropical forests are as uncertain as they are predictable. *Proceedings of the National Academy of Sciences of the United States of America*, *112*(26), 8013–8018. https://doi.org/10.1073/pnas.1500403112

Norden, N., Letcher, S., Boukili, V., Swenson, N., & Chazdon, R. (2012). Demographic drivers of successional changes in phylogenetic structure across life-history stages in plant communities. *Ecology*, *93*. https://doi.org/10.1890/10-2179.1

Ofoe, R., Thomas, R., Asiedu, S., Wang-Pruski, G., Fofana, B., & Abbey, L. (2023). Aluminum in plant: Benefits, toxicity and tolerance mechanisms. *Frontiers in Plant Science*, *13*. https://doi.org/10.3389/fpls.2022.1085998

Oksanen, A. J., Blanchet, F. G., Friendly, M., Kindt, R., Legendre, P., Mcglinn, D., Minchin, P. R., Hara,

R. B. O., Simpson, G. L., Solymos, P., Stevens, M. H. H., Szoecs, E., & Wagner, H. (2020). *Community Ecology Package* (Issue November, p. 298).

Ordoñez, J., Tovar, C., Walker, B., Wheeler, J., Ayala-Ruano, S., Aguirre-Carvajal, K., McMahon, S., & Cuesta, F. (2025). Phenological patterns of tropical mountain forest trees across the neotropics: evidence from herbarium specimens. *Proceedings of the Royal Society B: Biological Sciences*, *292*. https://doi.org/10.1098/rspb.2024.2748

Ordoñez, M.-C., Casanova Olaya, J. F., Galicia, L., & Figueroa, A. (2020). Soil Carbon Dynamics under Pastures in Andean Socio-Ecosystems of Colombia. *Agronomy*, *10*(4), 507. https://doi.org/10.3390/agronomy10040507

Ortiz, D., Moreno, F., & Díez, M. C. (2021). Photosynthesis, growth, and survival in seedlings of four tropical fruit-tree species under intense radiation. *Acta Amazonica*, *51*(1), 1–9. https://doi.org/10.1590/1809-4392202000752

Paine, C. E. T., Harms, K. E., Schnitzer, S. A., & Carson, W. P. (2008). Weak Competition Among Tropical Tree Seedlings : Implications for Species Coexistence. *Biotropica*, *40*(4), 432–440. https://doi.org/https://doi.org/10.1111/j.1744-7429.2007.00390.x

Patanè, C., Cavallaro, V., Avola, G., & D'Agosta, G. (2006). Seed respiration of sorghum [Sorghum bicolor (L.) Moench] during germination as affected by temperature and osmoconditioning. *Seed Science Research*, *16*(4), 251–260. https://doi.org/10.1017/SSR2006259

Pavoine, S., Baguette, M., & Bonsall, M. B. (2010). Decomposition of trait diversity among the nodes of a phylogenetic tree. *Ecological Monographs*, *80*(3), 485–507. https://doi.org/10.1890/09-1290.1

Pei, S., & Yeh, M. (2001). The discrete fractional cosine and sine transforms. *IEEE Trans. Signal Process.*, *49*, 1198–1207. https://doi.org/10.1109/78.923302

Peres-neto, P. R., Dray, S., & Braak, C. J. F. (2017). Linking trait variation to the environment : critical issues with community-weighted mean correlation resolved by the fourth-corner approach. *Ecography*, *40*, 806–816. https://doi.org/10.1111/ecog.02302

Pérez-Escobar, O. A., Zizka, A., Bermúdez, M. A., Meseguer, A. S., Condamine, F. L., Hoorn, C.,

Hooghiemstra, H., Pu, Y., Bogarín, D., Boschman, L. M., Pennington, R. T., Antonelli, A., & Chomicki, G. (2022). The Andes through time: evolution and distribution of Andean floras. *Trends in Plant Science*, *27*(4), 364–378. https://doi.org/10.1016/j.tplants.2021.09.010

Perez-Harguindeguy, N., Garnier, E., Lavorel, S., Poorter, H., Jaureguiberry, P., Cornwell, W. K., Craine, J. M., Gurvich, D. E., Urcelay, C., Veneklaas, E. J., Reich, P. B., Poorter, L., Wright, I. J., Ray, P., Enrico, L., Pausas, J. G., de Vos, A. C., Buchmann, N., Funes, G., … Cornelissen, J. H. C. (2013). New handbook for standardised measurement of plant functional traits worldwide. *Australian Journal of Botany*, *61*, 167–234. https://doi.org/10.1071/BT12225

Pérez, L. M., & Díaz, T. J. (2010). *Estimación del carbono contenido en la biomasa forestal aérea de dos bosques andinos en los departamentos de Santander y Cundinamarca*. Universidad Distrital Francisco José de Caldas.

Peterson, G., Elmqvist, T., Nyström, M., Norberg, J., Walker, B., Bengtsson, J., & Folke, C. (2003). Response diversity, ecosystem change, and resilience. *Frontiers in Ecology and the Environment*, *1*, 488–494. https://doi.org/10.1890/1540-9295(2003)001[0488:RDECAR]2.0.CO;2

Pickett, S. T. A., Collins, S. L., & Armesto, J. J. (1987). A hierarchical consideration of causes and mechanisms of succession. *Vegetatio*, *69*(1), 109–114. https://doi.org/10.1007/BF00038691

Pinho, B. X., de Melo, F. P. L., Arroyo-Rodríguez, V., Pierce, S., Lohbeck, M., & Tabarelli, M. (2018). Soil-mediated filtering organizes tree assemblages in regenerating tropical forests. *Journal of Ecology*, *106*(1), 137–147. https://doi.org/10.1111/1365-2745.12843

Piquer-Doblas, M., Correa-Londoño, G. A., & Osorio-Vélez, L. F. (2024). From Stand to Forest: Woody Plant Recruitment in an Andean Restoration Project. *Plants*, *13*(17), 1–17. https://doi.org/10.3390/plants13172474

Plue, J., Van Calster, H., Auestad, I., Basto, S., Bekker, R. M., Bruun, H. H., Chevalier, R., Decocq, G., Grandin, U., Hermy, M., Jacquemyn, H., Jakobsson, A., Jankowska-Błaszczuk, M., Kalamees, R., Koch, M. A., Marrs, R. H., Marteinsdóttir, B., Milberg, P., Måren, I. E., … Auffret, A. G. (2021). Buffering effects of soil seed banks on plant community composition in response to land use and climate. *Global Ecology and Biogeography*, *30*(1), 128–139. https://doi.org/10.1111/geb.13201

Polansky, L., & Robbins, M. M. (2013). Generalized additive mixed models for disentangling long-term trends, local anomalies, and seasonality in fruit tree phenology. *Ecology and Evolution*, *3*(9), 3141–3151. https://doi.org/10.1002/ece3.707

Poorter, L. (2009). Leaf traits show different relationships with shade tolerance in moist versus dry tropical forests. *New Phytologist*, *181*(4), 890–900. https://doi.org/https://doi.org/10.1111/j.1469-8137.2008.02715.x

Poorter, L., Amissah, L., Bongers, F., Hordijk, I., Kok, J., Laurance, S. G. W., Lohbeck, M., Martínez-Ramos, M., Matsuo, T., Meave, J. A., Muñoz, R., Peña-Claros, M., & van der Sande, M. T. (2023). Successional theories. *Biological Reviews*, *98*(6), 2049–2077. https://doi.org/10.1111/brv.12995

Poorter, L., & Bongers, F. (2006). Leaf Traits Are Good Predictors of Plant Performance across 53 Rain Forest Species. *Ecology*, *87*(7), 1733–1743. https://doi.org/https://doi.org/10.1890/0012-9658(2006)87[1733:LTAGPO]2.0.CO;2

Poorter, L., Bongers, F., Aide, T. M., Almeyda Zambrano, A. M., Balvanera, P., Becknell, J. M., Boukili, V., Brancalion, P. H. S., Broadbent, E. N., Chazdon, R. L., Craven, D., De Almeida-Cortez, J. S., Cabral, G. A. L., De Jong, B. H. J., Denslow, J. S., Dent, D. H., DeWalt, S. J., Dupuy, J. M., Durán, S. M., … Rozendaal, D. M. A. (2016). Biomass resilience of Neotropical secondary forests. *Nature*, *530*(7589), 211–214. https://doi.org/10.1038/nature16512

Poorter, L., Craven, D., Jakovac, C. C., van der Sande, M. T., Amissah, L., Bongers, F., Chazdon, R. L., Farrior, C. E., Kambach, S., Meave, J. A., Muñoz, R., Norden, N., Rüger, N., van Breugel, M., Almeyda Zambrano, A. M., Amani, B., Andrade, J. L., Brancalion, P. H. S., Broadbent, E. N., … Hérault, B. (2021). Multidimensional tropical forest recovery. *Science*, *374*(6573), 1370–1376. https://doi.org/10.1126/science.abh3629

Poorter, L., Rozendaal, D., Bongers, F., Almeida, D. J., Álvarez, F., Andrade, J., Villa, L. F. A., Becknell, J., Bhaskar, R., Boukili, V., Brancalion, P., César, R., Chave, J., Chazdon, R., Colletta, G. D., Craven, D., De Jong, B., Denslow, J., Dent, D., … Westoby, M. (2021). Functional recovery of secondary tropical forests. *Proceedings of the National Academy of Sciences*, *118*. https://doi.org/10.1073/pnas.2003405118

Poorter, L., Rozendaal, D. M. A., Bongers, F., de Almeida-Cortez, J. S., Almeyda Zambrano, A. M., Álvarez, F. S., Andrade, J. L., Villa, L. F. A., Balvanera, P., Becknell, J. M., Bentos, T. V., Bhaskar, R., Boukili, V., Brancalion, P. H. S., Broadbent, E. N., César, R. G., Chave, J., Chazdon, R. L., Colletta, G. D., … Westoby, M. (2019). Wet and dry tropical forests show opposite successional pathways in wood density but converge over time. *Nature Ecology and Evolution*, *3*(6), 928–934. https://doi.org/10.1038/s41559-019-0882-6

Poorter, L., Rozendaal, D. M. A., Bongers, F., de Jarcilene, S. A., Àlvarez, F. S., Luìs Andrade, J., Arreola Villa, L. F., Becknell, J. M., Bhaskar, R., Boukili, V., Brancalion, P. H. S., Cèsar, R. G., Chave, J., Chazdon, R. L., Colletta, G. D., Craven, D., de Jong, B. H. J., Denslow, J. S., Dent, D. H., … Westoby, M. (2021). Functional recovery of secondary tropical forests. *Proceedings of the National Academy of Sciences of the United States of America*, *118*(49). https://doi.org/10.1073/pnas.2003405118

Poschlod, P., Abedi, M., Bartelheimer, M., Drobnik, J., Rosbakh, S., & Saatkamp, A. (2013). Vegetation ecology, chapter 2: seed ecology and assembly rules in plant communities. *John Wiley and Sons*, 164–202. https://doi.org/10.1002/9781118452592.ch6

Puerta-Piñero, C., Muller-Landau, H., Calderón, O., & Wright, S. J. (2013). Seed arrival in tropical forest tree fall gaps. *Ecology*, *94 7*, 1552–1562. https://doi.org/10.1890/12-1012.1

Purschke, O., Schmid, B., Sykes, M., Poschlod, P., Michalski, S., Durka, W., Kühn, I., Winter, M., & Prentice, H. (2013). Contrasting changes in taxonomic, phylogenetic and functional diversity during a long-term succession: insights into assembly processes. *Journal of Ecology*, *101*. https://doi.org/10.1111/1365-2745.12098

R Core Team. (2024). *R: A Language and Environment for Statistical Computing* (4.4.3). R Foundation for Statistical Computing. https://www.r-project.org/

Rahbek, C., Borregaard, M. K., Colwell, R. K., Dalsgaard, B., Holt, B. G., Morueta-Holme, N., Nogues-Bravo, D., Whittaker, R. J., & Fjeldså, J. (2019). Humboldt's enigma: What causes global patterns of mountain biodiversity? *Science*, *365*(6458), 1108–1113. https://doi.org/10.1126/science.aax0149

Raj, R., Walker, J., Pingale, R., Nandan, R., Naik, B., & Adinarayana, J. (2021). Leaf area index estimation

using top-of-canopy airborne RGB images. *Int. J. Appl. Earth Obs. Geoinformation*, *96*, 102282. https://doi.org/10.1016/j.jag.2020.102282

Reich, P. B. (2014). The world-wide "fast-slow" plant economics spectrum: A traits manifesto. *Journal of Ecology*, *102*(2), 275–301. https://doi.org/10.1111/1365-2745.12211

Rico-Gray, V., & García-Franco, J. G. (1992). Vegetation and soil seed bank of successional stages in tropical lowland deciduous forest. *Journal of Vegetation Science*, *3*(5), 617–624. https://doi.org/10.2307/3235828

Ricotta, C., & Podani, J. (2017). On some properties of the Bray-Curtis dissimilarity and their ecological meaning. *Ecological Complexity*, *31*, 201–205. https://doi.org/10.1016/J.ECOCOM.2017.07.003

Ripley, B., Venables, B., Bates, D. M., & Brianripleyr-projectorg, M. B. R. (2025). *Package 'MASS.'*

Rodrigo, J., & Herrero, M. (2002). Effects of pre-blossom temperatures on flower development and fruit set in apricot. *Scientia Horticulturae*, *92*(2), 125–135. https://doi.org/10.1016/S0304-4238(01)00289-8

Rodrigues, A. A., Filho, S. C. V., Müller, C., Rodrigues, D. A., Sales, J. de F., Zuchi, J., Costa, A. C., Rodrigues, C. L., da Silva, A. A., & Barbosa, D. P. (2019). Tolerance of Eugenia dysenterica to aluminum: Germination and plant growth. *Plants*, *8*(9), 1–15. https://doi.org/10.3390/plants8090317

Rosbakh, S., Pacini, E., Nepi, M., & Poschlod, P. (2018). An Unexplored Side of Regeneration Niche: Seed Quantity and Quality Are Determined by the Effect of Temperature on Pollen Performance. *Frontiers in Plant Science*, *9*. https://doi.org/10.3389/fpls.2018.01036

Rozendaal, D., Suarez, D. R., De Sy, V., Avitabile, V., Carter, S., Yao, C. A., Alvarez-Davila, E., Anderson-Teixeira, K., Araujo-Murakami, A., Arroyo, L., Barca, B., Baker, T., Birigazzi, L., Bongers, F., Branthomme, A., Brienen, R., Carreiras, J., Gatti, C., Cook-Patton, S., … Herold, M. (2021). Aboveground forest biomass varies across continents, ecological zones and successional stages: refined IPCC default values for tropical and subtropical forests. *Environmental Research Letters*, *17*. https://doi.org/10.1088/1748-9326/ac45b3

Rubiano, K., Clerici, N., Norden, N., & Etter, A. (2017). Secondary Forest and Shrubland Dynamics in a

Highly Transformed Landscape in the Northern Andes of Colombia (1985–2015). *Forests*, *8*(6), 216. https://doi.org/10.3390/f8060216

Rungrojtrakool, P., Tiansawat, P., Jampeetong, A., Shannon, D. P., & Chairuangsri, S. (2021). Soil seed banks of tree species from natural forests, restoration sites, and abandoned areas in Chiang Mai, Thailand. *Forest and Society*, *5*(1), 167–180. https://doi.org/10.24259/fs.v5i1.11612

Saatkamp, A., Cochrane, A., Commander, L., Guja, L. K., Jimenez-Alfaro, B., Larson, J., Nicotra, A., Poschlod0, P., Silveira, F. A. O., Cross, A. T., Dalziell, E. L., Dickie, J., Erickson, T. E., Fidelis, A., Fuchs, A., Golos, P. J., Hope, M., Lewandrowski, W., Merritt, D. J., … Walck, J. L. (2018). A research agenda for seed-trait functional ecology. *New Phytologist*, *221*(4), 1764–1775. https://doi.org/10.1111/nph.15502

Sanaphre-Villanueva, L., Dupuy, J., Andrade, J., Reyes-García, C., Paz, H., & Jackson, P. (2016). Functional Diversity of Small and Large Trees along Secondary Succession in a Tropical Dry Forest. *Forests*, *7*, 163. https://doi.org/10.3390/F7080163

Santiago, L., De Guzman, M., Baraloto, C., Vogenberg, J., Brodie, M., Hérault, B., Fortunel, C., & Bonal, D. (2018). Coordination and trade-offs among hydraulic safety, efficiency and drought avoidance traits in Amazonian rainforest canopy tree species. *The New Phytologist*, *218 3*, 1015–1024. https://doi.org/10.1111/nph.15058

Santos de Oliveira, C., de Sousa Messeder, J. V., Lopez Teixido, A., Reis Arantes, M. R., & Oliveira Silveira, F. A. (2021). Vegetative and reproductive phenology in a tropical grassland–savanna–forest gradient. *Journal of Vegetation Science*, *32*(2), 1–16. https://doi.org/10.1111/jvs.12997

Satdichanh, M., Huaixia, Yan, K., Dossa, G., Winowiecki, L., Vågen, T., Gassner, A., Xu, J.-C., & Harrison, R. (2018). Phylogenetic diversity correlated with above-ground biomass production during forest succession: Evidence from tropical forests in Southeast Asia. *Journal of Ecology*, *107*, 1419–1432. https://doi.org/10.1111/1365-2745.13112

Sherlock, B., & Kakad, Y. (2001). Windowed discrete cosine and sine transforms for shifting data. *Signal Process.*, *81*, 1465–1478. https://doi.org/10.1016/S0165-1684(01)00033-0

Shipley, B., Lechowicz, M., Wright, I. J., & Reich, P. B. (2006). Fundamental Trade-Offs Generating the

Worldwide Leaf Economics Spectrum. *Ecology*, *87*(3), 535–541.

Sierra, C. A., del Valle, J. I., Orrego, S. A., Moreno, F. H., Harmon, M. E., Zapata, M., Colorado, G. J., Herrera, M. A., Lara, W., Restrepo, D. E., Berrouet, L. M., Loaiza, L. M., & Benjumea, J. F. (2007). Total carbon stocks in a tropical forest landscape of the Porce region, Colombia. *Forest Ecology and Management*, *243*(2–3), 299–309. https://doi.org/10.1016/j.foreco.2007.03.026

Silva, J. P. G. da, Marangon, L. C., Feliciano, A. L. P., Ferreira, R. L. C., Torres, J. E. de L., & Santos, W. B. dos. (2019). Soil Seed Bank in the Tropical Rainforest Inserted in Agricultural Matrix, Northeast Region of Brazil. *Journal of Experimental Agriculture International*, *30*(4), 1–11. https://doi.org/10.9734/jeai/2019/46619

Smith, R. (2017). Solutions for loss of information in high-beta-diversity community data. *Methods in Ecology and Evolution*, *8*. https://doi.org/10.1111/2041-210X.12652

Smith, S. A., & Brown, J. W. (2018). Constructing a broadly inclusive seed plant phylogeny. *American Journal of Botany*, *105*(3), 302–314. https://doi.org/10.1002/ajb2.1019

Soriano, D., Orozco-Segovia, A., Mrquez-Guzmn, J., Kitajima, K., Gamboa-De Buen, A., & Huante, P. (2011). Seed reserve composition in 19 tree species of a tropical deciduous forest in Mexico and its relationship to seed germination and seedling growth. *Annals of Botany*, *107*(6), 939–951. https://doi.org/10.1093/aob/mcr041

Sousa, T. R., Costa, F. R. C., Bentos, T. V., Leal Filho, N., Mesquita, R. C. G., & Ribeiro, I. O. (2017). The effect of forest fragmentation on the soil seed bank of Central Amazonia. *Forest Ecology and Management*, *393*, 105–112. https://doi.org/10.1016/j.foreco.2017.03.020

Souza, D., Sfair, J., De Paula, A. S., Barros, M. F., Rito, K., & Tabarelli, M. (2019). Multiple drivers of aboveground biomass in a human-modified landscape of the Caatinga dry forest. *Forest Ecology and Management*. https://doi.org/10.1016/J.FORECO.2018.12.042

Stefanidis, K., Oikonomou, A., Dimitrellos, G., Tsoukalas, D., & Papastergiadou, E. (2023). Relationships between Environmental Factors and Functional Traits of Macrophyte Assemblages in Running Waters of Greece. *Diversity*, *15*(9). https://doi.org/10.3390/d15090949

Tebby, C., Joachim, S., Van Den Brink, P., Porcher, J., & Beaudouin, R. (2017). Analysis of community-level mesocosm data based on ecologically meaningful dissimilarity measures and data transformation. *Environmental Toxicology and Chemistry*, *36*. https://doi.org/10.1002/etc.3701

Terborgh, J., Nuñez, N. H., Loayza, P. A., & Valverde, F. C. (2017). Gaps contribute tree diversity to a tropical floodplain forest. *Ecology*, *98 11*, 2895–2903. https://doi.org/10.1002/ecy.1991

Umaña, M., Condit, R., Condit, R., Pẽrez, R., Turner, B., Wright, S. J., Comita, L., & Comita, L. (2020). Shifts in taxonomic and functional composition of trees along rainfall and phosphorus gradients in central Panama. *Journal of Ecology*, *109*, 51–61. https://doi.org/10.1111/1365-2745.13442

Uriarte, M., Muscarella, R., & Zimmerman, J. (2018). Environmental heterogeneity and biotic interactions mediate climate impacts on tropical forest regeneration. *Global Change Biology*, *24*. https://doi.org/10.1111/gcb.14000

van Breugel, M., Bongers, F., & Martínez-Ramos. (2007). Species Dynamics during Early Secondary Forest Succession: Recruitment, Mortality and Species Turnover. *Biotropica*, *39*(5), 610–619.

Vázquez-Ramírez, J., & Venn, S. (2023). Snow, fire and drought: How alpine and treeline soil seed banks are affected by simulated climate change. *Annals of Botany*. https://doi.org/10.1093/aob/mcad184

Violle, C., Navas, M. L., Vile, D., Kazakou, E., Fortunel, C., Hummel, I., & Garnier, E. (2007). Let the concept of trait be functional! *Oikos*, *116*(5), 882–892. https://doi.org/10.1111/j.0030-1299.2007.15559.x

Walters, M. B., & Reich, P. B. (2000). SEED SIZE, NITROGEN SUPPLY, AND GROWTH RATE AFFECT TREE SEEDLING SURVIVAL IN DEEP SHADE. *Ecology*, *81*(7), 1887–1901. https://doi.org/https://doi.org/10.1890/0012-9658(2000)081[1887:SSNSAG]2.0.CO;2

Westoby, M. (1998). A leaf-height-seed (LHS) plant ecology strategy scheme. *Plant and Soil*, *199*(2), 213–227. https://doi.org/10.1023/A:1004327224729

Williams-Linera, G., Bonilla-Moheno, M., & López-Barrera, F. (2016). Tropical cloud forest recovery: the role of seed banks in pastures dominated by an exotic grass. *New Forests*, *47*(3), 481–496. https://doi.org/10.1007/s11056-016-9526-8

Williamson, G., Mesquita, R., & Bentos, T. (2008). Reproductive Phenology of Central Amazon Pioneer Trees. *Tropical Conservation Science*, *1*, 186–203. https://doi.org/10.1177/194008290800100303

Wright, I. J., Reich, P. B., Westoby, M., Ackerly, D. D., Baruch, Z., Bongers, F., Cavender-Bares, J., Chapin, T., Cornellssen, J. H. C., Diemer, M., Flexas, J., Garnier, E., Groom, P. K., Gulias, J., Hikosaka, K., Lamont, B. B., Lee, T., Lee, W., Lusk, C., … Villar, R. (2004). The worldwide leaf economics spectrum. *Nature*, *428*(6985), 821–827. https://doi.org/10.1038/nature02403

Wright, J. S. (2002). Plant diversity in tropical forests: a review of mechanisms of species coexistence. *Oecologia*, *130*(1), 1–14. https://doi.org/10.1007/s004420100809

Wright, S. J., & Calderón, O. (2006). Seasonal, El Nino and longer term changes in flower and seed production in a moist tropical forest. *Ecology Letters*, *9*(0), 35–44. https://doi.org/10.1111/j.1461-0248.2005.00851.x

Wright, S. J., & Calderón, O. (2018a). Solar irradiance as the proximate cue for flowering in a tropical moist forest. *Biotropica*, *50*. https://doi.org/10.1111/btp.12522

Wright, S. J., & Calderón, O. (2018b). Solar irradiance as the proximate cue for flowering in a tropical moist forest. *Biotropica*, *50*(3), 374–383. https://doi.org/10.1111/btp.12522

Wright, S. Joseph, & van Schaik, C. P. (1994). Light and the Phenology of Tropical Trees. *The American Naturalist*, *143*(1), 192–199. https://doi.org/10.1086/285600

Wu, Y., & Shen, Y. B. (2021). Seed Coat Structural and Permeability Properties of Tilia miqueliana Seeds. *Journal of Plant Growth Regulation*, *40*(3), 1198–1209. https://doi.org/10.1007/s00344-020-10179-0

Yan, P., He, N., Yu, K., Xu, L., & Van Meerbeek, K. (2023). Integrating multiple plant functional traits to predict ecosystem productivity. *Communications Biology*, *6*. https://doi.org/10.1038/s42003-023-04626-3

Yang, D., & Li, W. (2013). Soil seed bank and aboveground vegetation along a successional gradient on the shores of an oxbow. *Aquatic Botany*, *110*, 67–77. https://doi.org/10.1016/j.aquabot.2013.05.004

Yao, J., & Ding, H. (2024). Nonlinear Responses of Vegetation Phenology to Climate Change and Urbanization: A Case Study in Beijing, China. *IEEE Journal of Selected Topics in Applied Earth Observations and Remote Sensing*, *17*, 5390–5402. https://doi.org/10.1109/JSTARS.2024.3367734

Yaseen, M., Khan, W. R., Bahadur, S., Batool, F., Khalid, F., Ahmed, U., & Ashraf, M. (2023). Intra- and inter-specific responses of plant functional traits to environmental variables: implications for community ecology in the tropical monsoonal dwarf forest on Hainan Island. *Frontiers in Forests and Global Change*, *6*. https://doi.org/10.3389/ffgc.2023.1198626

Zalamea, P., Sarmiento, C., Arnold, A., Davis, A., & Dalling, J. (2015). Do soil microbes and abrasion by soil particles influence persistence and loss of physical dormancy in seeds of tropical pioneers? *Frontiers in Plant Science*, *5*. https://doi.org/10.3389/fpls.2014.00799

Zanne, A. E., Tank, D. C., Cornwell, W. K., Eastman, J. M., Smith, S. A., Fitzjohn, R. G., McGlinn, D. J., O'Meara, B. C., Moles, A. T., Reich, P. B., Royer, D. L., Soltis, D. E., Stevens, P. F., Westoby, M., Wright, I. J., Aarssen, L., Bertin, R. I., Calaminus, A., Govaerts, R., … Beaulieu, J. M. (2014). Three keys to the radiation of angiosperms into freezing environments. *Nature*, *506*(7486), 89–92. https://doi.org/10.1038/nature12872

Zelený, D. (2018). Which results of the standard test for community- - weighted mean approach are too optimistic ? *Journal of Vegetation Science*, *29*(6), 953–966. https://doi.org/https://doi.org/10.1111/jvs.12688

Zhang, H., Qi, W., John, R., Wang, W., Song, F., & Zhou, S. (2015). Using functional trait diversity to evaluate the contribution of multiple ecological processes to community assembly during succession. *Ecography*, *38*, 1176–1186. https://doi.org/10.1111/ECOG.01123

Zhang, X., Ni, X., Hědenec, P., Yue, K., Wei, X., Yang, J., & Wu, F. (2022). Litter facilitates plant development but restricts seedling establishment during vegetation regeneration. *Functional Ecology*. https://doi.org/10.1111/1365-2435.14200

Zhang, Z.-T., Song, X., Xiao, W.-F., Gao, B.-J., & Guo, Z.-L. (2009). Characteristics of soil seed banks in logging gaps of forests at different succession stages in Changbai Mountains. *Ying Yong Sheng Tai Xue Bao = The Journal of Applied Ecology / Zhongguo Sheng Tai Xue Xue Hui, Zhongguo Ke*

Xue Yuan Shenyang Ying Yong Sheng Tai Yan Jiu Suo Zhu Ban, *20*, 1293–1298.

Zhou, L., Thakur, M. P., Jia, Z., Hong, Y., Yang, W., An, S., & Zhou, X. (2023). Light effects on seedling growth in simulated forest canopy gaps vary across species from different successional stages. *Frontiers in Forests and Global Change*, *5*. https://doi.org/10.3389/ffgc.2022.1088291

Zimmerman, J., Wright, S. J., Calderón, O., Pagan, M., & Paton, S. (2007). Flowering and fruiting phenologies of seasonal and aseasonal neotropical forests: the role of annual changes in irradiance. *Journal of Tropical Ecology*, *23*, 231–251. https://doi.org/10.1017/S0266467406003890

Zirbel, C., Bassett, T., Grman, E., Grman, E., & Brudvig, L. (2017). Plant functional traits and environmental conditions shape community assembly and ecosystem functioning during restoration. *Journal of Applied Ecology*, *54*, 1070–1079. https://doi.org/10.1111/1365-2664.12885